

STOCHASTIC FLOW SEQUENCE GENERATION  
AND ASPINALL UNIT OPERATIONS

By

KENNETH C NOWAK

B.S., Rensselaer Polytechnic Institute, 2006

A thesis submitted to the faculty of the Graduate School of the University of  
Colorado in partial fulfillment of the requirement for the degree of  
Master of Science  
Department of Civil, Environmental, and Architectural Engineering

2008

This thesis entitled:  
Stochastic Flow Sequence Generation  
and Aspinall Unit Operations  
written by Kenneth C Nowak  
has been approved for the  
Department of Civil, Environmental, and Architectural Engineering

---

Balaji Rajagopalan

---

Edith Zagona

---

Kenneth Strzepek

Date \_\_\_\_\_

The final copy of this thesis has been examined by the signatories, and we find that both the content and the form meet acceptable presentation standards of scholarly work in the above mentioned discipline.

Kenneth C Nowak (MS, Civil, Environmental, and Architectural Engineering)

Stochastic Flow Sequence Generation and Aspinall Unit Operations

Thesis directed by Professor Balaji Rajagopalan

The Aspinall Unit is comprised of three reservoirs that lie on the western slope of Rocky Mountains and regulate approximately 50% of the Gunnison River Basin drainage. Since its completion in 1977, the Unit's primary objectives have been generation of hydropower, storage for consumptive use, flood prevention, and recreation. Currently, an Environmental Impact Statement (EIS) is being prepared to benefit endangered fish species found in the Gunnison River, focusing on habitat management by prescribing beneficial flows. Thus, the implication of this additional demand/objective is of importance to water managers.

Southwestern water management and planning are increasingly discussed topics, given the recent, unprecedented drought (1999-2004). While this period marked the worst drought on record for the Colorado River Basin, paleo reconstructed flows dating back to the 1500's suggest that such events are not uncommon. As a result, when assessing the impact of the recommended fish flows (RFF) on pre-existing objectives, it is important to consider a wide range of hydrologies that include extended periods of drought and surplus.

This work aims to develop synthetic hydrologies that can be used to assess the implications of meeting the RFF on current operations of the Aspinall Unit through the following steps. Stochastic flow sequence generation techniques based on observed data only are first investigated, followed by approaches to incorporate paleo

reconstructed data. The selected methods are then employed to generate synthetic traces which are eventually used as inputs to a Decision Support System (DSS) model of the Gunnison Basin. In order to be used as such, these traces are disaggregated from an annual single site value to intervening flows throughout the basin at a monthly timestep. Last, a DSS model is developed and employed to demonstrate the usefulness of the stochastic flow sequences.

## **Dedication**

For my parents and brother, who have always encouraged my endeavors,  
whatever they may be.

## **Acknowledgements**

This work would not have been possible without the help of many individuals.

First, I would like to thank my advisor, Dr. Balaji Rajagopalan, committee member Dr. Edith Zagona and also Dr. Jim Prairie. Without their constant guidance and patience throughout my work I would not have been able to accomplish and learn all that I have. I thank the staff at the Center for Advanced Decision Support for Water and Environmental Systems for providing a great environment in which to work; their willingness to help has made the challenges of this process attainable. Last, I gratefully thank the Bureau of Reclamation for their funding of this research work.

## Contents

CHAPTER 1: INTRODUCTION.....	1
1.1 Background.....	1
1.1.1 Western United States Water Resources.....	1
1.1.2 Gunnison River Basin and Aspinall EIS.....	3
1.1.3 Recommended Fish Flows (RFF).....	5
1.2 Need for Stochastic Flow Sequence Generation.....	7
1.3 Outline.....	7
CHAPTER 2: DEVELOPMENT OF STOCHASTIC FLOW SEQUENCES BASED ON OBSERVED DATA.....	10
2.1 Introduction.....	10
2.2 Background.....	11
2.3 Description of Stochastic Methods.....	12
2.3.1 ARMA.....	12
2.3.2 ISM.....	14
2.3.3 K-Nearest Neighbor Time Series Resampling.....	14
2.3.4 Modified KNN.....	18
2.4 Evaluation of Methods.....	20
2.5 Results.....	23
2.6 System Risk.....	28
2.6 Summary and Discussion.....	30
CHAPTER 3: DEVELOPMENT OF STOCHASTIC FLOW SEQUENCES BASED ON OBSERVED AND PALEO DATA.....	32

3.1 Introduction.....	32
3.2 Paleo Data.....	33
3.2 Methods.....	35
3.2.1 Block Resampling (Block).....	36
3.2.2 Homogeneous Markov (HM).....	36
3.2.3 Block Homogeneous Markov (BHM) .....	37
3.2.4 Non-Homogeneous Markov (NHM).....	38
3.2.5 KNN Flow Magnitude Resampling .....	42
3.3 Evaluation of Methods.....	43
3.4 Results.....	45
3.5 Summary and Discussion.....	56
CHAPTER 4: SPACE-TIME DISAGGREGATION OF FLOW SEQUENCES.....	59
4.1 Introduction.....	59
4.2 Disaggregation Techniques.....	61
4.3 KNN Space-Time Disaggregation .....	63
4.4 Model Evaluation.....	66
4.5 Results.....	66
4.6 Summary .....	78
CHAPTER 5: ASPINALL UNIT OPERATIONS MODELING .....	79
5.1 Introduction.....	79
5.2 Water Management and Need for Modeling Tools .....	79
5.3 Aspinall EIS .....	81
5.4 Basin Description and Operations .....	83

5.4.1 General Overview .....	83
5.4.2 Taylor Park.....	86
5.4.3 Blue Mesa .....	87
5.4.4 Morrow Point and Crystal.....	88
5.5 Modeling.....	88
5.5.1 No Action.....	89
5.5.1.1 Taylor Park Reservoir.....	89
5.5.1.2 Blue Mesa Reservoir.....	90
5.5.1.3 Morrow Point Reservoir .....	90
5.5.1.4 Crystal Reservoir .....	91
5.5.2 RFF Policy .....	91
5.6 Validation and Results .....	93
5.7 Summary.....	104
CHAPTER 6: CONCLUSION AND RECOMMENDATION FOR FUTURE WORK	107
6.1 Conclusions.....	107
6.1.1 Observed Data Techniques .....	107
6.1.2 Paleo Techniques .....	108
6.1.3 Flow Disaggregation.....	109
6.1.4 Application of Synthetic Flows to Gunnison Operations Model.....	109
6.2 Future Work.....	110
6.2.1 Further Development of Paleo Techniques.....	110
6.2.2 Climate Change and Water Management .....	111
REFERENCES .....	112

APPENDIX A RFF RIVERWARE RULES ..... 116

## Figures

Figure 1 United States population change map. (source: <a href="http://www.CensusScope.org">www.CensusScope.org</a> ).....	2
Figure 2 Gunnison River at Grand Junction, CO annual hydrograph.....	4
Figure 3 Gunnison River Basin. (source: USBR 2004b).....	5
Figure 4 PACF (left) and ACF (right) for USGS gauge number 09152500 from 1906- 2005. ....	13
Figure 5 Lag-1 KNN technique. ....	16
Figure 6 Modified KNN. (source: Prairie et al., 2006).....	19
Figure 7 Mean (left) and standard deviation (right) for 100 simulations. ....	20
Figure 8 Median annual flow for various numbers of simulations using KNN.....	21
Figure 9 Definition of surplus and drought statistics.....	22
Figure 10 Distributional statistics for KNN, Modified KNN and AR-1 traces. ....	24
Figure 11 Annual Flow PDFs (acre-ft/yr) of KNN (left), Modified KNN (center) and AR-1 (right). The red line depicts the observed PDF. ....	25
Figure 12 Surplus length histograms. KNN (left), Modified KNN (center) and AR-1 (right). ....	26
Figure 13 Drought length histograms. KNN (left), Modified KNN (center) and AR-1 (l right). ....	26
Figure 14 Surplus volume histograms. KNN (left), Modified KNN (center) and AR-1 (right). ....	27
Figure 15 Drought deficit histograms. KNN (left), Modified KNN (center) and AR-1 (right). ....	27
Figure 16 Observed drought histogram .....	28

Figure 17 Observed surplus histogram .....	28
Figure 18 Sequent peak algorithm. KNN (left), Modified KNN (center) and AR-1 (right). .....	30
Figure 19 PDFs of storage required to meet a demand of 1.65 MAF. The red vertical line represents the live storage capacity of the Gunnison Basin. KNN (left), Modified KNN (center) and AR-1 (right).....	30
Figure 20 Paleo reconstructed flows for the Colorado River at Lee’s Ferry, AZ.....	34
Figure 21 Wet/dry state time series for observed data (top) and four paleo reconstructions. ....	35
Figure 22 Paleo reconstructed flows for Gunnison River near Grand Junction, CO with 5-year smoothing. ....	35
Figure 23 Wet-wet (blue dashed) and dry-dry (solid red) transition probabilities from the BHM technique. ....	38
Figure 24 Wet-wet (blue dashed) and dry-dry (solid red) transition probabilities from the NHM technique.....	40
Figure 25 Definition of drought/surplus statistics. ....	45
Figure 26 Distributional statistics for Block, HM, BHM and NHM traces.....	46
Figure 27 Annual PDFs (acre-ft/yr) of traces generated using Block (upper left), HM (upper right BHM (lower left) and NHM (lower right) techniques. The observed PDF is shown in red.....	47
Figure 28 Surplus length histograms of Block (upper left), HM (upper right), BHM (lower left) and NHM (lower right) techniques.....	48

Figure 29 Drought length histograms of Block (upper left), HM (upper right), BHM (lower left) and NHM (lower right) techniques.....	49
Figure 30 Surplus volume histograms of Block (upper left), HM (upper right), BHM (lower left) and NHM (lower right) techniques.....	52
Figure 31 Drought deficit histograms of Block (upper left), HM (upper right), block BHM (lower left) and NHM (lower right) techniques.....	53
Figure 32 Sequent peak of Block (upper left), HM (upper right), BHM (lower left) and NHM (lower right) techniques. The red dashed line represents maximum live storage of the Aspinall Unit and Taylor Reservoir, while the dotted blue line shows the observed data trace.....	54
Figure 33 PDFs of storage required to meet a 1.65 MAF demand. The vertical red line is live storage of the Gunnison Basin. Block (upper left), HM (upper right), BHM (lower left) and NHM (lower right) techniques.....	56
Figure 34 Gunnison Basin and disaggregation sites.....	61
Figure 35 Space-time disaggregation schematic.....	64
Figure 36 Annual flow PDF (acre-ft/yr) at site 4.....	67
Figure 37 Annual flow PDF (acre-ft/yr) at site 3.....	67
Figure 38 Annual flow PDF (acre-ft/yr) at site 2.....	67
Figure 39 Annual flow PDF (acre-ft/yr) at site 1.....	68
Figure 40 Monthly flow PDFs (acre-ft/yr) at site 4.....	69
Figure 41 Monthly flow PDFs (acre-ft/yr) at site 3.....	70
Figure 42 Monthly flow PDFs (acre-ft/yr) at site 2.....	71
Figure 43 Monthly flow PDFs (acre-ft/yr) at site 1.....	72

Figure 44 Two step spatial disaggregation. ....	74
Figure 45 Monthly statistics at the index gauge. ....	74
Figure 46 Monthly statistics at site 4. ....	75
Figure 47 Monthly statistics at site 3. ....	75
Figure 48 Monthly statistics at site 2. ....	76
Figure 49 Monthly statistics at site 1. ....	76
Figure 50 Temporal correlations at site 4. ....	77
Figure 51 Spatial correlations at monthly and annual timesteps. ....	78
Figure 52 Gunnison River Basin. (source: USBR, 2004b).....	84
Figure 53 Gunnison River natural flow hydrograph near Grand Junction. ....	86
Figure 54 Riverware model. ....	89
Figure 55 Probability (%) of not meeting fish flows with NHM data inputs, RFF policy shown as dashed and NA policy as solid. ....	94
Figure 56 Probability (%) of not meeting fish flows under RFF policy with results from NHM data inputs shown as dashed and computed natural flow inputs as solid. .	94
Figure 57 Annual hydropower generation for Morrow Point under NHM and computed natural flow data inputs. ....	96
Figure 58 Monthly and annual spill at Blue Mesa under RFF policy with NHM inputs (top) and computed natural flow data input (bottom). ....	98
Figure 59 Monthly and annual spill at Blue Mesa under NA policy with NHM inputs (top) and computed natural flow data input (bottom). ....	99
Figure 60 Blue Mesa Reservoir Storage under RFF policy with NHM inputs (top) and RFF policy with computed natural flow data inputs (bottom). ....	100

Figure 61 Blue Mesa Reservoir Storage under NA policy with NHM inputs (top) and NA policy with computed natural flow data inputs (bottom).....	101
Figure 62 Taylor Park Reservoir Storage RFF policy with NHM inputs (top) and computed natural flow data inputs (bottom).....	101
Figure 63 Taylor Park Reservoir Storage under NA policy with NHM inputs (top) and NA policy with computed natural flow data inputs (bottom).....	102
Figure 64 Modeled flows at USGS gauge 09152500 under RFF policy and NHM input data. Blue circles represent average computed natural flow, red triangles the average modeled flow results using computed natural flow inputs and green squares the average historic data at this location, all from 1977-2006.....	103
Figure 65 Modeled flows at USGS gauge 09152500 under NA policy and NHM input data. Blue circles represent average computed natural flow, red triangles the average modeled flow results using computed natural flow inputs and green squares the average historic data at this location, all from 1977-2006.....	103
Figure 66 Crystal spill results from modeling with NHM data and NA policy.....	105
Figure 67 Crystal spill results from modeling with KNN data and NA policy .....	105

## Tables

Table 1 HM TPM (left is current state, top is future state).....	37
Table 2 Hydrologic categories. (source: USFWS, 2003) .....	83
Table 3 Gunnison River spring flow recommendations. (source: USFWS, 2003).....	83
Table 4 Summer, fall and winter recommended flow ranges for Gunnison River. (source: USFWS, 2003).....	83

# **CHAPTER 1: INTRODUCTION**

## **1.1 Background**

### **1.1.1 Western United States Water Resources**

The recent extended period of drought (1999-2004) throughout the southwestern United States and Colorado River Basin in particular, has raised considerable concern about the ability to reliably provide water to the area's growing population while protecting the environment and endangered species. During this period, Lakes Powell and Mead experienced marked declines in storage, spurring alarm not only about the climate and growing demand, but the management of water in the Colorado Basin as a whole. The Colorado Basin supplies water to seven "basin states" (Wyoming, Colorado, Utah, Nevada, Arizona, New Mexico and California) and to parts of Mexico. Furthermore, thirty-six species of fish are native to the basin, four of which are listed as endangered and found nowhere else in the world. As a result, water use and allocation have come under intense scrutiny.

Since the early 1900's, the southwest has grown over 1500% compared to the United States national average of approximately 225%. Figure 1 depicts this trend over a ten year period spanning 1990-2000. In particular, Arizona and New Mexico have become new retirement hotspots, while southern California and Las Vegas continue to sprawl (Chourre and Wright, 1997). The influx of water users to the area, combined with the demand for amenities such as golf courses and manicured lawns, has further stressed this region. The current water management compacts between basin states have several detractors. Agreements were based on limited data that suggest a much wetter climate and overall greater availability of water. Several

accords guarantee water by volume, instead of a percent-based approach, which can create a rather lopsided allocation during dry years. Also, population growth and location are difficult to anticipate, and thus water is not always available to places that need it most. Climate change projections suggest that water in the southwest will become scarcer in the future. Now, more than ever, understanding potential hydrologic scenarios and the implications on water management is of great importance.

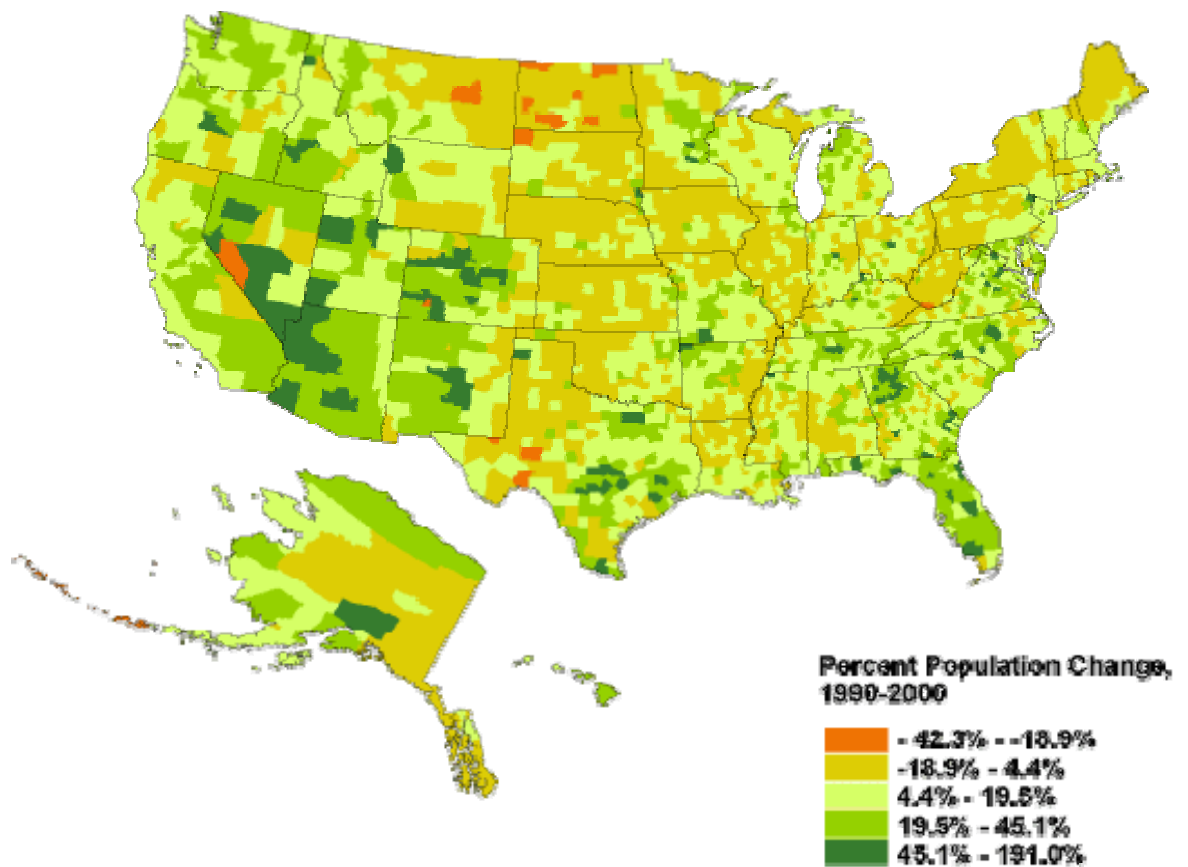


**Figure 1 United States population change map. (source: [www.CensusScope.org](http://www.CensusScope.org))**

These aspects are underscored in the Gunnison River Basin, one of the important tributaries of the Colorado River, which serves as a microcosm to the issues faced on a larger scale in the Colorado River Basin. In particular, efforts are

underway in this basin to devise reservoir operating strategies to help sustain aquatic habitat under increasing stress to the area's water resources from conflicting demands and changing climate. Hence, the Gunnison River Basin is the focus of this study.

### **1.1.2 Gunnison River Basin and Aspinall EIS**

The hydrology of much of the Colorado Basin including the Gunnison, is primarily driven by spring snowmelt run-off, shown by the computed natural flow hydrograph at Grand Junction (Figure 2). Natural flow data is maintained by the Bureau of Reclamation and has anthropogenic impacts removed (Prairie and Callejo, 2005). Thus, it is the best estimate available of the actual basin hydrology. As to be expected, peak demands tend to occur in summer months, primarily for irrigation purposes. In order to reliably provide water to users, there are numerous dams, from which water can be released and controlled as necessary. These structures can greatly alter the riparian environment by inundating large areas, disrupting natural streamflows and in general, negatively impacting the fish habitat (Gosset et al., 2006; Rieman et al., 2001; Thompson and Rahel, 1998). Within the Gunnison Basin, several species have become endangered including the Razorback Sucker and the Colorado Pikeminnow. Federal action to protect critical habitat for these fish, in accordance with the National Environmental Policy Act, has resulted in the ongoing preparation of the Aspinall Unit Operations Environmental Impact Statement (EIS). The Aspinall Unit is a series of reservoirs that regulate approximately half of the Gunnison River Basin, which, in its entirety, drains 8,000 square miles on the western slope of the Rocky Mountains, before its confluence with the Colorado in Grand Junction, CO. The map below (Figure 3) illustrates the basin and three reservoirs

(Crystal, Morrow Point and Blue Mesa) that comprise the Aspinall Unit. Other noteworthy components of the basin include Taylor Reservoir, located on Taylor River, the Uncompahgre Diversion Project and the Black Canyon of the Gunnison National Park, just downstream of the Aspinall Unit. The EIS aims to develop operating guidance and criteria to assist in meeting recommended fish flows (RFF) for the endangered species, while continuing to meet the pre-existing objectives of the Unit (USBR, 2004a).

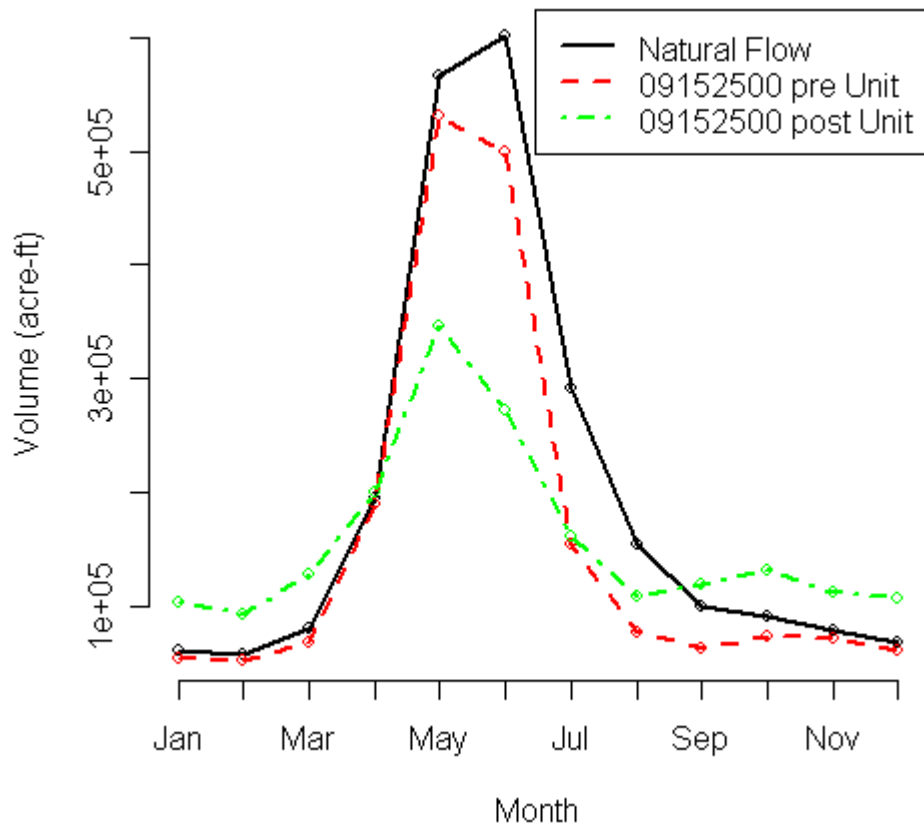


**Figure 2 Gunnison River at Grand Junction, CO annual hydrograph.**

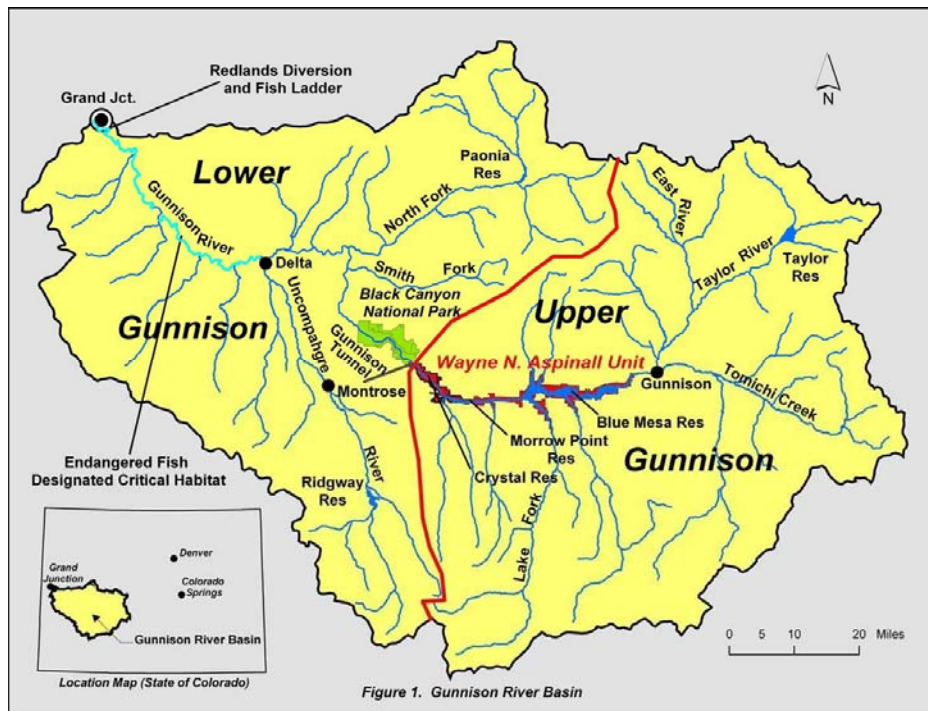


Figure 3 Gunnison River Basin. (source: USBR 2004b)

### 1.1.3 Recommended Fish Flows (RFF)

The largest impact of the Aspinall Unit has been the alteration of the river's natural hydrograph. As a result of holding back water for the dry summer months, typical spring peak flows have been severely reduced. This can be clearly seen in Figure 2, which shows the pre and post Aspinall Unit hydrographs, as well as the computed natural flow hydrograph (Prairie and Callejo, 2005). The pre Unit hydrograph is comprised of data observed at USGS gauge number 09152500 near Grand Junction, prior to the start of Aspinall Unit construction in 1963. This hydrograph is very similar to the natural flow plot for the January to May period, but differs in the summer to early fall. The discrepancy is due to the Gunnison Diversion Tunnel (1909), in which water is delivered to the Uncompahgre Basin from the Gunnison during the irrigation season, resulting in the reduced summer flows. The post Unit hydrograph is developed from the same USGS gauge data, but after 1977,

when construction was completed. The impact of the reservoirs is quite noticeable; peak flows have been reduced while during the other seasons flow has been augmented for irrigation and hydropower. Overall, the difference in total annual volume between the pre and post unit hydrographs is about 1%, with the post unit being slightly less. This is a small difference and is most likely due to the increased losses due to evaporation from the three reservoirs.

The RFF set forth by the US Fish and Wildlife Service mandate high flow releases in late spring, hoping to inundate flood plains/generate off-channel habitats rich in food for adult staging/growth, while providing effective sediment transport to remove silt and restore cobble bed breeding habitat (USFWS, 2003). Late spring/early summer high flows also serve as a spawning cue for the fish. Required flows for a given year are based on the forecasted April –July inflow to the basin; which is used to assign one of six hydrologic states. There are six states that range from wet to dry. Each of the six hydrologic categories specify the number of days for which there should be ½ fullbank discharge and fullbank discharge, in addition to instantaneous peak flow ranges. Also, summer, fall and winter flows are established based on hydrologic category to provide baseflows that promote survival of the young (USFWS, 2003). All flows are specified at the United States Geologic Survey (USGS) gauge near Grand Junction (09152500).

Understanding the year-to-year variability in streamflow is critical to obtaining insight into the potential risk of inability to meet these fish flows and developing realistic and sustainable reservoir operating guidelines. To this end, the following integrated components are essential – (i) simple and robust streamflow

simulation techniques and (ii) a realistic decision support tool that encapsulates the operations and rules of the basin and can be driven by a variety of streamflow scenarios to obtain system risk and reliability estimates. This research develops a variety of synthetic hydrologies for that purpose and a simple DSS model to demonstrate their utility in work such as the Aspinall Unit Operations EIS study.

### **1.2 Need for Stochastic Flow Sequence Generation**

When assessing the Aspinall Unit operations under the new strains of fish flow requirements, it is important to model the system under a variety of plausible flow scenarios – especially extreme conditions beyond what has been observed. Historical data are always limited; therefore, tools are necessary to generate plausible flow scenarios that are statistically consistent with the observed data. Paleo reconstructions of streamflow that extend back several centuries are also available, albeit with reduced reliability (Hidalgo et al., 2000; Woodhouse et al., 2006). Thus, a stochastic flow generation tool is desired that is (i) simple, (ii) robust, (iii) data driven and (iv) able to incorporate information from the paleo reconstructions to provide a realistic and rich variety of streamflow sequences. This motivates the first part of this research. In the second component, a decision support tool is developed for basin operations that can be driven by these stochastic sequences and show their value in providing system risk and reliability when meeting the RFF. The outline of the thesis describing the various chapters is as follows.

### **1.3 Outline**

Chapter 2 will introduce basic parametric and non-parametric techniques for the generation of stochastic flow sequences for the Gunnison River at Grand Junction.

Specifically, the Index Sequential Method (ISM) (Ouarda et al., 1997), K-Nearest Neighbor (KNN) bootstrap (Lall and Sharma, 1996), Modified K-Nearest Neighbor (Prairie et al., 2006) and Auto Regressive Moving Average (ARMA) (Thomas and Fiering, 1962; Salas et al., 1982; Harms and Campbell, 1967) models are discussed. ISM is widely utilized for its simplicity and ability to replicate observed statistics very well. Its main drawback is that the sequence and magnitude of flows are restricted to that of the observed – essentially, it repeats the flows in the exact manner as observed. The KNN bootstrap technique can generate a wide range of flow sequences while retaining the observed magnitude of flows – this provides a richer variety in the sequences while preserving the observed statistics. Prairie et al.’s (2006) Modified KNN also generates a wide range of sequences while retaining observed statistics, but in addition, produces previously unseen flow magnitudes. ARMA models have the ability to generate a wide variety of values, beyond those observed, but struggle to reproduce non-Gaussian distributions. This chapter will elaborate on the implementation of these methods, contrast advantages and drawbacks and compare the results from the traces generated.

Paleo reconstructed flow data can provide insight into long-term streamflow and more importantly, on the hydrologic state (wet/dry) variability – however, the reconstructed flow magnitudes are less reliable, as they are based on regression equations developed between tree ring growth and streamflow during the contemporary period (Hidalgo et al. 2000). Nonetheless, it is prudent to harness this information and incorporate it into a streamflow generation technique. To this end, Chapter 3 will develop a technique that combines Markov chain-based methods that

with a KNN bootstrap, in order to generate streamflow scenarios incorporating the observed and paleo information. The different combination methods are presented, compared and discussed in this chapter.

The above methods provide annual streamflow traces for the Gunnison River near Grand Junction. However, for work such as the EIS study, flow scenarios are often needed at several locations throughout the basin at monthly time scales. This requires the generated annual flows to be disaggregated in space and time. Chapter 4 will adapt the non-parametric space-time disaggregation technique (Prairie et al., 2006) for this purpose to provide monthly flows at key sites in the Gunnison Basin. The results will be compared with historical data to ensure effective disaggregation of flows from Chapters 2 and 3.

In Chapter 5, a decision support tool in Riverware (Zagona et al., 2001) will be presented. This is a modification of the Aspinnall Unit operations developed by Regonda (2006). The key change is the development of operational rules to meet the RFF. The monthly flow scenarios generated from the previous chapter will be used to drive this decision support tool. This will provide scenarios of hydropower generation, pool elevations, and fish flow violations and the consequent risk estimates. This information illustrates the benefit from stochastic traces in providing guidance when making necessary modifications to operating policies.

Chapter 6 will provide an overall summary of the work, addressing both the techniques used and results from Riverware modeling. This section will also provide recommendations for future work and improvements.

## **CHAPTER 2: DEVELOPMENT OF STOCHASTIC FLOW SEQUENCES BASED ON OBSERVED DATA**

### **2.1 Introduction**

Devising effective water resources and flood plain management strategies require a realistic estimation of the risk of various streamflow related events. As mentioned earlier, when assessing the Aspinall Unit operations under the new strains of fish flow requirements, it is important to model the system under a variety of plausible flow scenarios – especially extreme conditions beyond what has been observed. This requires a tool that can generate realistic flow scenarios that are statistically similar to the observed data but provide a rich flow sequence variety.

Several stochastic techniques have been developed and prevalent among them are traditional (parametric) linear stochastic techniques in an Auto Regressive Moving Average (ARMA) regression framework (Thomas and Fiering, 1962; Salas et al., 1982, Harms and Campbell, 1967). Recently, nonparametric techniques have been developed that are versatile and simple, and seem to provide an attractive alternative (Lall and Sharma, 1996; Prairie et al., 2006; Sharma et al., 1997). Another method most widely used in practice is resampling chunks of historical data – i.e., Index Sequential Method (ISM) (Ouarda et al., 1997).

In this chapter, the objective is to apply the above suite of techniques to streamflow generation at USGS gauge number 09152500 in the Gunnison River Basin, a key gauge in the basin for the EIS analysis. The observed data are available for the period 1906 –2005, as natural flow from the U.S. Bureau of Reclamation (USBR) (Prairie and Callejo, 2005). The above mentioned techniques are assessed for their ability to capture a variety of statistics while also attempting to generate

longer periods of drought and surplus. A background on the stochastic streamflow generation is provided, followed by a brief description of four generation techniques – (i) ARMA, (ii) K-Nearest Neighbor (KNN) Bootstrap, (iii) Modified KNN (iv) ISM – widely used by USBR. The statistics used for comparison are then presented, followed by the results from the simulations and discussion.

## 2.2 Background

Given a time series  $X_t, t = 1, 2, \dots, N$ , a typical time series model is of the form

$$X_t = f(X_{t-1}, X_{t-2}, \dots, X_{t-p}) + Z_t$$

**Equation 1**

where  $Z_t$  is the model error (or residual) that is assumed to be normally distributed with a mean of 0 and variance  $\sigma^2$ . If the function  $f$  is linear and fitted to the entire data set, then the above form is an Auto Regressive (AR) model and all aspects of regression theory apply (Loucks et al., 1981, Chatfield, 2004). The function  $f$ , as can be seen in Equation 1, captures the time dependency in the time series. If there are random jumps (i.e., financial time series) in the data in addition to time dependency, then the above model is modified to Equation 2.

$$X_t = f(X_{t-1}, X_{t-2}, \dots, X_{t-p}, Z_{t-1}, \dots, Z_{t-q}) + Z_t$$

**Equation 2**

If  $f$  is linear and fitted to the entire data set, then it is an Auto Regressive Moving Average (ARMA). The inclusion of past residuals captures the shock component, and the past time series value captures that dependency. The order ‘p’ and ‘q’ have to be appropriately estimated from the data. The ARMA framework (Loucks et al., 1981, Chatfield, 2004) is the staple of hydrologic time series modeling.

While this framework is easy and has a rich background from linear regression theory, it has several drawbacks. Chiefly, (i) the function  $f$  is linear and fitted globally to the entire data – so any global or local nonlinearities that might be present in the data cannot be captured, (ii) the model assumes the data to be normally distributed - if not, the data must be transformed to normality before model fitting – which can be quite difficult in practice and (iii) statistics modeled and captured in the transformed space are not guaranteed to be captured in the original space when they are back-transformed

Nonparametric techniques, which estimate the function  $f$  ‘locally’ at each point, provide an attractive alternative by offering a data-driven and flexible approach (Lall, 1995). There are several nonparametric approaches (see Lall, 1995 for an overview), but the general philosophy is to identify a ‘locale’ or ‘neighborhood’ around the current ‘feature’ and then either fit a function to the points (Prairie et al., 2005) in the neighborhood or resample from them (Lall and Sharma, 1996). The local estimation provides the capability to capture any arbitrary features present in the data. These techniques can be viewed as variations of a block bootstrap of the observed data, also known as Index Sequential Method (ISM) (Ouarda et al., 1997). This very simple approach is widely used by the Bureau of Reclamation. These methods are further described in the following section.

## **2.3 Description of Stochastic Methods**

### **2.3.1 ARMA**

As mentioned earlier, the ARMA framework is the staple of traditional time series analysis as well as hydrologic time series modeling. The linear form of this model is given as:

$$X_t = \alpha_1 X_{t-1} + \dots + \alpha_p X_{t-p} + Z_t + \beta_0 Z_t + \beta_1 Z_{t-1} + \dots + \beta_q Z_{t-q}$$

**Equation 3**

where  $p$  and  $q$  represent the model order,  $\alpha$  the AR coefficients,  $\beta$  the MA coefficients and  $\sigma^2$  the error variance. The method of moments or maximum likelihood technique (Chatfield, 2004) is used to estimate  $\alpha$  and  $\beta$  from the data. Typically, objective criteria such as Akaike Information Criterion (AIC) are used to identify the optimal model order (e.g., AR1MA1, AR2MA1). Visual inspection of the Auto Correlation Function (ACF) and Partial Auto Correlation Function (PACF) can also help provide insights into the model order. From theory (Loucks et al., 1981; Chatfield et al. 2004), an AR model of order ( $p$ ) is appropriate if the PACF of the time series is insignificant beyond lag  $p$ . Likewise, a MA model of order ( $q$ ) is appropriate if the ACF of the time series is insignificant beyond lag  $q$ . For annual streamflow at USGS gauge number 09152500, the ACF and PACF are shown in Figure 4. From the PACF it can be seen that an AR-1 model is adequate.

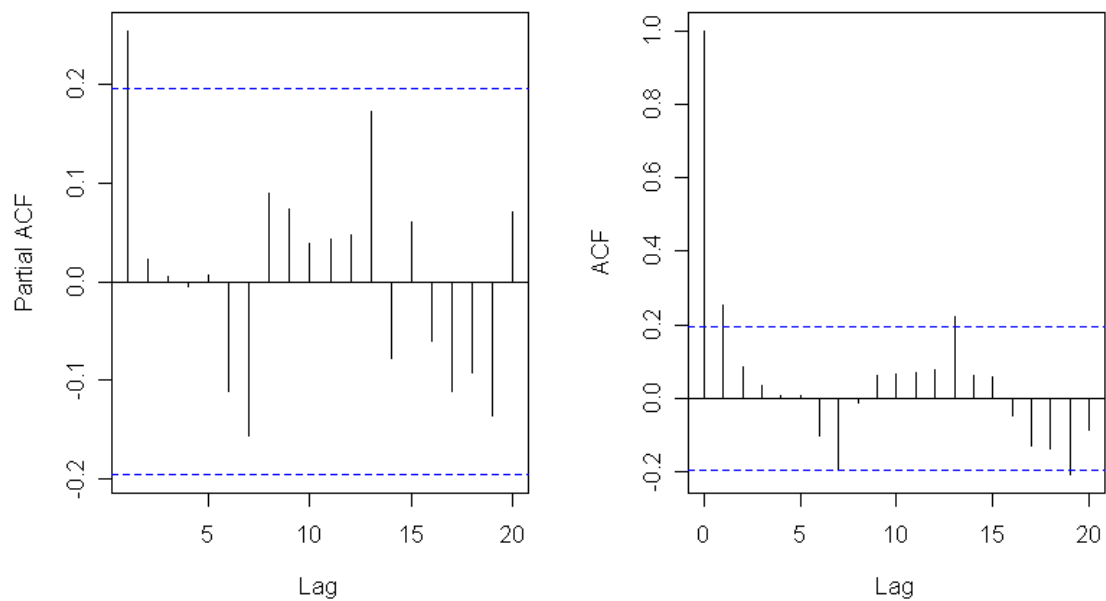


**Figure 4 PACF (left) and ACF (right) for USGS gauge number 09152500 from 1906-2005.**

Thus, the AR(1) model for this data is:

$$X_t = \alpha X_{t-1} + Z_t$$

Equation 4

### 2.3.2 ISM

The Index Sequential Method (ISM) (Ouarda et al., 1997) uses a sequential block bootstrap of the observed data in order to generate flow sequences. Each sequence is of the desired simulation length (in this case, 30 years). For 100 years of data, we can have 100 blocks of 30-year sequences (when the end of the data record is reached it is wrapped around to the start of the record). To illustrate, the first sequence will be data from 1906 to 1935; the second from 1907 to 1936, and so on; the last sequence will be data of 2005 along with 1906 to 1934. By re-sampling the observed data in sequential 30 year blocks (1906-1935, 1907-1936, etc.) with wrapping (i.e., 2005-1934), ISM can potentially generate events longer than that of the observed. While this method is simple to implement and captures all the statistics and features of the observed data quite well (by design), it is limited to 100 specific sequences, most of which are seen in the observed data.

### 2.3.3 K-Nearest Neighbor Time Series Resampling

The KNN bootstrap technique (Lall and Sharma, 1996) is a modification of the ISM. Rather than selecting an entire (30-year) block at once, the trace is generated one year at a time. As a result, a key difference between the two methods is that unlike ISM, where only the observed year sequences can be obtained, KNN can generate a variety of sequences. This technique has been applied to multivariate, multi-site, daily weather generation (Rajagopalan and Lall, 1999; Yates et al., 2003).

The implementation algorithm of the lag-1 KNN time series resampling technique is described below.

(i) Begin by randomly selecting a year, say,  $t$ , with corresponding flow  $x_t$ .

(ii) Next, the  $K$  number of nearest neighbors of  $x_t$  are identified from the historical observations. The value of  $K$  is typically the square root of the length of the historic data. This choice has been found to work well in previous studies (Lall and Sharma, 1996). Note that the nearest neighbors are a set of historical years.

(iii) Weights are assigned to each of the  $K$  neighbors – with highest weight to the nearest neighbor and least to the farthest. Lall and Sharma (1996) have shown that weight function choice has little impact on results.

(iv) One of the neighbors (a historic year) is randomly selected using the weight function, say, year  $j$ . The flow corresponding to year  $j+1$ ,  $x_{j+1}$ , becomes the simulated flow for the second year.

(v) Steps ii through iv are repeated to obtain the desired number of flow sequences.

This process is depicted in Figure 5.

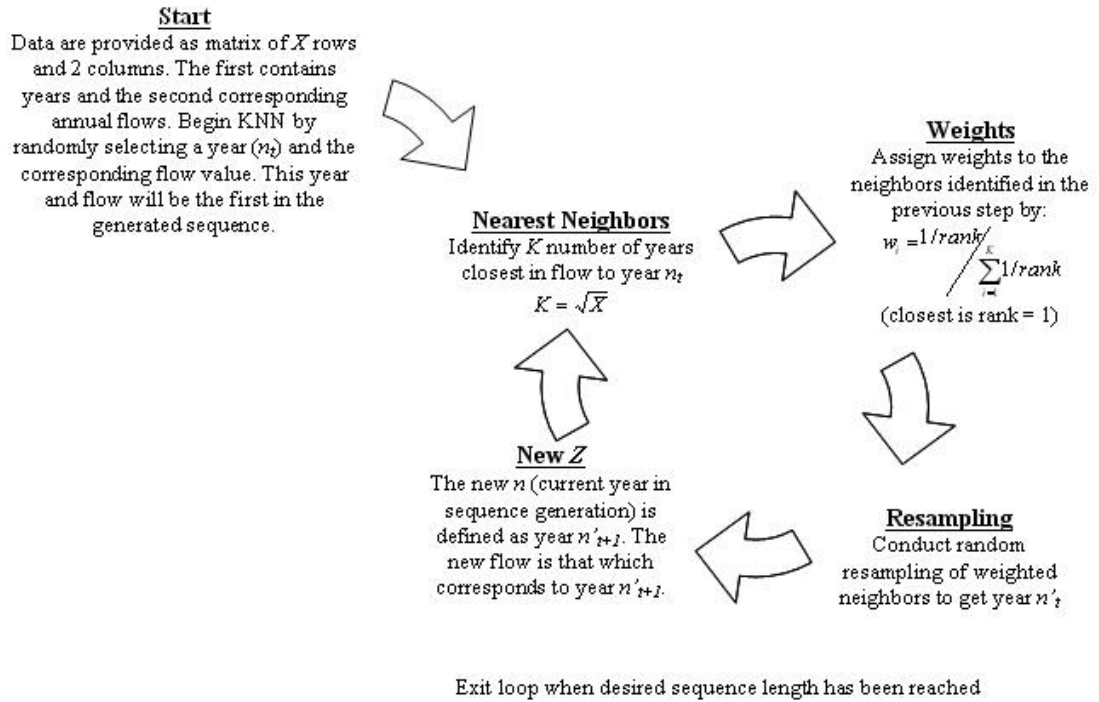


Figure 5 Lag-1 KNN technique.

The following is a KNN lag-1 example, based on Figure 5.

**Example data (X=16):**

Year	Flow (acre-ft/yr)
1950	844.8
1951	1375.4
1952	1039.8
1953	1124.5
1954	1310.4
1955	728.0
1956	646.5
1957	1077.5
1958	1229.5
1959	1432.8
1960	1472.1
1961	927.9
1962	1065.3
1963	819.0
1964	1373.2
1965	524.1

- (i) Select a year at random to be the first year in the generated sequence. Say, current year ( $t$ ) = 1956 (646.acre-ft/yr)

**Generated sequence (so far):**

Year Number	Year	Flow (acre-ft/yr)
1	1956	646.5
2		

(ii) Identify  $K$  nearest neighbors to year 1956 based on flow ( $K = \sqrt{X}$ ,  $K=4$ )

(Note: 1965 is one of the 4 closest neighbors, but cannot be selected because there is no flow information after 1965)

**Neighbors for 1956:**

Rank	Year	Flow (acre-ft/yr)	Delta
1	1956	646.5	0
2	1955	728.0	81.5
3	1963	819.0	172.5
4	1950	844.8	198.3

(iii) Assign weights to neighbors by:

$$w_i = \frac{1/\text{rank}_i}{\sum_{i=1}^K 1/\text{rank}_i}$$

(iv) Conduct a random resampling of the weighted neighbors to obtain a single neighbor for this iteration ( $j$ ). Say  $j=1963$  in this case. The next year in the generated sequence is year  $j+1$  (1964), and its corresponding flow.

**Generated sequence (so far):**

Year Number	Year	Flow (acre-ft/yr)
1	1956	646.5
2	1964	1373.2
3		

(v) 1964 now becomes the current year ( $t$ ) and steps 2-6 are repeated until the desired sequence length is reached.

### 2.3.4 Modified KNN

One of the aspects of the KNN resampling approach is that no new values can be generated – which might be desired by some users and applications. To address this, Prairie et al. (2006) proposed a modification of the KNN resampling approach. The methodology is abstracted from Prairie et al. (2006) and described below.

(i). A local polynomial is fit for each month dependent on the previous month (as in Figure 6):

$$y_t = g(y_{t-1}) + e_t$$

#### Equation 5

where  $g(y_{t-1})$  = local polynomial fitted as described above.

(ii). The residuals ( $e_t$ ) from the fit are saved.

(iii). Once we have the simulated value of the flow for the current month ( $y_{t-1}^*$ ), we estimate the mean flow of the next month ( $\hat{y}_t^*$ ) from Equation 5, not including the residual.

(iv). KNN of  $y_{t-1}^*$  (these are highlighted in Figure 6) are obtained.

(v). The neighbors are weighted using the following weight function.

$$W(i) = \frac{1/i}{(\sum_{i=1}^K 1/i)}$$

#### Equation 6

This weight function gives more weight to the nearest neighbor and less weight to the farthest neighbor. The weights are normalized to create a probability mass function or “weight metric.” Other weight functions with the same philosophy (i.e., more

weights to nearest neighbors and lesser weights to farther neighbors) can be used as well. Little or no sensitivity was found to the choice of the weight function.

(vi). One of the neighbors is resampled using the “weight metric” obtained from Equation 5, above. Consequently, its residual ( $e_t^*$ ) is added to the mean estimate ( $\hat{y}_t^*$ ). Thus, the simulated value for the next timestep becomes:

$$y_t^* = \hat{y}_t^* + e_t^*$$

**Equation 7**

(vii). Steps (i)–(vi) are repeated for other months to obtain an ensemble of simulations. The output from steps (i) and (ii) can be saved for each month and used for successive years.

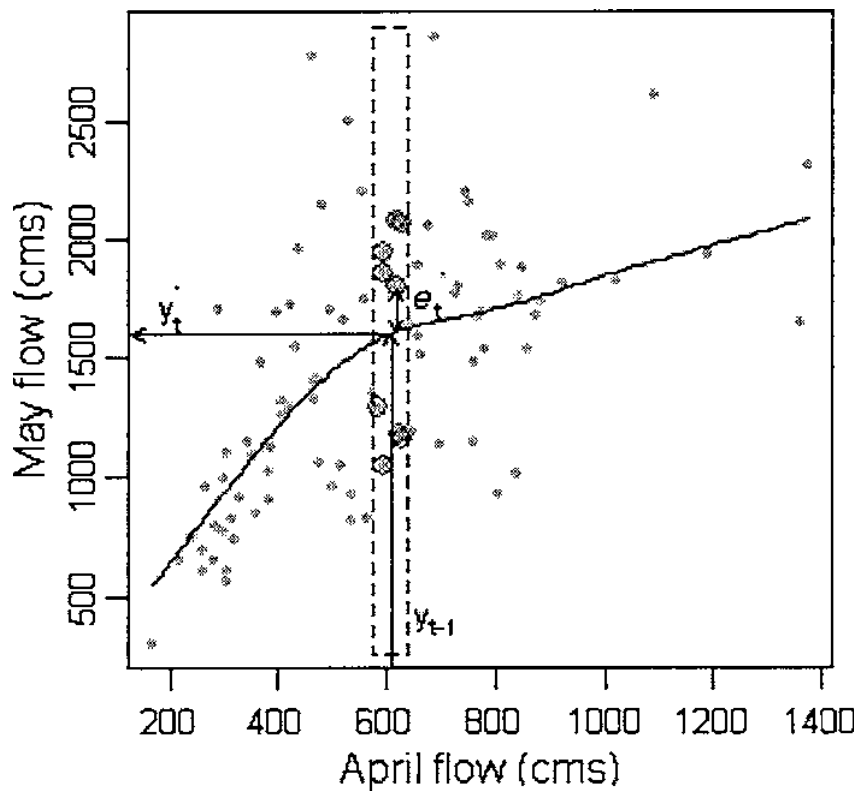


Figure 6 Modified KNN. (source: Prairie et al., 2006)

## 2.4 Evaluation of Methods

A suite of statistics are computed from the simulations, compared against that of the historic data and presented as boxplots. The ‘box’ in the boxplot represents the interquartile range, the horizontal line inside the box is the median, the whiskers correspond to the 5th and 95th percentiles and values beyond the whiskers are shown as points. The value of a statistic computed from the historical data is shown as a dashed red line. When the observed statistic lies within the interquartile range, it can be inferred that the simulations adequately capture the statistic.

The distributional statistics computed are mean, standard deviation, coefficient of skew, lag-1 correlation, maximum and minimum. In addition, probability density functions (PDFs) of the simulations are provided.

For the KNN, Modified KNN and AR-1 methods described earlier, 1,000 simulations, 30 years in length were generated. For ISM, however, traces are limited to 100 simulations, the length of historical data. All the methods reproduce the mean and standard deviation (Figure 7). The ISM produces a limited range of mean and standard deviations – this is because its simulations are restricted to the observed sequence.

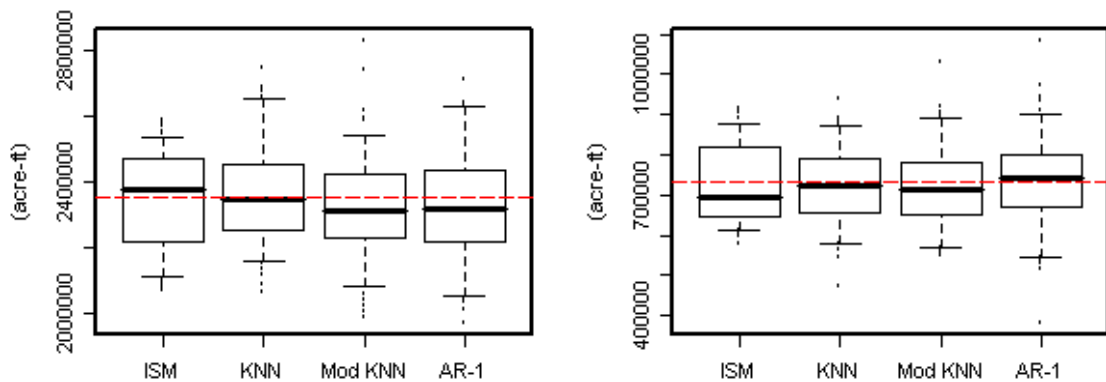


**Figure 7 Mean (left) and standard deviation (right) for 100 simulations.**

It should be noted that bootstrap techniques such as KNN are sensitive to the number of simulations, i.e., sampling variability (Efron, 1982). To placate concerns regarding the decision to generate 1,000 traces, simulations of several sizes were generated - 10 through 10,000 and the median for each was computed, shown as boxplots (Figure 8). The interquartile ranges and whiskers are almost identical for simulations of more than 100, and the outlier range begins to stabilize for runs with 250 to 1000 simulations. There is, however, a slight increase in the range of outliers when 10,000 simulations are generated. This can always be expected when more simulations are generated, and furthermore, these values represent less than 0.5% of the all the simulated traces, which is not overly significant. This exercise suggests that 1,000 simulations is a sufficient number to address sampling variability. Consequently, comparisons are provided for the three methods – AR1, KNN and Modified KNN.

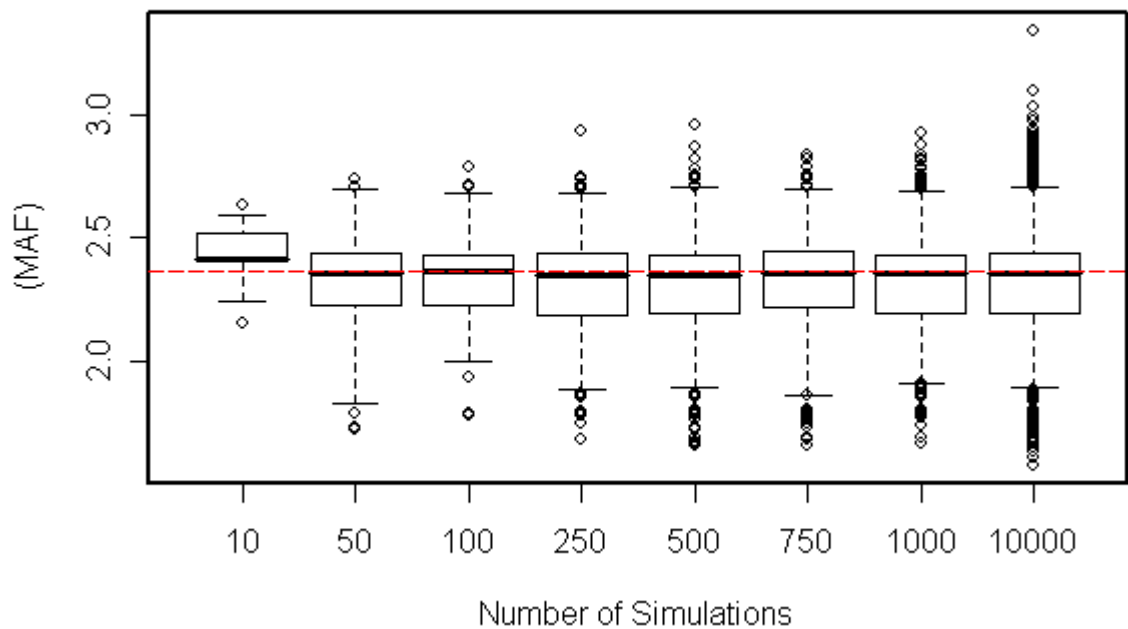


**Figure 8 Median annual flow for various numbers of simulations using KNN.**

For water resources management, particularly reservoir operations, periods of drought and surplus are critical for system reliability – therefore, a suite of spell statistics are computed and depicted in Figure 9. For the work that follows, a drought period is simply a series of consecutive years for which all flows are less than the observed median value. A drought deficit refers to the difference in water volume between median flow for the length of the drought and the actual volume of water for that period, or how much water it would take to bring all years in a drought to median flow. Likewise, a surplus period is consecutive years for which annual flows are above the median. The volume of water above the median flow for that time is termed a surplus.

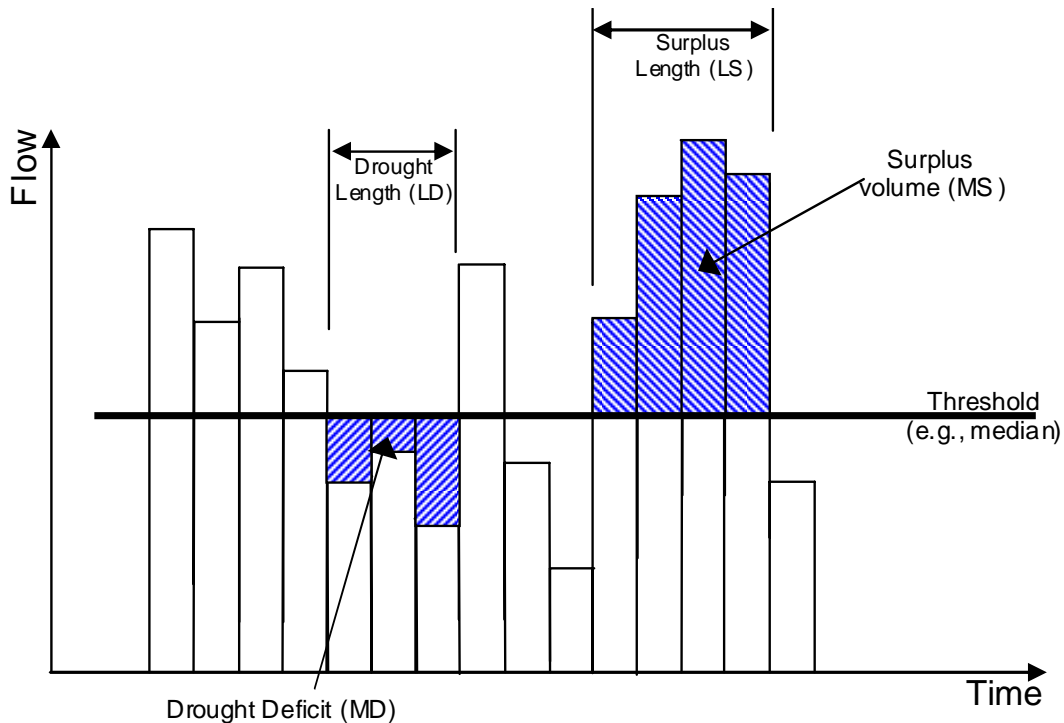


**Figure 9 Definition of surplus and drought statistics.**

As would be expected, it is important to assess both the length and magnitude of these drought/surplus periods. For example, a 10 year drought can seem rather

severe, but if all of those years are just slightly below the drought/surplus threshold, the impact on reservoir operations is most likely small. Conversely, a 3 year drought with significantly reduced inflow can strain even the largest of reservoirs quickly. Thus, histograms of drought/surplus and length/magnitude are provided for all simulation methods.

## **2.5 Results**

All the methods capture the mean, standard deviation and lag-1 auto correlation very well. The nonparametric methods capture the skew well, but the AR-1 method under-simulates this statistic. This is because the AR method generates a normal distribution which has a skew of zero, whereas, the nonparametric methods are data driven. The nonparametric KNN method cannot generate values outside the maximum and minimum of the observed data, while the modified KNN and AR-1 can (Figure 10). However, the nonparametric methods capture the non-normality feature of the observed data very well, but the AR-1 method reproduces a normal distribution (Figure 11). This is one key advantage of the nonparametric techniques.

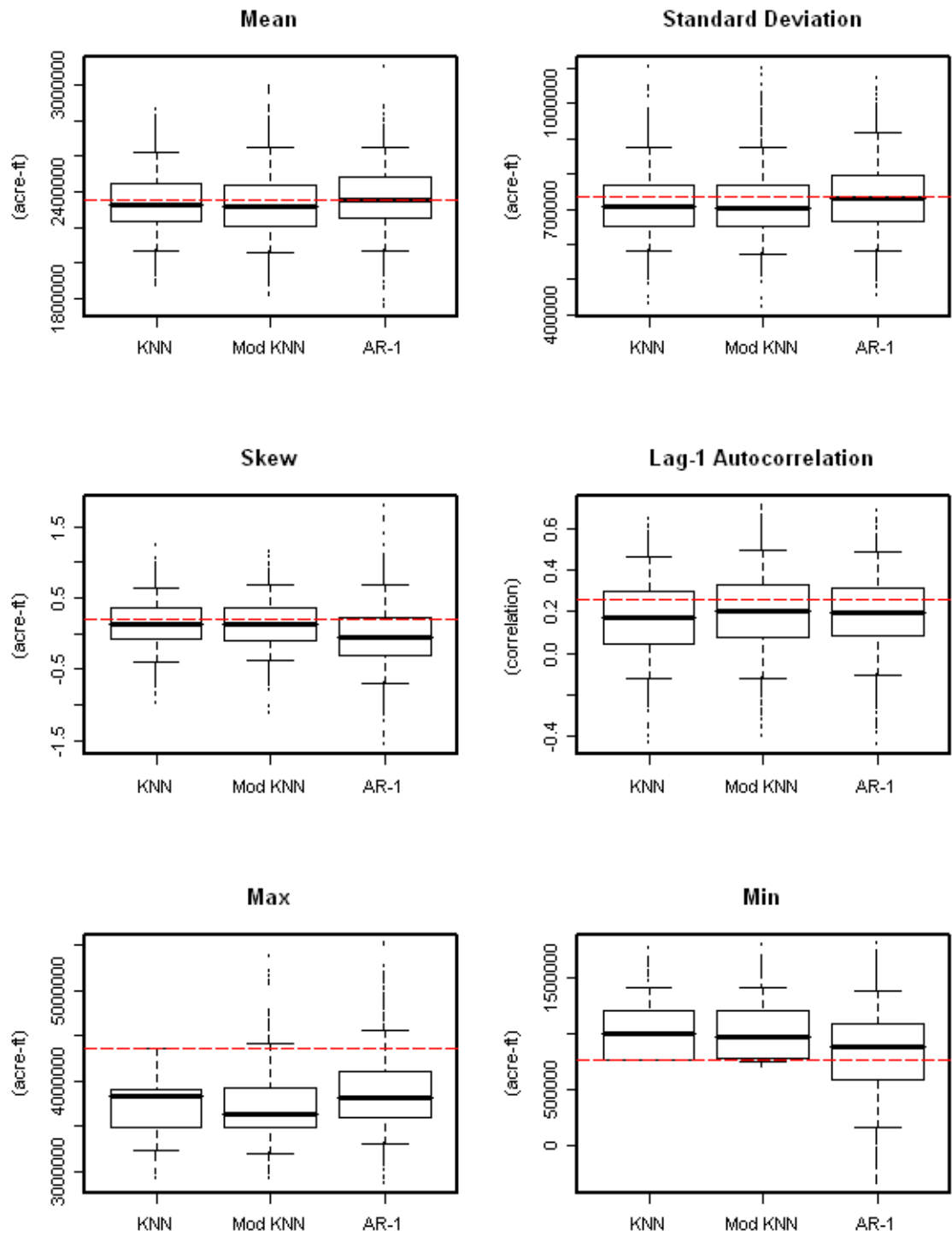


**Figure 10** Distributional statistics for KNN, Modified KNN and AR-1 traces.

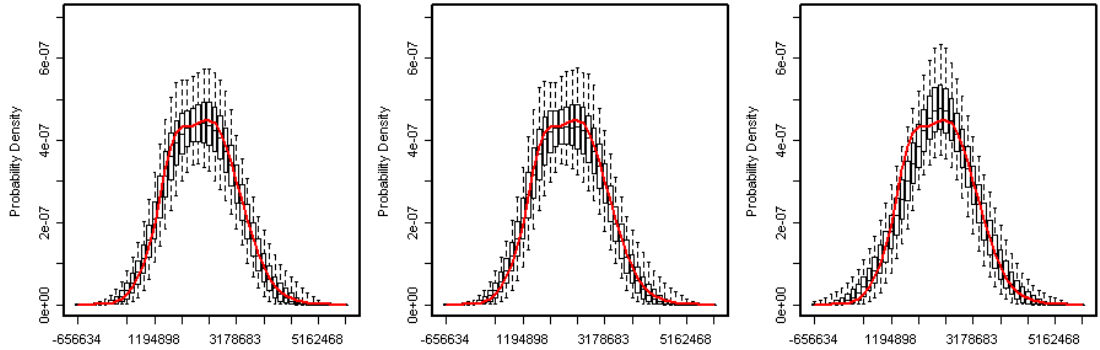


**Figure 11 Annual Flow PDFs (acre-ft/yr) of KNN (left), Modified KNN (center) and AR-1 (right). The red line depicts the observed PDF.**

Figure 12 shows the surplus length distributions of the three methods. All three techniques show periods of surplus longer than that of the observed (6 years), albeit with somewhat low probability. The two KNN-based methods show almost identical surplus distributions. This is logical, as they are both effectively bootstraps of the observed data. The spells from AR-1 show reduced probability, especially at lower spell lengths. Similar observation can be made for the drought length (Figure 13), surplus volume (Figure 14) and deficit volumes (Figure 15). For comparison, the observed surplus and drought histograms are provided (Figure 16 and Figure 17). While the observed drought and surplus values are clearly exceeded by the techniques put forth, it is with limited probability. The non parametric techniques show approximately 2% probability of exceeding the max observed event for drought and surplus. The AR model has slightly higher probabilities (roughly 3.3%).

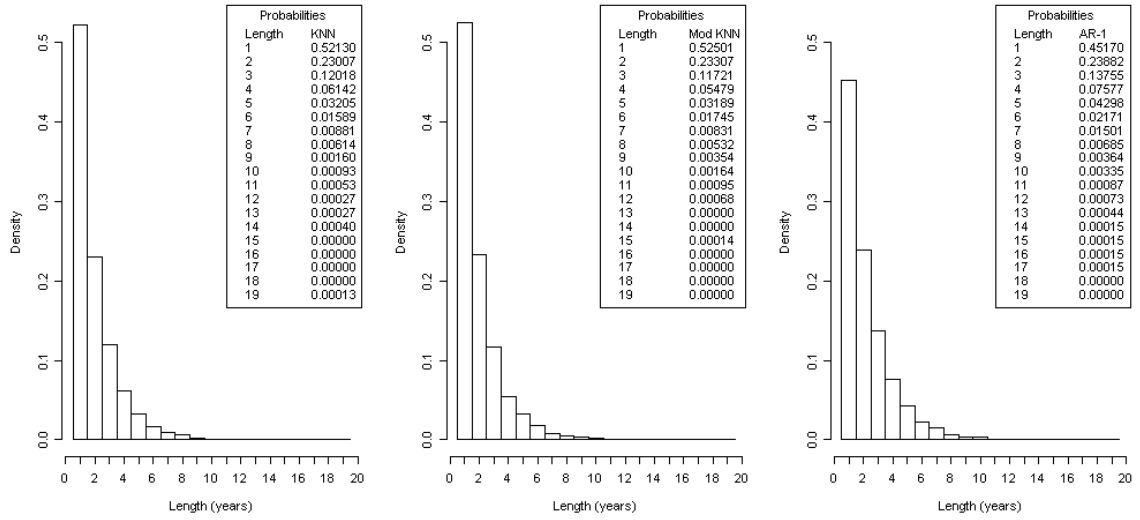


Figure 12 Surplus length histograms. KNN (left), Modified KNN (center) and AR-1 (right).

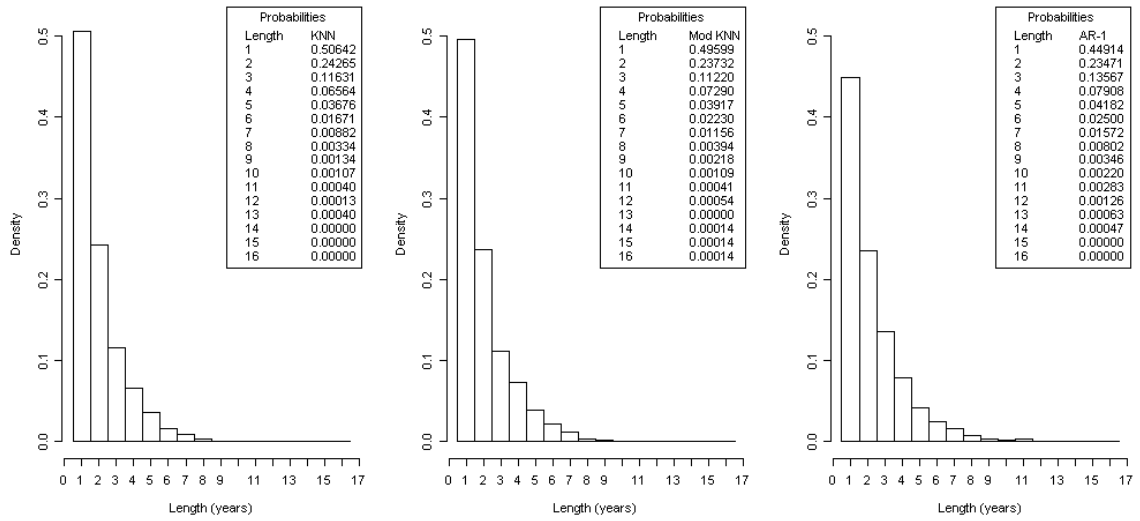
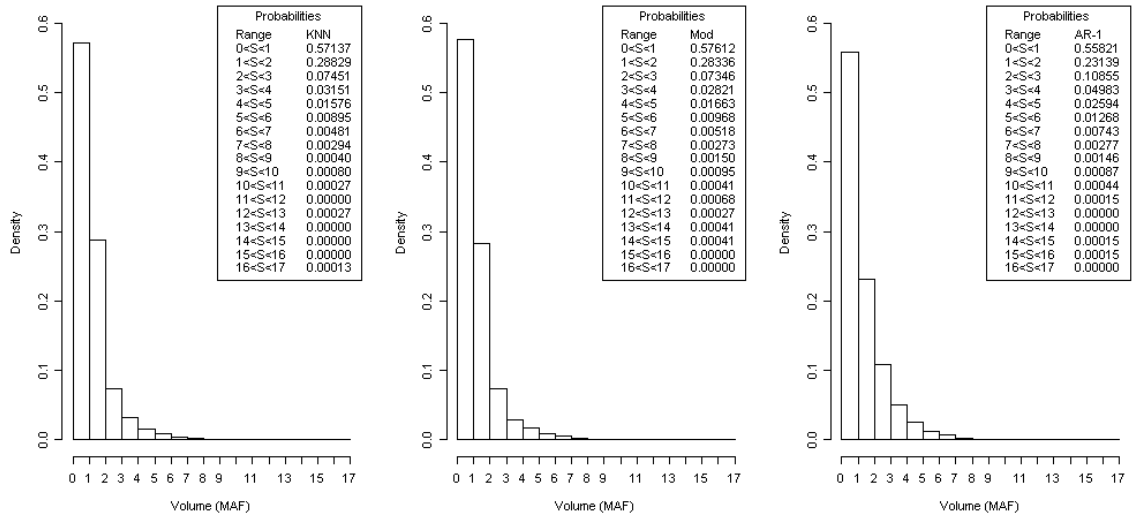
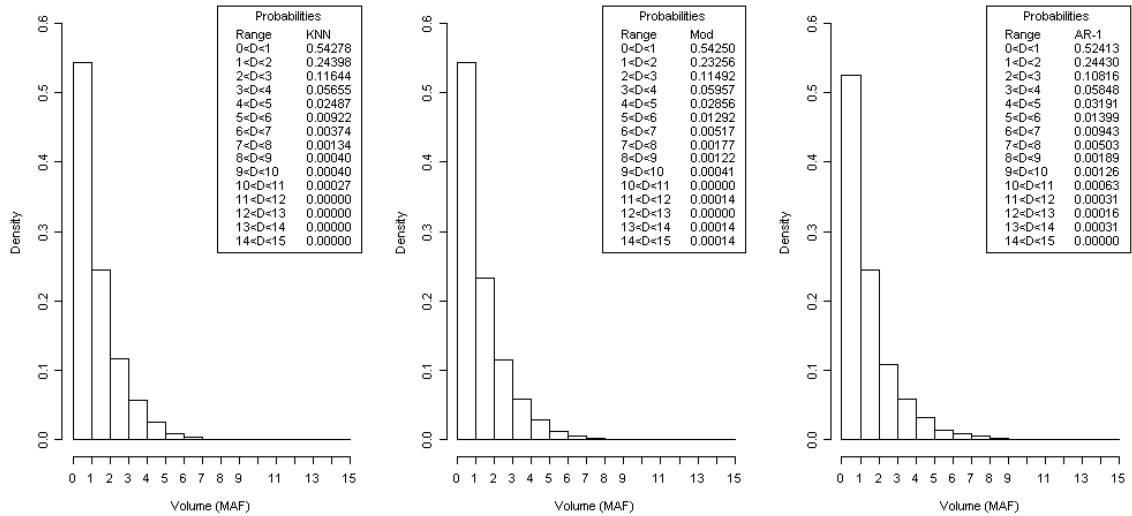


Figure 13 Drought length histograms. KNN (left), Modified KNN (center) and AR-1 (right).



**Figure 14 Surplus volume histograms. KNN (left), Modified KNN (center) and AR-1 (right).**



**Figure 15 Drought deficit histograms. KNN (left), Modified KNN (center) and AR-1 (right).**

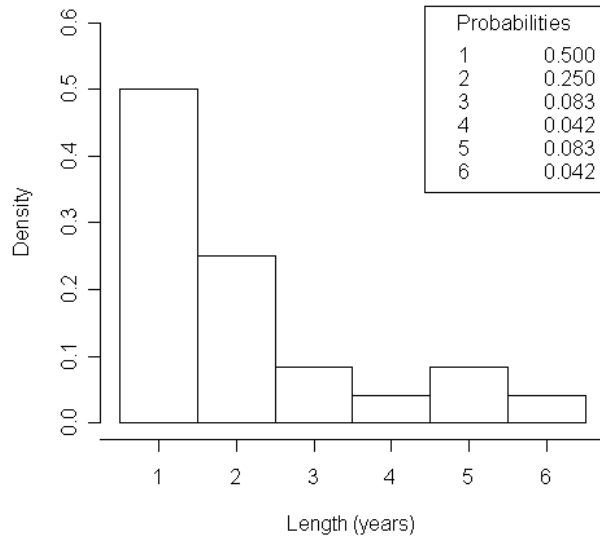


**Figure 16 Observed drought histogram**

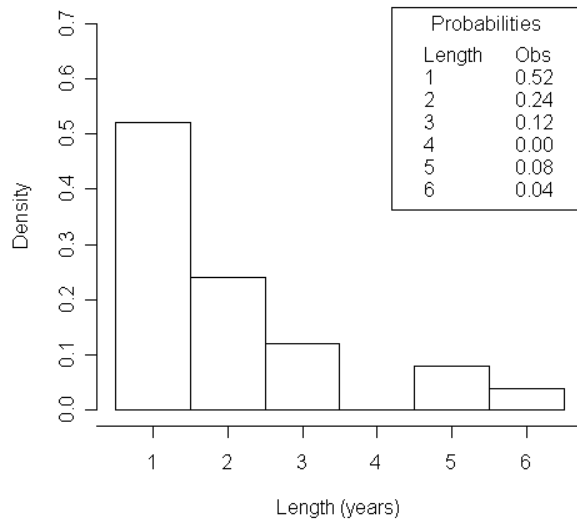


**Figure 17 Observed surplus histogram**

## 2.6 System Risk

The drought and surplus statistics described above are sensitive to the threshold (in this case the long-term median flow) choice. This is somewhat subjective, especially since the metric changes as the observed data set grows with time. An alternate method to quantify water availability is considered. Termed the sequent peak algorithm (Loucks et al., 1981), this approach quantifies the storage capacity needed to meet different demands for a given flow sequence. As a result, this method obviates the need to define a drought threshold, and instead provides a

robust system-wide measure of the ability to meet demands. The following briefly describes implementation of this technique:

$$S_i^i = \begin{cases} S_{i-1}^i + d - y_i \\ 0 \end{cases}$$
$$S_c = \max[S_1^i, \dots, S_N^i]$$

$S_i$  is the storage at timestep  $i$ ,  $d$  is the demand or yield,  $y_i$  is the streamflow from a sequence at time  $i$ , and  $S_c$  is the storage capacity. This algorithm is also widely used for designing reservoir capacities.

Storage is computed for each demand level for each simulated sequence, resulting in boxplots shown in Figure 18. It can be seen that all three methods provide considerable variability in the storage, as to be expected. The combined live storage of the Aspinall Unit and Taylor Park is approximately 1.07 MAF (Western, 2007; United States, 2004) and is shown by a red dashed line for reference. For a system demand of 1.65 MAF, the storage requirement for the observed trace is almost exactly 1.07 MAF, suggesting 100% reliability. However, both nonparametric simulations show about 25% of storage requirements are above 1.07 MAF, suggesting only 75% reliability. This variability from the KNN simulations can provide a better estimate of the system reliability, which is important in management decisions. Last, AR-1 shows about 50% reliability for a demand of 1.65 MAF, given the available storage. This is a result of the skew toward smaller flow values, and thus, may not be completely appropriate for management of the Aspinall Unit. Figure 19 shows PDFs of required storage to meet the demand of 1.65 MAF.

The sequent peak method assumes a static demand that must be met each year. From that point of view, it provides an overly simplistic model of reservoir operations

and results in a conservative estimate of storage requirements. To gain further insight into reliability of various system components, the simulations should be used to drive a decision support model that incorporates the complexity of reservoir operation.

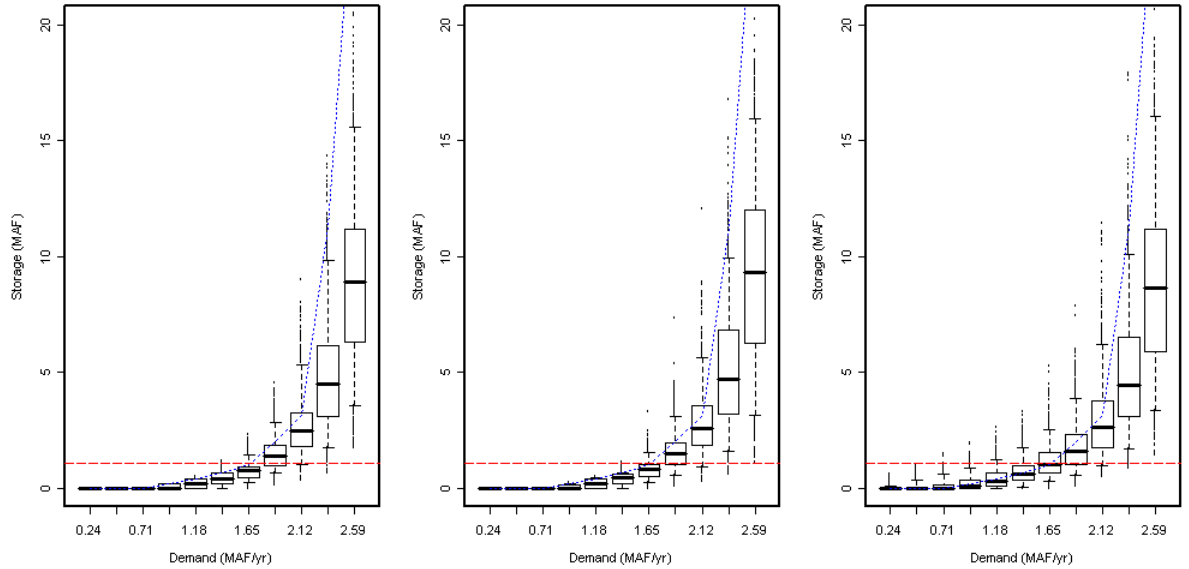


**Figure 18** Sequent peak algorithm. KNN (left), Modified KNN (center) and AR-1 (right).

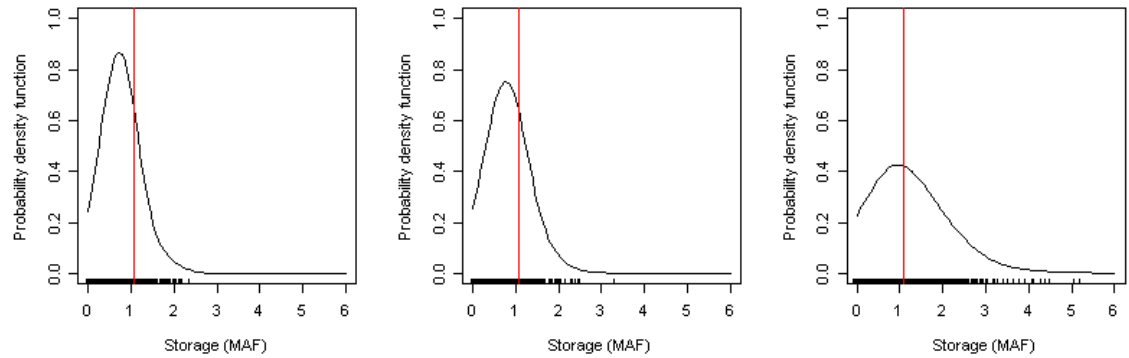


**Figure 19** PDFs of storage required to meet a demand of 1.65 MAF. The red vertical line represents the live storage capacity of the Gunnison Basin. KNN (left), Modified KNN (center) and AR-1 (right).

## 2.6 Summary and Discussion

The purpose of investigating a variety of modeling techniques is undoubtedly to generate more varied traces beyond that of the commonly used ISM. Equally important to introducing increased variability is proper model selection. Thus, by these two criteria, both KNN approaches provide a satisfactory combination of

statistical validation and variance. The advantage of the traditional KNN approach is that it is simpler to implement, as it only resamples the observed values. This ensures that the magnitudes are all realistic, because they have been documented in past years. While this may not seem overly significant, it may prove crucial in convincing skeptical managers and stakeholders to consider “new” techniques. The Modified KNN does not have these benefits; in fact, its strength over the traditional approach lies in the ability to introduce more variability by simulating previously unseen values. Clearly, this may be perceived as either advantageous or a drawback, depending on the purpose and goals of the work.

In conclusion, the nonparametric stochastic techniques investigated in this chapter have proven superior compared to traditional approaches such as an AR-1 model. Model selection, however, is impacted not only by the effectiveness of meeting goals, but also by the intended audience.

## **CHAPTER 3: DEVELOPMENT OF STOCHASTIC FLOW SEQUENCES BASED ON OBSERVED AND PALEO DATA**

### **3.1 Introduction**

The Gunnison River Basin experienced the worst drought on record during 2000-2004. This event impacted the entire Colorado Basin and raised serious concerns regarding water availability and quality over much of the western United States. Since this period was one of the severe droughts in recorded history, many water managers wondered if this was perhaps an anomaly that should have little impact on basin operations and management. However, paleo reconstructions of streamflow for the pre-observational period in the basins show droughts of greater magnitude and duration with higher frequency, indicating that the recent drought is not unusual. While the system was able to withstand the recent dry period and all major water delivery obligations were met, insight from paleo data will help provide water managers with better estimates of system risk and consequently, lead to better management strategies in the future. Clearly, this calls for combining the rich information provided by paleo reconstructions with the observed streamflow record in stochastic models, enabling the generation of realistic flow scenarios required for robust water resources planning and management. To this end, Chapter 3 proposes several techniques for such a combination, followed by an evaluation of the stochastic flow simulations.

Paleo reconstructed flows utilized in this work were developed by Woodhouse et al. (2006) at USGS gauge number 09152500 for the period of 1569-1997, and they are used along with the natural (observed) streamflow (Prairie and Callejo, 2005) for the 1906-2005 period. Four methods are examined that combine these two data sets,

capitalizing on their individual strengths to produce robust flow sequences. The central aspect of these methods is the use of hydrologic state (i.e., wet or dry) sequencing from the paleo reconstructions and magnitudes from the observed data. The rationale for this is discussed in the follow sections. Streamflow traces are generated using these techniques and are evaluated on their ability to capture a suite of statistics, while extending drought and surplus attributes beyond the observed range. The investigation concludes with a summary of the results and identification of a recommended technique.

### **3.2 Paleo Data**

Paleo reconstructed flow data are generally created by fitting a regression model to observed flow values and the corresponding portion of tree ring cores. This provides a relationship between tree ring growth and streamflow, allowing for the back-extrapolation of flows as far as the core samples permit. The outcome of the reconstruction is dependant upon a number of choices made throughout the process – site and species selection are chief among them (Hidalgo et al., 2000). An ideal site has a variety of tree species that provide sensitivity to both wet and dry periods, displayed by tree ring growth. In addition to site and species choice, model selection to represent the streamflow-ring growth relationship greatly impacts the reconstructions. This is illustrated in Figure 20, where four reconstructions (indicated in the figure) for the Colorado River at Lee’s Ferry, AZ gauge are presented. Reconstruction variability is mainly due to the factors mentioned above. In this case, the reconstructions completed by Hidalgo et al. (2000) differ significantly from the rest. This variability and the fact that regression based reconstructions do not capture

the entire variability have resulted in a reluctance to use these reconstructed flows for water management purposes.

Nevertheless, the reconstructions agree quite well on the hydrologic state (i.e., a wet or dry) in any year – as can be seen in Figure 20. Defining the wet and dry year based on a threshold of the observed median flow, the states from the reconstructions are shown in Figure 21. Analysis of the data in Figure 21 shows that three or more reconstructions agree on the hydrologic state 88% of the time, while all four methods agree 65% of the time on an annual basis. This is a clear indication that the paleo reconstructions are quite good at providing the hydrologic state information. Thus, a combination of the two data sets entails using the state information from the reconstructed period and the magnitude information from the observed record. This forms the rationale for the methods proposed in this chapter below.

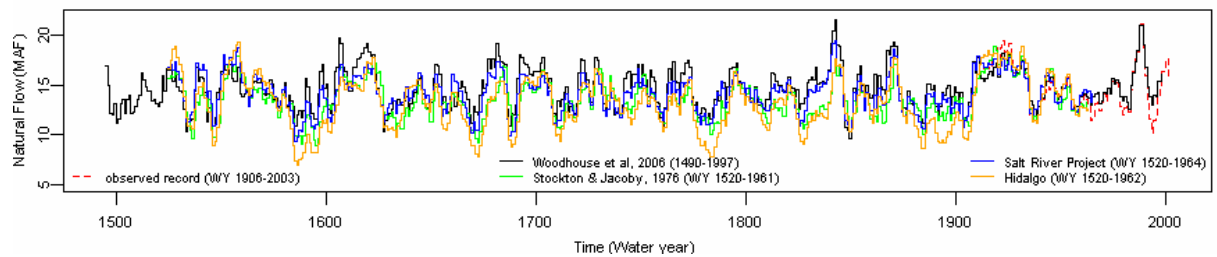


**Figure 20 Paleo reconstructed flows for the Colorado River at Lee's Ferry, AZ.**

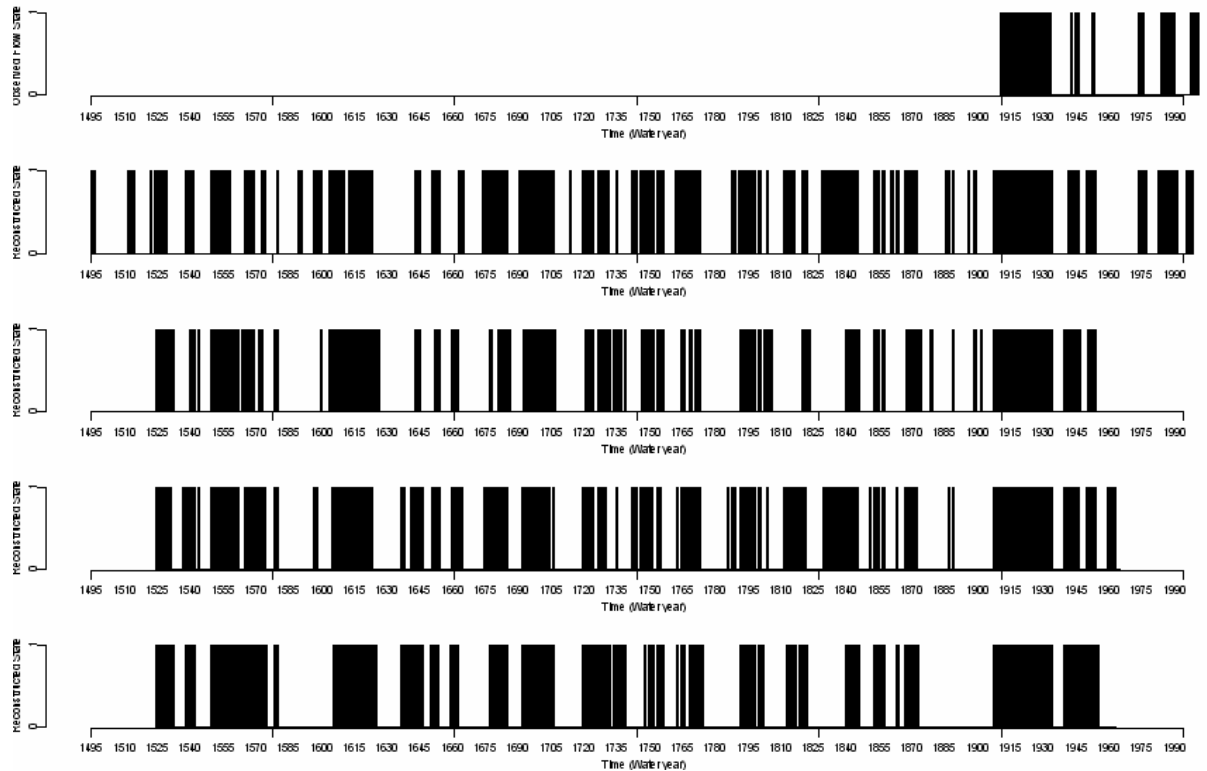


**Figure 21** Wet/dry state time series for observed data (top) and four paleo reconstructions.

Woodhouse et al. (2006) completed the reconstructions used in this work for the Gunnison River near Grand Junction, CO (USGS gauge 09152500) for the period 1569 to 1997 shown in Figure 22.

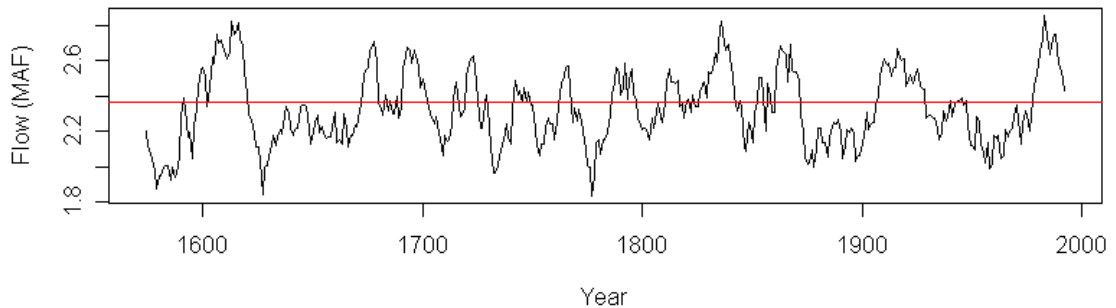


**Figure 22** Paleo reconstructed flows for Gunnison River near Grand Junction, CO with 5-year smoothing.

### 3.2 Methods

As previously stated, the methods considered here involve two steps – (i) model/simulate the hydrologic state and (ii) model/simulate the streamflow

magnitude. The median flow of the 100 year observed period is used as the threshold to define the wet (1) or dry(0) state – this is approach is widely used by a number of groups, including the United States Bureau of Reclamation (USBR). Upon obtaining the binary state sequence ( $S_t, t = 1, 2, ..N$ ) of the paleo record, four techniques are applied to model the state sequence; (1) block resampling of the binary, (2) homogeneous Markov model, (3) block homogeneous Markov model and (4) non-homogeneous Markov model. These methods are used to generate hydrologic state sequences for a desired length (in this case 30 years), followed by a K-Nearest Neighbor (KNN) resampling of the observed flows to assign magnitudes. The process in which the binary traces are generated distinguishes one method from another. These methods are described below.

### **3.2.1 Block Resampling (Block)**

This is the most basic approach, which selects a random block of 30 years and the associated hydrologic state information is selected (i.e., bootstrapped) from the paleo record. The resampling is repeated many times to obtain an ensemble of sequences. This technique captures the multi-year dependency, but the sequences are limited to those seen in the paleo record.

### **3.2.2 Homogeneous Markov (HM)**

This method and the two that follow differ from the block resampling technique because they generate new, unseen binary sequences, while the block resampling, as mentioned above, is limited to the sequences in the paleo record. This is possible through a two state, first order Markov model (Rajagopalan et al., 1996) – which results in four possible transitions from one year to the next (wet to wet, wet to

dry, dry to dry, and dry to wet). The probability of experiencing a particular transition is estimated as a proportion from the entire paleo data period. For example, the wet-wet transition is computed as a percentage representing the number of times a wet year is followed by a wet year – resulting in a transition probability matrix (TPM) that provides the probability of transiting to any state in the next year from any state in the current year. Table 1 is an example of a TPM; note that the probabilities sum to 1 across the rows.

	<b>W</b>	<b>D</b>	<b>Sum</b>
<b>W</b>	0.5275229	0.4724771	1
<b>D</b>	0.5047619	0.4952381	1

**Table 1** HM TPM (left is current state, top is future state).

The TPM is used to generate sequences of hydrologic states (1 or 0). Markov chains are very popular in modeling rainfall occurrences (Rajagopalan and Lall, 1999; Apipattanavis et al., 2007) and have been shown to capture spell statistics quite well.

Since the TPM is fitted over the entire paleo record and provides an average estimate of the transitions, it is not very effective at modeling the temporal variability (or epochal behavior) of the wet and dry spells present in the data (see Figure 22).

The following two methods address this deficiency.

### **3.2.3 Block Homogeneous Markov (BHM)**

To capture the epochal variability, the strengths of the previous two methods were combined to form a block homogeneous Markov model (BHM). In this approach, a random block (of say 30 years) and the associated paleo binary state information are selected, and the TPM is computed for this block. Then, a 30-year

state sequence is generated from the estimated transition probability matrix. This approach captures the epochal variability better while still being simple to implement.

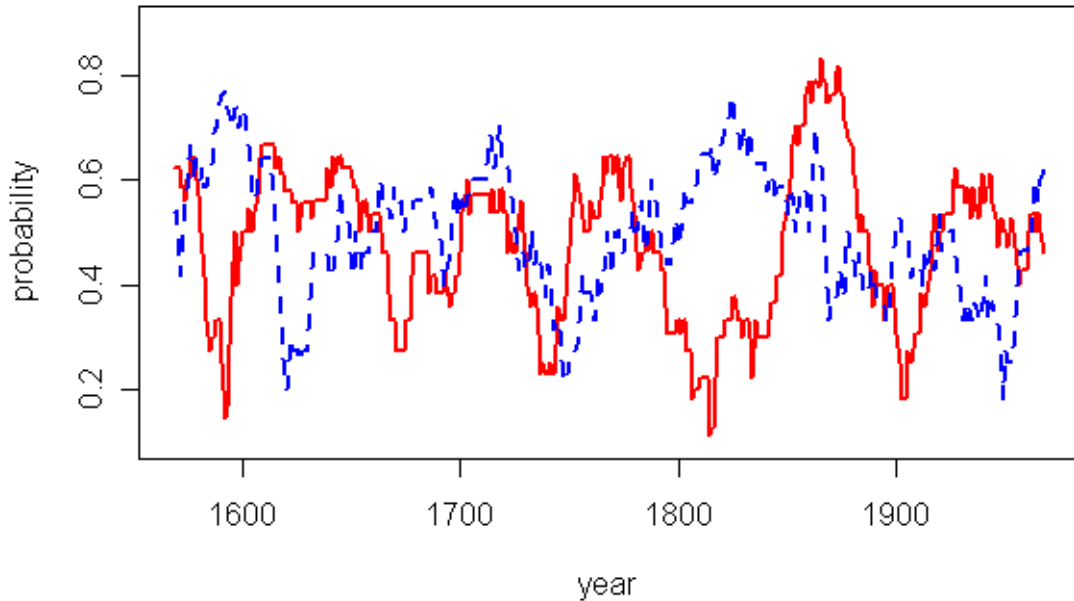


**Figure 23** Wet-wet (blue dashed) and dry-dry (solid red) transition probabilities from the BHM technique.

### 3.2.4 Non-Homogeneous Markov (NHM)

This final method is a natural extension of the BHM approach described above. In this method, a transition probability matrix is estimated for each year using a kernel estimator (Rajagopalan et al., 1996), thus modeling the temporal nonhomogeneity. This method was developed and implemented on the Colorado River Basin (Prairie et al., 2008) and was found to be highly effective at generating longer periods of drought and surplus. A brief description is provided below while referring the reader to this paper for further details. Additional information can also be found in Rajagopalan, et al. (1996) and Rajagopalan, et al. (1997).

The four local transition probabilities for each year  $t$ , can be determined from the probabilities of transitioning from a dry to wet state ( $P_{dw}$ ) and a wet to dry state ( $P_{wd}$ ). The probability of transitioning from a dry to dry state is found as

$P_{dd} = 1 - P_{dw}$ , and the probability of transitioning from a wet to wet state is found as  $P_{ww} = 1 - P_{wd}$ , as described previously. These transition probabilities are calculated based on years in the range  $[t - h_0 \text{ to } t + h_0]$  as:

$$P_{dw}(t) = \frac{\sum_{i=2}^n K\left(\frac{t-t_i}{h_{dw}}\right) S_t [1 - S_{t-1}]}{\sum_{i=2}^n K\left(\frac{t-t_i}{h_{dw}}\right) S_t}$$

**Equation 8**

$$P_{wd}(t) = \frac{\sum_{i=2}^n K\left(\frac{t-t_i}{h_{wd}}\right) [1 - S_t] S_{t-1}}{\sum_{i=2}^n K\left(\frac{t-t_i}{h_{wd}}\right) [1 - S_t]}$$

**Equation 9**

where  $K(\cdot)$  = the kernel function;  $h_0$  is kernel bandwidth for the transition of interest ( $dw$  or  $wd$ );  $S_t$  = system hydrologic state (1 = wet, 0 = dry) at time  $t$ ;  $S_{t-1}$  = system hydrologic state at time  $t - 1$ ;  $t$  = year of interest; and  $n$  = the number of values in the window  $t - h_0$  to  $t + h_0$ . The kernel function  $K$  is defined as:

$$K(x) = \frac{3h}{(4h^2 - 1)} (1 - x^2)$$

**Equation 10**

where  $x = \left(\frac{t-t_0}{h}\right)$ ,  $|x| \leq 1$ ,  $t$  is the year of interest, and  $t_0$  is the transition of interest.

The bandwidth provides a window overlaying the current year, over which the suite of transition probabilities is calculated. The value of  $h$  is optimized for years

transitioning from wet and then again for years transitioning from dry. Optimization is accomplished using a method defined as:

$$\text{LSCV}(h) = \frac{1}{n} \sum_{i=1}^n [1 - \hat{P}_{-t_i}(t_i)]^2$$

**Equation 11**

where  $n$  = the number of  $dw$  or  $wd$  transition within the window  $[t - h_0$  to  $t + h_0]$ ;

and  $\hat{P}_{-t_i}(t_i)$  = the estimate of the transition probability ( $\hat{P}_{dw}$  or  $\hat{P}_{wd}$ ) at year  $t$  dropping the information on year  $t$ .

The LSCV is calculated for a suite of  $h$  values; the  $h$  ultimately selected results in the smallest LSCV value. Once  $h$  values have been selected for transitions from both wet and dry years, transition probabilities can be calculated for each year.

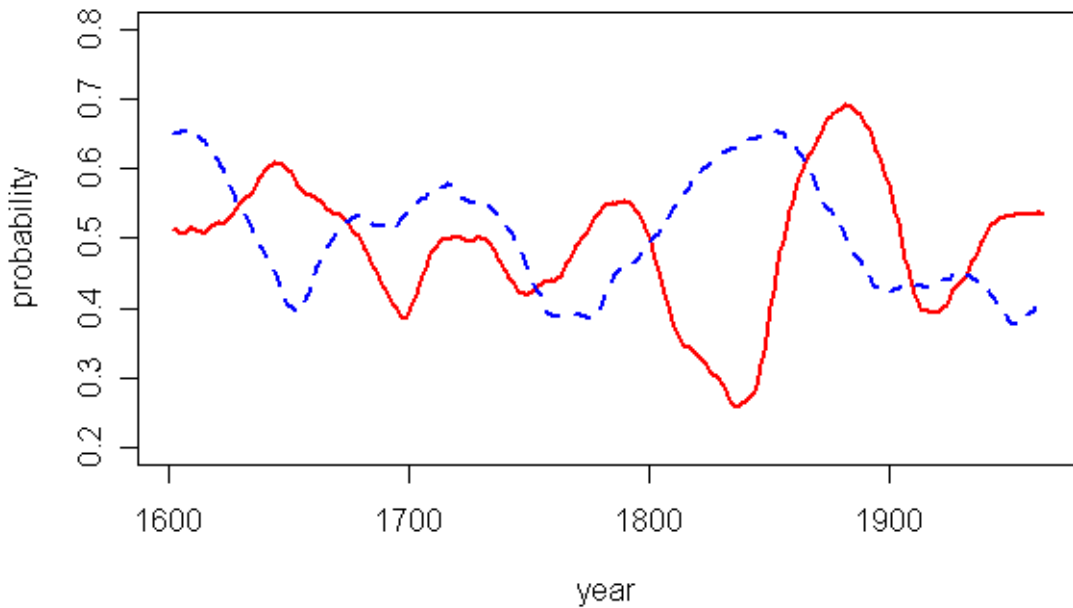


**Figure 24 Wet-wet (blue dashed) and dry-dry (solid red) transition probabilities from the NHM technique.**

Of note, when optimizing the band width ( $h$ ), it is necessary to determine a wet band width representative of transitions which start with a wet year, and a dry

band width representative of transitions which begin with a dry year. Since this work deals with a two state model, there are two possible transitions that can be optimized for both the wet ( $ww$  and  $wd$ ) and dry ( $dd$  and  $dw$ ) band widths. Ideally, there will be a clear LSCV minimum for at least one of the two possible transitions that can be used to determine each bandwidth. This is not always the case however, and thus, bandwidth selection can be somewhat at the discretion of the individual.

From encountering this situation (where the LSCV function decays instead of reaching a minimum value) in working with other data, several useful findings are reported. The most effective way to approach such a scenario is to develop a minimum delta LSCV threshold. Therefore, if the LSCV value from one band width to the next fails to change by a significant amount, that bandwidth can be declared the effective minimum. When developing this threshold, it should be kept in mind that very small bandwidths can introduce undue variability, while large  $h$  values result in over-smoothing of the probabilities. Furthermore, large band widths can significantly reduce the number of years upon which transition probabilities can be calculated. For example, a bandwidth of 60 years results in 120 years of paleo record that cannot be used to compute transition probabilities. Thus, in this example, a band width of 60 represents more than a 25% “reduction” in data. It is difficult to assign hard-fast rules for these situations due to the uniqueness of each dataset; however, the above should serve as a guide for these issues.

The simulation proceeds as before, by resampling a block of years from the paleo record. Using the TPM estimates for each year, the hydrologic state is

generated for each of the years in the block. The nonhomogeneity of the TPM is the key aspect of this method and enables modeling of the epochal behavior.

### 3.2.5 KNN Flow Magnitude Resampling

Once the desired number of binary traces have been generated, via any of the above described methods, the flow magnitudes are obtained from the observed data. To accomplish this, a KNN conditional resampling approach (Prairie et al., 2008) is employed, conditioned on the hydrologic state of the previous and current year. This model can be described as the conditional probability density function (PDF):

$$f(x_t | S_t, S_{t-1}, x_{t-1})$$

#### Equation 12

where the flow at the current time ( $x_t$ ) is conditioned on the current system state ( $S_t$ ), previous system state ( $S_{t-1}$ ) and previous flow ( $x_{t-1}$ ).

The following description of the KNN flow magnitude resampling is abstracted from Prairie et al. (2008). Simulation from this conditional PDF is achieved by a KNN bootstrap method (Lall and Sharma, 1996; Rajagopalan and Lall, 1999). Typically, K nearest neighbors are identified in the observational data of the current feature vector [ $S_t, S_{t-1}, x_{t-1}$ ]. One of the neighbors is selected, based on a metric that gives highest probability to the nearest neighbor and lowest to the farthest. The corresponding streamflow of the selected neighbor is the simulated value for the current time.

This case is unique in that the feature vector includes discrete and continuous variables. Further, the discrete variables indicate system state as 0 or 1 (i.e., dry or wet), while the continuous variable is a considerably larger value. If this disparity in

magnitude is not considered in the neighbor choice the state information will not influence the neighbor choice. The neighbor would then be chosen base solely on  $x_{t-1}$ . Therefore, determination from the feature vector ( $v_t=[S_t, S_{t-1}, x_{t-1}]$ ) is split into two steps. First, the discrete variables are identified as members in one of the four categories ( $ww, wd, dw, dd$ ) identified from the state vector ( $[S_t, S_{t-1}]$ ). In the second step, the K-nearest neighbors of  $x_{t-1}$  that lie within the appropriate category are identified. The flow for the following year,  $x_t$ , corresponding to the neighbor selected for  $x_{t-1}$  is then sampled.

In this work,  $K_j = n_j$ , where  $j = 1, \dots, 4$  representing the four state categories and  $n$  is the number of values in each category. With a larger observational data set, the number of nearest neighbors can also be based on the heuristic scheme  $K = \sqrt{n}$  (Lall and Sharma, 1996), following the asymptotic arguments of Fukunaga (1990). Objective criteria, such as Generalized Cross Validation (GCV), can also be used. The  $K_j$  neighbors were weighted with the function:

$$W(i) = \left(\frac{1}{i}\right) / \left(\sum_{i=1}^K \frac{1}{i}\right).$$

**Equation 13**

### **3.3 Evaluation of Methods**

A suite of statistics are computed from the simulations and compared against that of the observed data using boxplots. The ‘box’ in the boxplots represents the interquartile range (IQR), the horizontal line inside the box is the median, the whiskers correspond to the 5th and 95th percentiles and values beyond the whiskers are shown as points. The value of a statistic computed from the historical data is

shown as a red triangle. When the observed statistic lies within the IQR, it can be inferred that the simulations adequately capture the statistic.

The distributional statistics of the flow magnitudes computed for comparison with the observed are mean, standard deviation, skewness, lag-1 correlation, maximum and minimum. In addition to the above-mentioned statistics, probability density functions (PDFs) are fit to the simulations and presented as boxplots to show variability.

The main idea behind the combined approaches developed is to generate a rich variety of wet and dry sequences that are critical for water management – especially the EIS. Thus, statistics on periods of drought and surplus are computed – these are same as described in Chapter 2. Figure 25 below depicts the various drought and surplus statistics considered. To compare drought and surplus periods generated by the different methods, histograms are provided to display drought/surplus length/magnitude distributions.

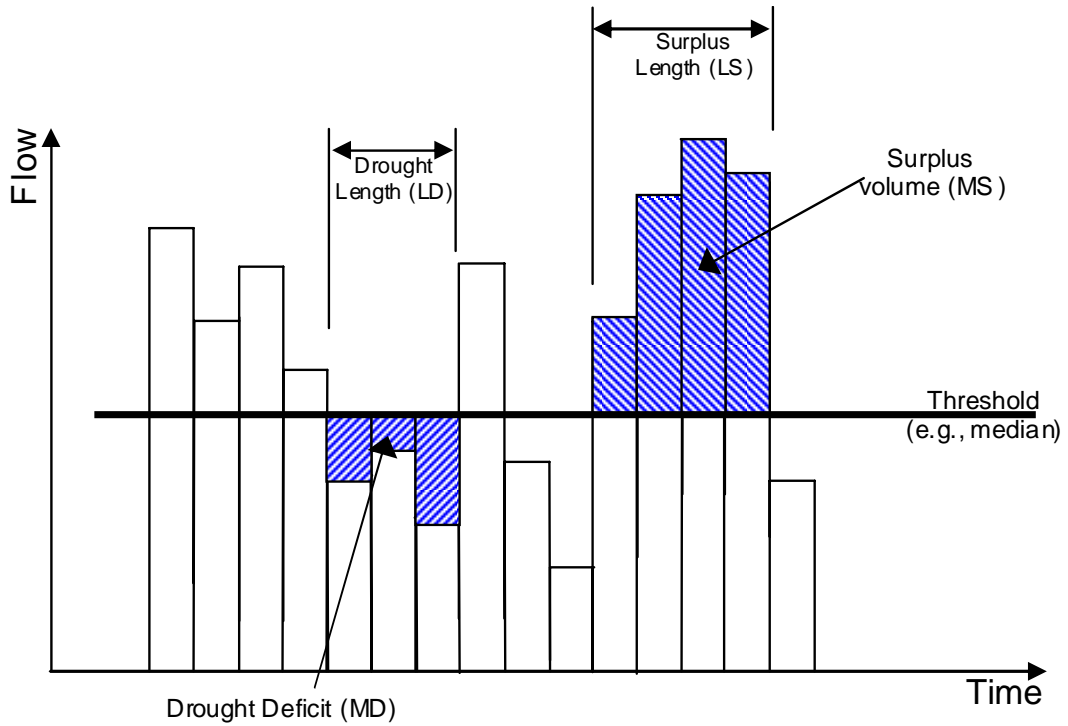


**Figure 25 Definition of drought/surplus statistics.**

### 3.4 Results

Figure 26 shows the suite of basic statistics of the flow magnitude computed for the four paleo methods employed in this investigation, with the red line representing the respective statistic of the observed data for the observed period. All methods capture the observed mean, standard deviation and skew quite well – this is to be expected, as the methods generate flows by resampling the historical data. However, it is worth mentioning that the block HM method has the widest IQR, as well as the widest total range of values, indicating its effectiveness at introducing variability. The lag-1 autocorrelation, maximum and minimum statistics are under-simulated by the methods. These statistics would all be captured if flow sequences were generated as the same length as the observed period (i.e., 100 years long instead of 30 years) and based on the observed period, as opposed to generating 30 year

sequences in a two step process based on the paleo and observed data – as seen in Chapter 2.

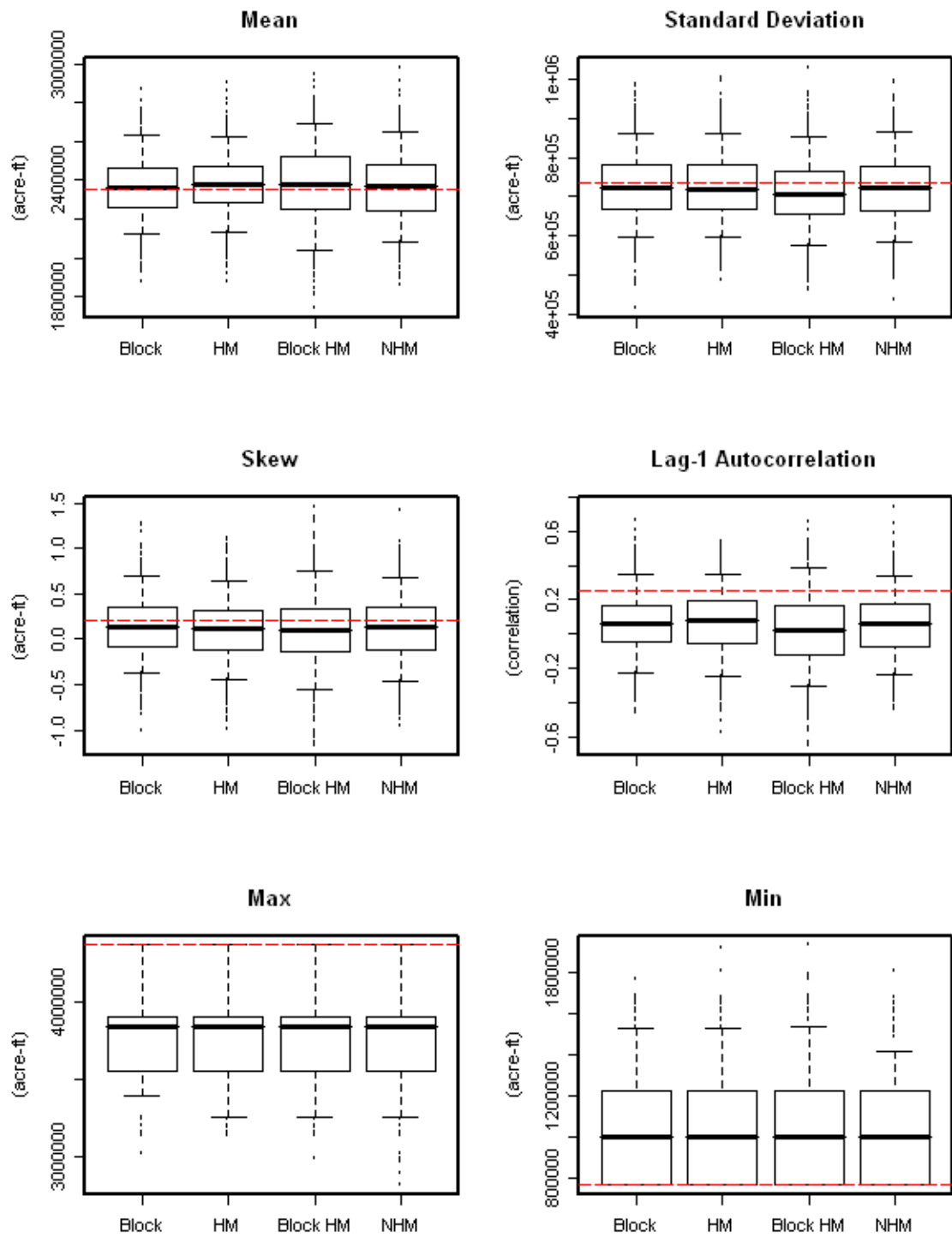
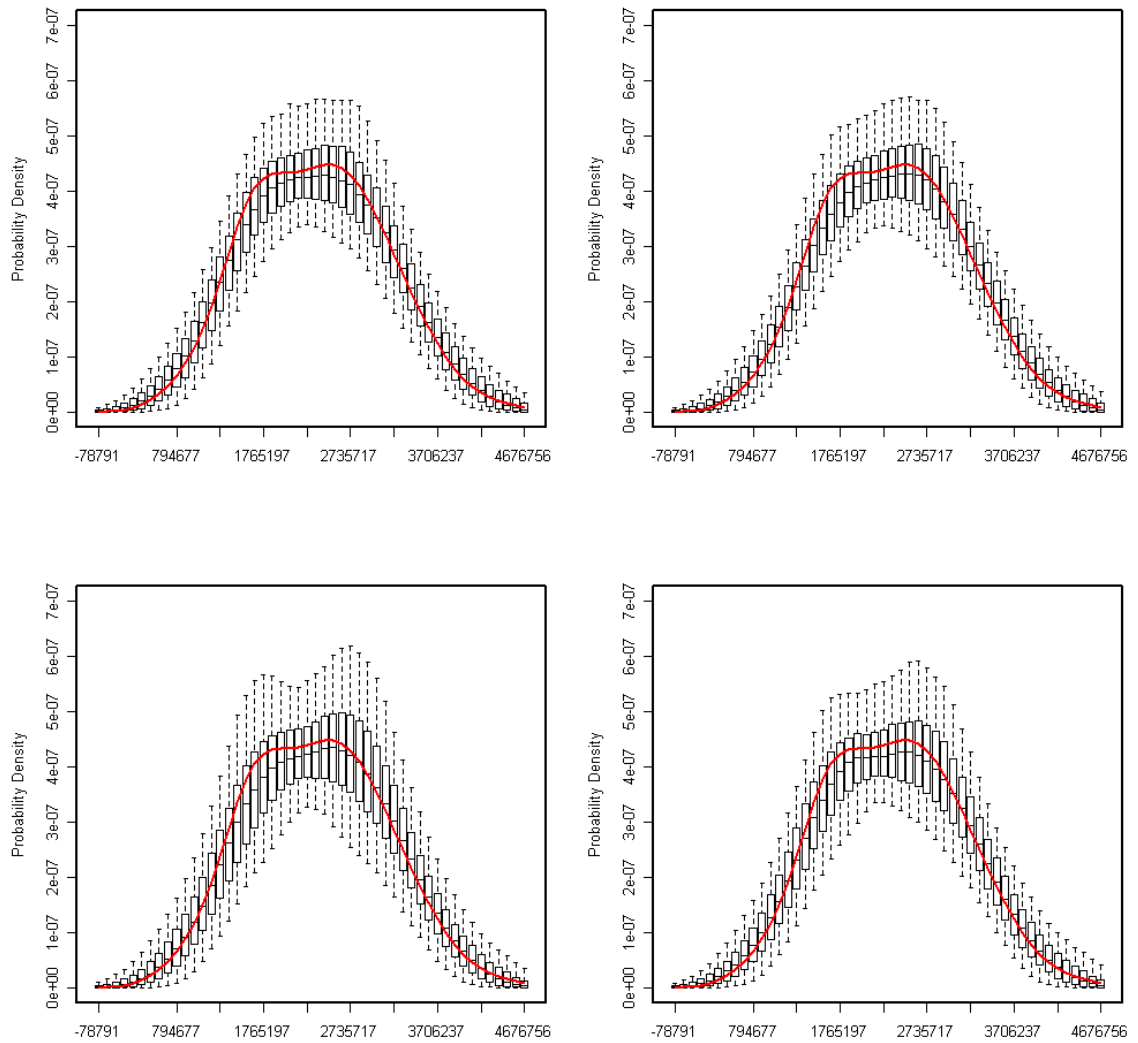
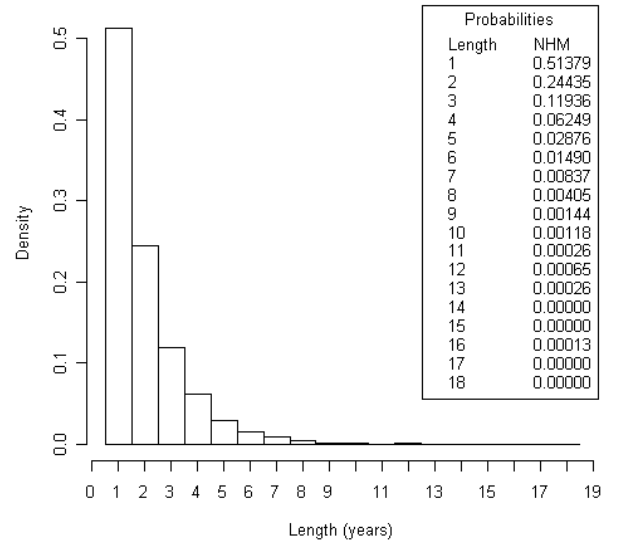
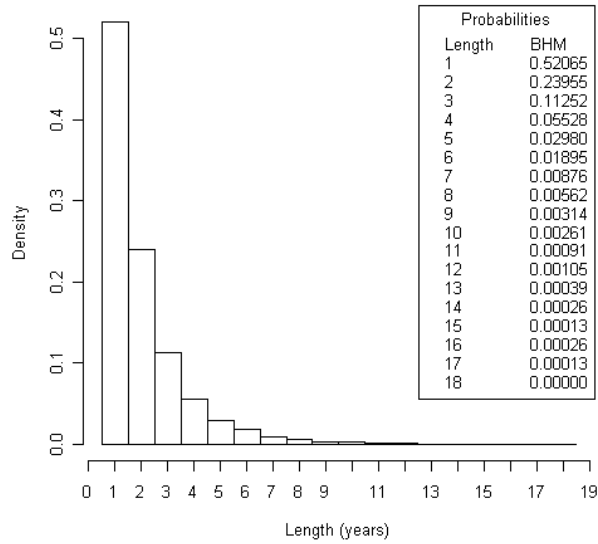
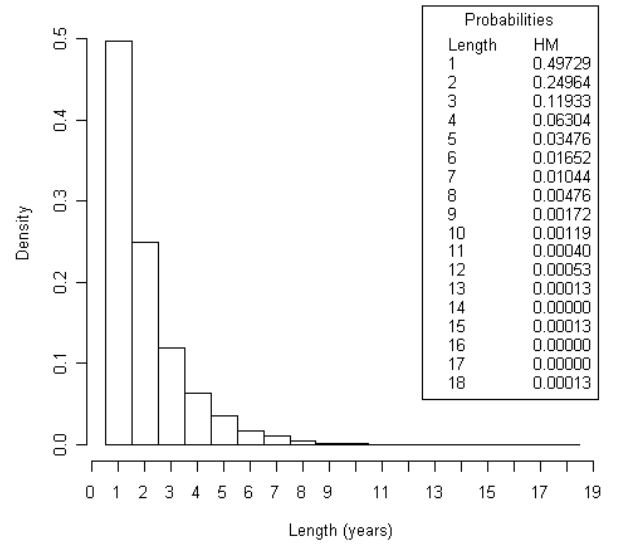
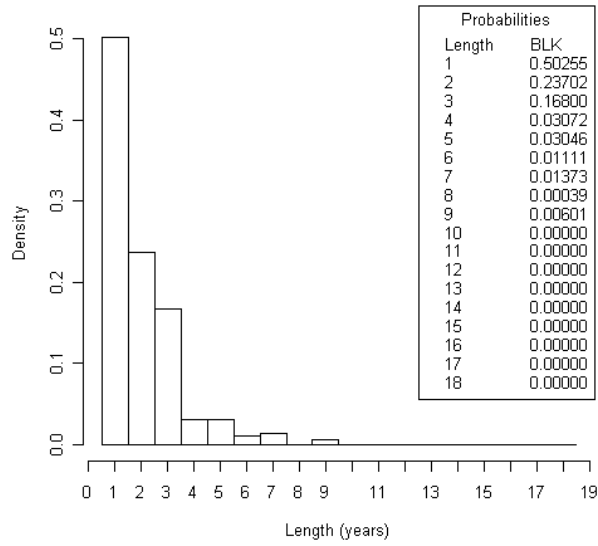


Figure 26 Distributional statistics for Block, HM, BHM and NHM traces.

The PDFs of the historical flows are well captured in all the methods (Figure 27) – consistent with the fact the flow magnitudes are generated from resampling the observed flows. This helps in capturing the non-Gaussian shape of the PDF present in the observed data – a unique advantage offered by this approach over traditional parametric techniques.



**Figure 27 Annual PDFs (acre-ft/yr) of traces generated using Block (upper left), HM (upper right) BHM (lower left) and NHM (lower right) techniques. The observed PDF is shown in red.**



**Figure 28 Surplus length histograms of Block (upper left), HM (upper right), BHM (lower left) and NHM (lower right) techniques.**

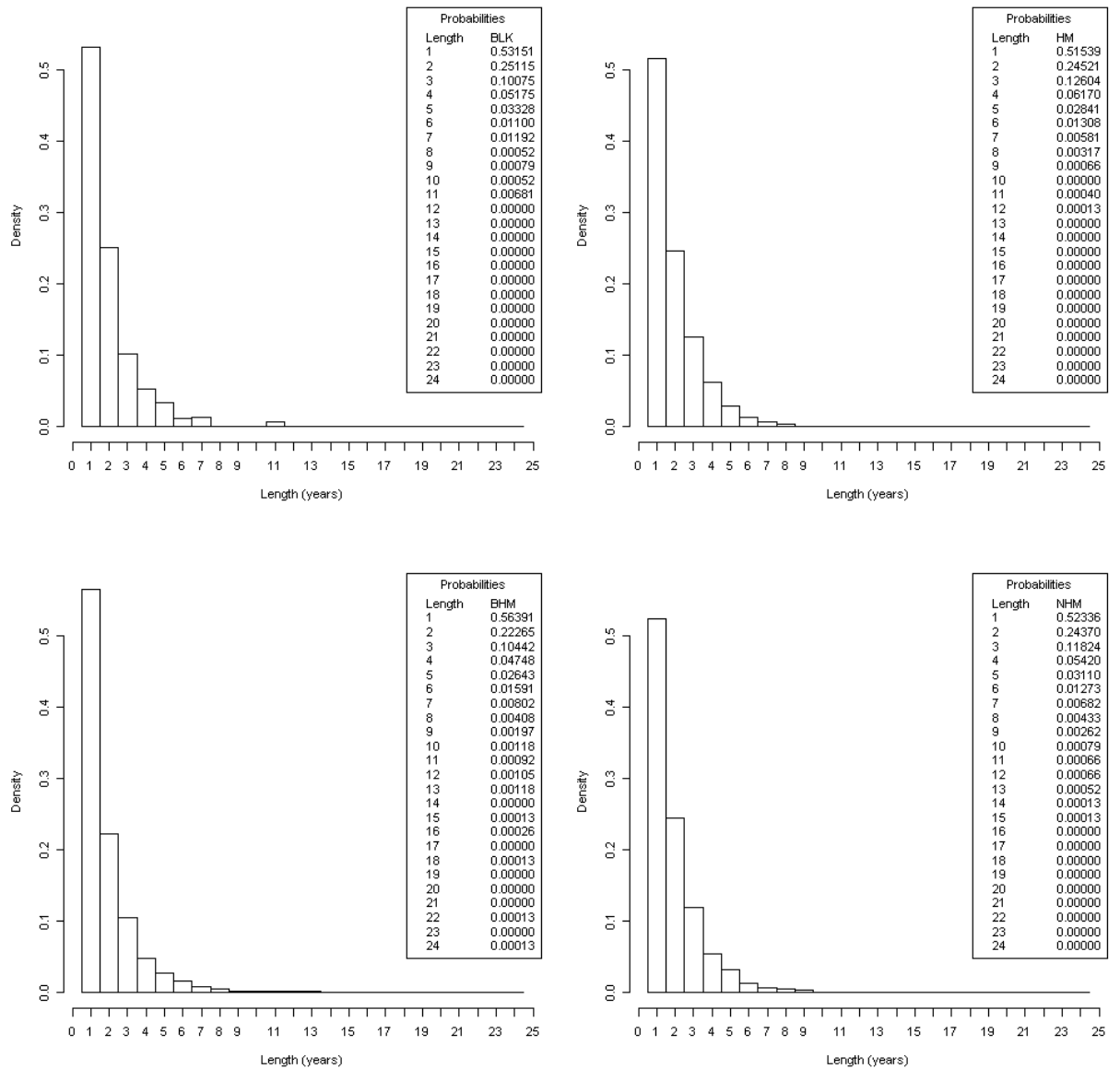


**Figure 29 Drought length histograms of Block (upper left), HM (upper right), BHM (lower left) and NHM (lower right) techniques.**

Figure 28 and Figure 29 show surplus and drought length distributions of the four methods investigated. As to be expected, the block method is limited to both the longest drought and longest surplus seen in the paleo data (11 and 9 years, respectively). The other techniques all generate periods of drought and surplus that extend beyond those observed, with the maximum drought reaching 24 years in length and the maximum surplus reaching 18 years. It should be noted that the

probabilities of exceeding the longest observed drought (6 years) and surplus (6 years) are similar very similar to those seen in Chapter 2 (approximately 2%); however, with the paleo techniques, that probability is spread over a wider range of lengths. Also, the HM results show a considerably higher probability of exceeding the observed surplus than the observed drought.

The transition probabilities of most importance when discussing drought and surplus periods are wet to wet ( $ww$ ) and dry to dry ( $dd$ ). These probabilities are shown as time series for the block homogeneous technique in Figure 23 and for the non-homogeneous approach in Figure 24. Even though there are more wet than dry events in the paleo record (210 vs. 219), the NHM and BHM methods both produce longer periods of drought than surplus. This is directly linked to the distribution of  $ww$  and  $dd$  transition probabilities. As seen in Figure 23 and Figure 24, the  $dd$  curve has one obvious peak with magnitudes greater than any seen in the  $ww$  plot. Thus, when this region is selected, there is potential to generate the extended periods of drought, even though on average the  $ww$  transition probability is greater.

The HM method produces the longest surplus period, albeit only by 1 year, compared to the BHM approach. This can be attributed to the slightly higher  $ww$  and  $dw$  transition probabilities, as seen in Table 1. The slight preference to transition to wet from dry and then stay wet not only accounts for the extended surplus periods generated by the HM technique, but also the relatively short drought periods shown in Figure 29. This is also supported by the increased probability of exceeding the maximum observed surplus length, as discussed earlier.

Figure 30 and Figure 31 show surplus and deficit volume distributions, respectively. It should be noted that the HM model can generate deficits and surplus volumes greater than that from the paleo, given the resampling of observed values. Nonetheless, it is clear that the other three methods still have considerable advantage in terms of drought/surplus magnitudes, as they generate longer drought/surplus lengths. Similar to the drought and surplus length histograms, the HM, BHM and NHM methods all generate deficit and surplus magnitudes greater than that of the observed. Furthermore, the BHM and NHM techniques both generate larger deficits than surpluses. There is, however, no skew in the HM towards larger surplus volumes. This is not unrealistic, as length and magnitude distributions are not synonymous. In fact, the magnitude of a drought/surplus periods is probably more important than the length because ten years of flow slightly below the median will not greatly impact operations, while three years of very low flow can be crippling to the system.

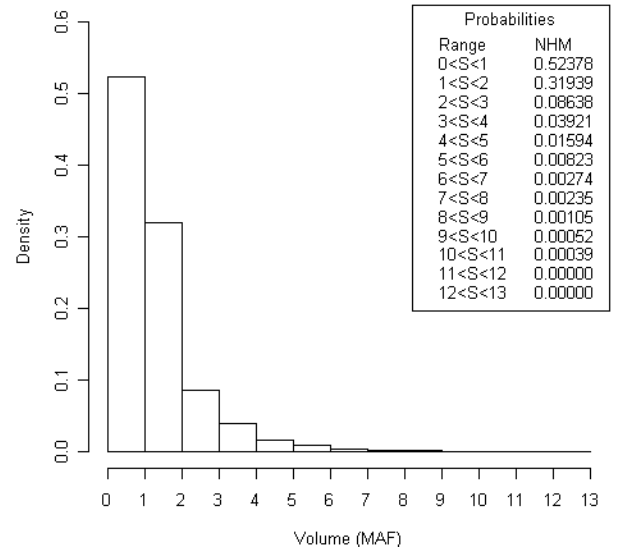
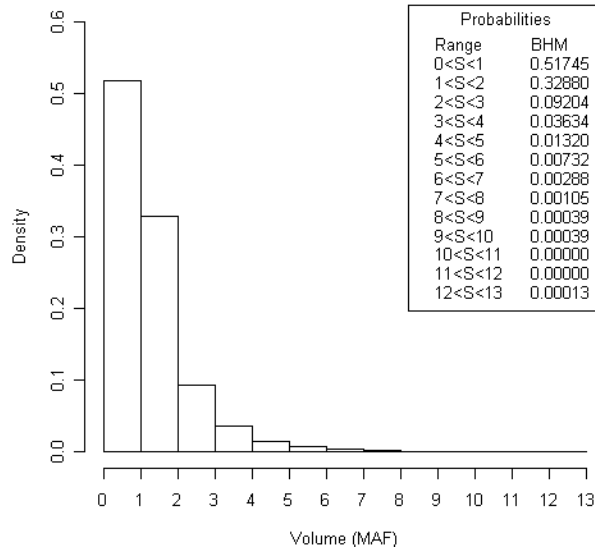
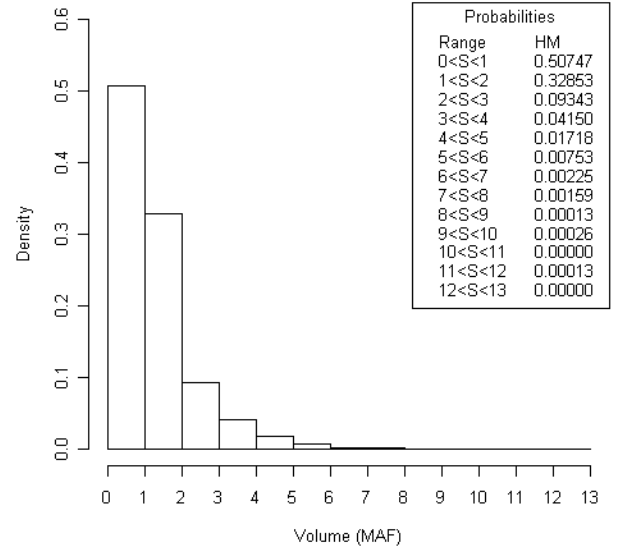
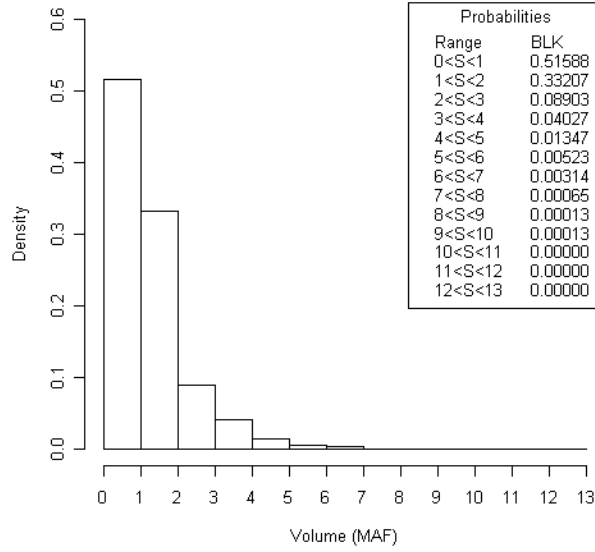


**Figure 30 Surplus volume histograms of Block (upper left), HM (upper right), BHM (lower left) and NHM (lower right) techniques.**

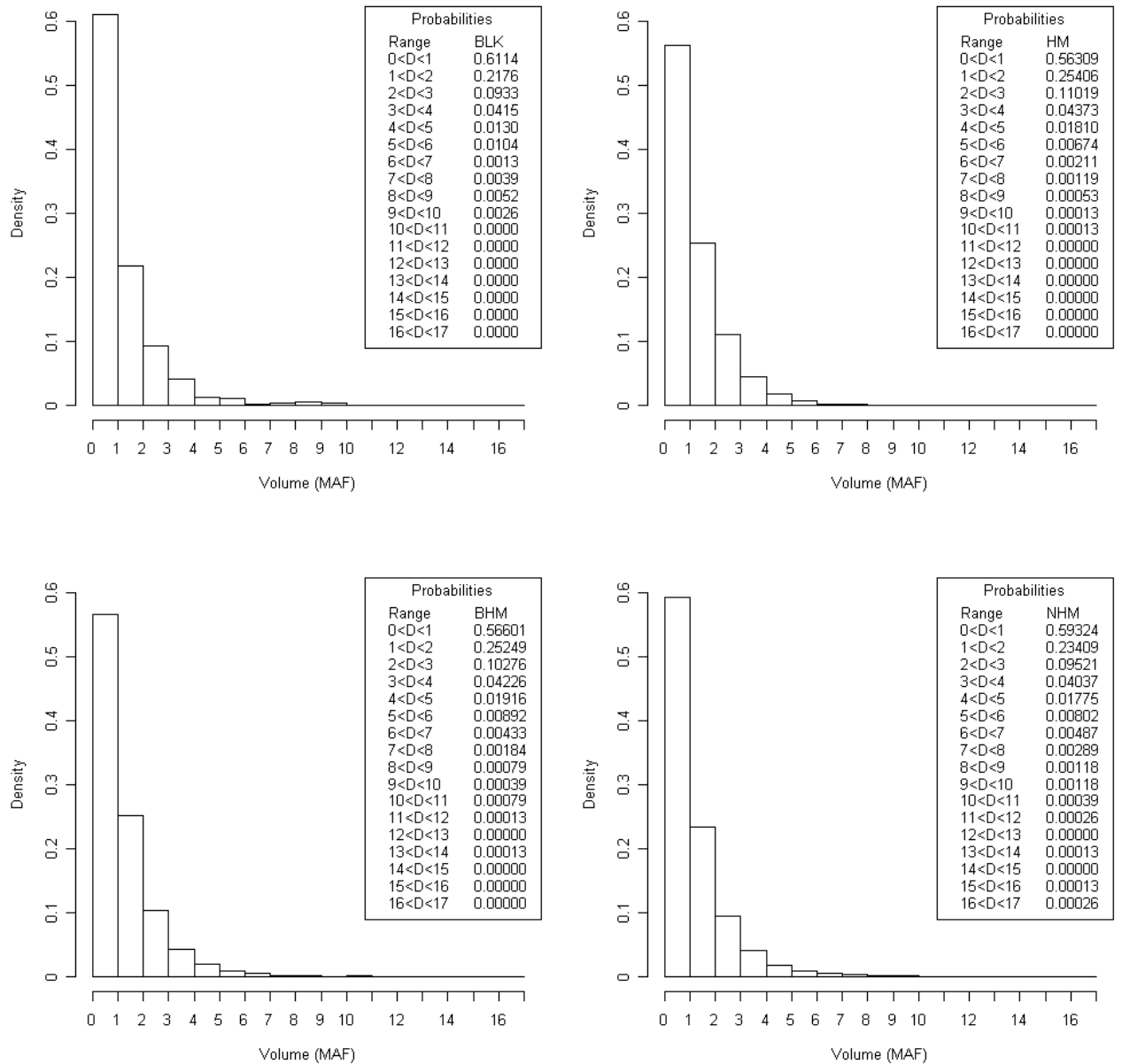


**Figure 31 Drought deficit histograms of Block (upper left), HM (upper right), block BHM (lower left) and NHM (lower right) techniques.**

As discussed in Chapter 2, the sequent peak algorithm offers an attractive alternative to quantifying system risk. Instead of selecting a drought or surplus threshold as done for the above histograms, the sequent peak approach determines a necessary storage for a given demand and flow sequence. As a result, water

managers can quickly assess the ability to meet demands from the storage-yield plots such as those in Figure 32.

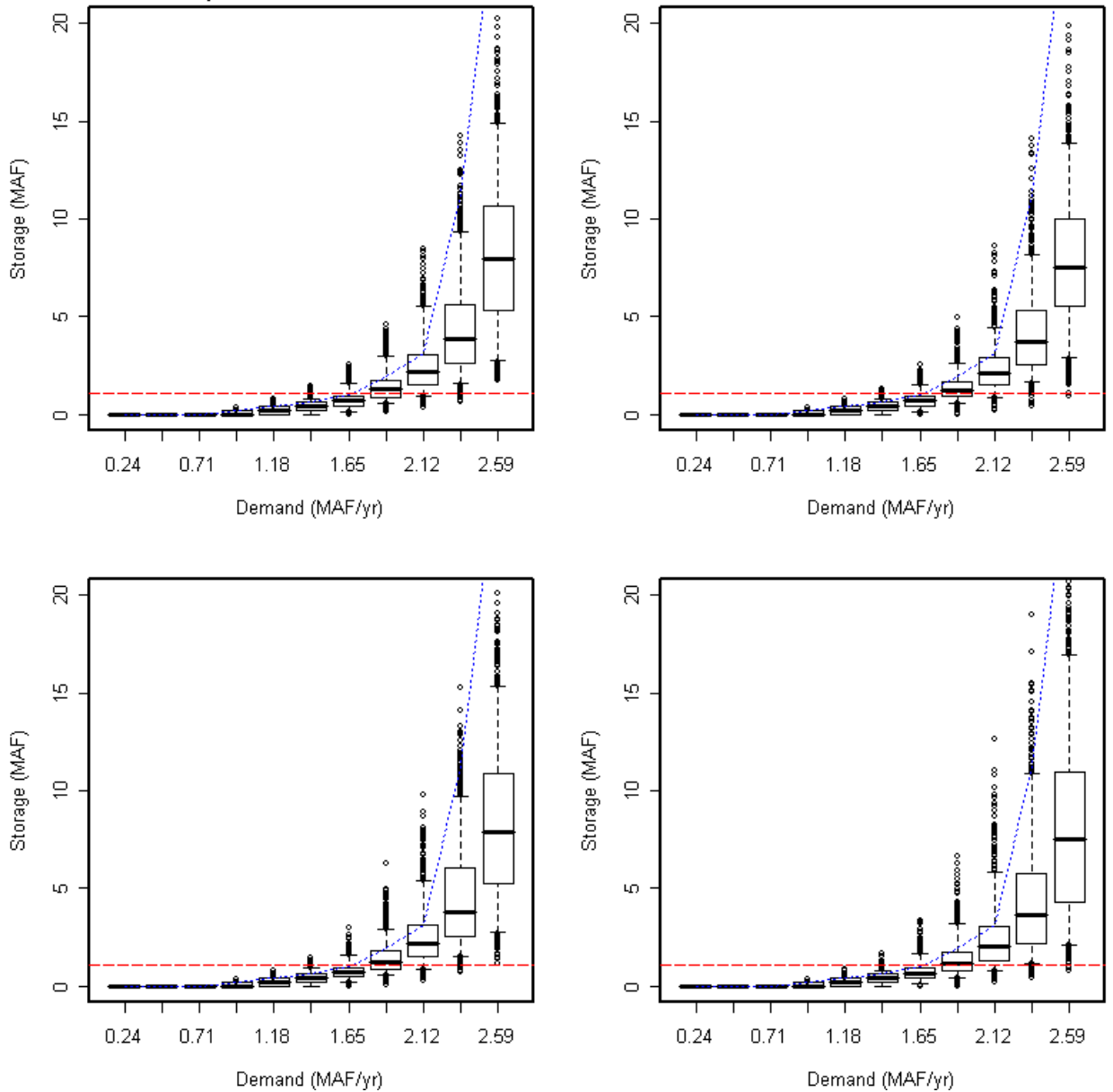


**Figure 32** Sequent peak of Block (upper left), HM (upper right), BHM (lower left) and NHM (lower right) techniques. The red dashed line represents maximum live storage of the Aspinall Unit and Taylor Reservoir, while the dotted blue line shows the observed data trace.

The sequent peak analysis of the traces generated with the paleo techniques is not unlike that of the KNN and Modified KNN from Chapter 2. The observed data (blue dotted line) indicate that a demand of 1.65 MAF/yr can be met given the current

storage (horizontal dashed red line). However, the boxplots for the generated traces indicate a slight decrease in reliability compared to those from the non-paleo stochastic simulations in Chapter 2. Figure 33 shows a more detailed picture by providing PDFs of the required storages. Given the long wet and dry sequences generated from these methods, the storage requirements are also higher – indicated by a higher number of storage values beyond the whiskers in the above figure. The simulations from the paleo methods suggest a lower reliability, which is important information for future management planning.

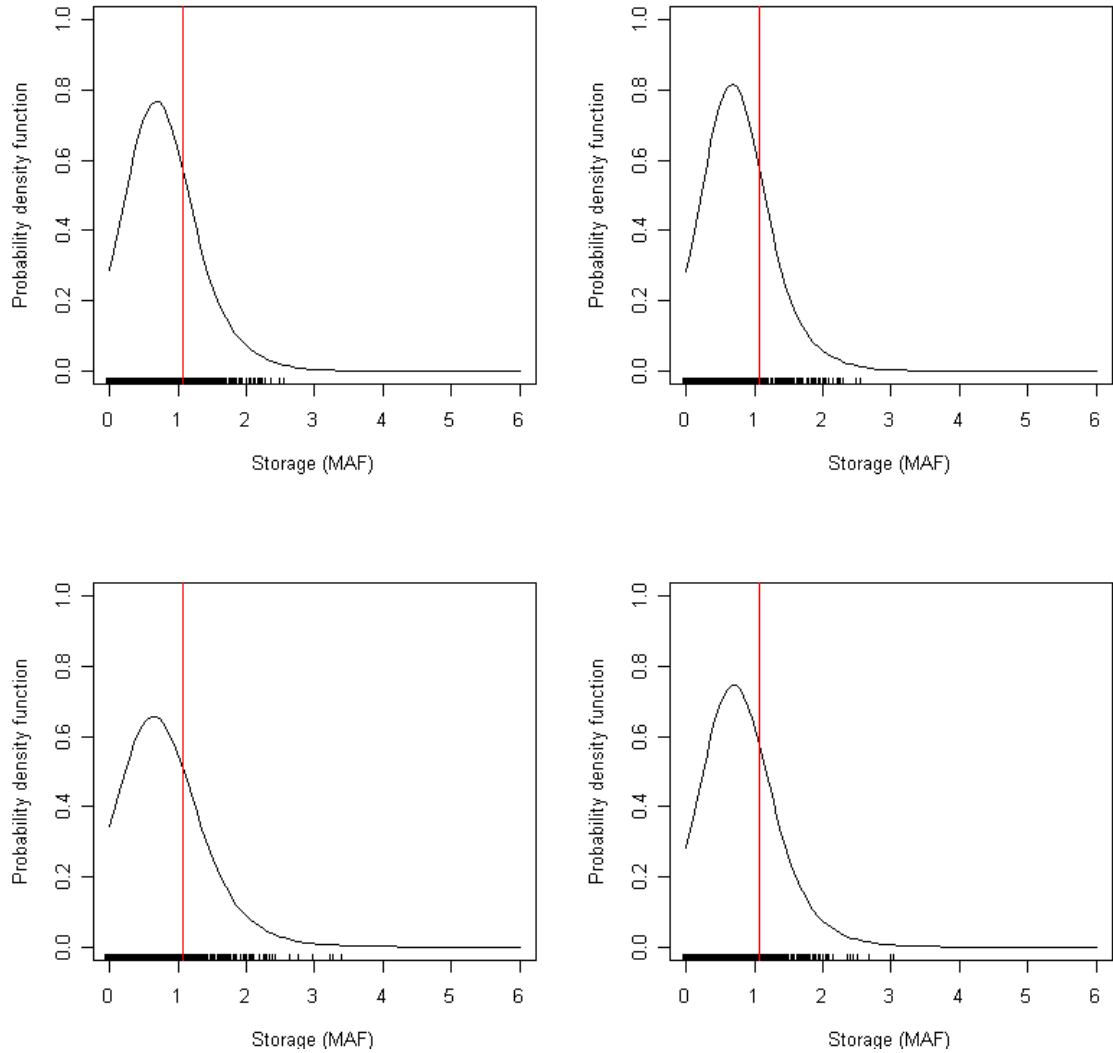


**Figure 33 PDFs of storage required to meet a 1.65 MAF demand. The vertical red line is live storage of the Gunnison Basin. Block (upper left), HM (upper right), BHM (lower left) and NHM (lower right) techniques.**

### 3.5 Summary and Discussion

Four different methods for generating flow sequences combining paleo reconstructions and observed record were presented. These techniques are unique and offer a way to combine the strong aspects – hydrologic state information of the paleo record and the magnitude information from the observed data.

As shown in the statistical validation, all four techniques capture the distributional statistics of the streamflow. Within those techniques, there are apparent

strengths and weaknesses for each, especially for the drought and wet spells. The Block method is the most limited in terms of drought and surplus spells, as it can only reproduce the maximum lengths experienced in the paleo reconstruction, and there are a limited number of unique sequences to be resampled. However, it is very simple to implement, which can be an important strength for some applications. The HM is an improvement in that it generates new, unseen state sequences, but includes a major detractor - the transition probabilities are overly smoothed and represent the average for the entire paleo reconstruction period. Therefore, some of the epochal nature of the variability in the data is not well reproduced- a main goal of including the paleo data. From this perspective, there is perhaps more merit to using the Block approach than the HM.

The BHM provides a reasonable compromise between the two above-mentioned techniques, but may result in an undue bias toward a particular transition, evidenced by Figure 23. The NHM is an improved version of the BHM method, as it computes the transition probability for each year using a kernel based estimator. Additionally, by computing the transition probabilities at each year of the paleo, the occasional wet/dry year that breaks up an epoch can be reproduced, making for the most realistic sequencing.

As discussed in Chapter 2, technique selection is a blend of intended use, goals and audience. For the purpose of this research, the non-homogeneous Markov approach is selected. It accomplishes the goals of introducing paleo sequencing, generates extended periods of drought and surplus and produces perhaps the most

realistic traces. These flows will be disaggregated in space and time (Chapter 4) to drive the Riverware decision model (in Chapter 5).

## **CHAPTER 4: SPACE-TIME DISAGGREGATION OF FLOW SEQUENCES**

### **4.1 Introduction**

Flow scenarios are required at several locations in a basin, simultaneously maintaining spatial correlations, in order to investigate basin-wide water management strategies and system reliability. This is precisely the case for the model developed in Chapter 5 for the Gunnison Basin. The majority of the Gunnison is dominated by the operation of the Aspinall Unit, and thus, inflow to the various reservoirs is crucial in evaluating the operating policies under the added strain of fish flows. Furthermore, the majority of water arrives in the form of spring snow melt, and peak demands occur during summer for the purpose of agricultural irrigation. Therefore, multi-site, seasonal modeling of the basin and operations is paramount for the understanding of these complex, non-stationary systems. In maintaining a parsimonious approach, typically, annual flows are generated at a downstream gauge using techniques described in the previous chapters, and then disaggregated spatially and temporally (i.e., monthly) using stochastic disaggregation techniques (Valencia and Schakke, 1973; Salas et al., 1980; Koutsoyiannis, 1992; Tarboton et al., 1997).

In this study, the nonparametric disaggregation technique proposed by Prairie et al. (2007) is employed to generate streamflows at four locations in the Gunnison Basin that will serve as inputs to the decision analysis in the next chapter. Figure 34 shows a map detailing the Gunnison Basin and four locations to which the cumulative flow will be disaggregated. The highest location (site 1) lies on the Taylor River and represents all flow entering the system above Taylor Reservoir. Site 2 is located a

considerable distance downstream and captures intervening flow between Taylor and Blue Mesa Reservoirs. Local inflows between Blue Mesa and Crystal reservoirs are represented at site 3. Last, the remaining drainage between Crystal Reservoir and Grand Junction is presented at site 4. The sum of all intervening flow values results in the total in-stream flow below site 4.

The disaggregation will be conducted using intervening flow values – i.e., flows within each reach. This is convenient because the intervening flows add up to the total flow at the downstream location (Site 4), also known as index gauge, and they are directly input into the decision model

A brief background of stochastic disaggregation and a description of the nonparametric technique adapted is provided, followed by its application to the basin.

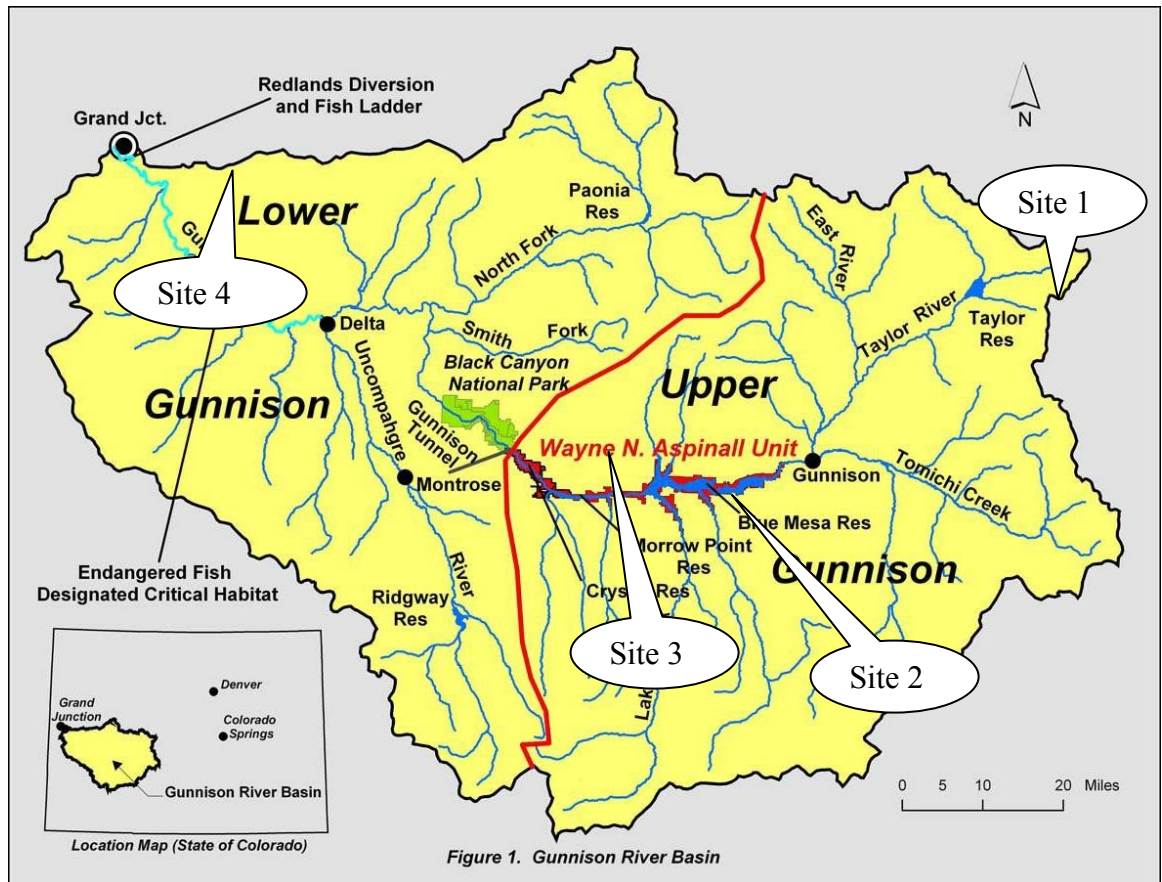


Figure 34 Gunnison Basin and disaggregation sites.

#### 4.2 Disaggregation Techniques

Early disaggregation models were based on the work of Valencia and Schaake (1973), which employed a linear technique. This approach is represented by Equation 14, where  $X_t$  represents the disaggregate variables (e.g., monthly flows) at time  $t$ ,  $Z_t$  is the aggregate variable (e.g., annual flow) and  $V_t$  is a vector of random values from a normal distribution. The elements of  $X_t$  sum to  $Z_t$ , also known as the summability criteria, which is an important element for generating space-time streamflows on a river network. Model parameters contained in matrix  $A$  and  $B$  are estimated such that the simulations preserve the cross correlation between and among the variables. The

aggregate variable is typically generated from a simple stochastic model such as AR-1, and this is disaggregated using the model below.

$$X_t = AZ_t + BV_t$$

**Equation 14**

The general form of Equation 14 is rather similar to an ARMA model; and therefore, it suffers from similar drawbacks described in Chapter 2. Specifically, this linear disaggregation scheme requires data to be normally distributed, and as previously mentioned, this is not always the case in hydrologic data. Therefore, non-Gaussian data must be transformed to a normal distribution before the above model is fit. The simulations are generated in this transformed space and then back-transformed to the original space – consequently, the statistics (especially the summability) are not guaranteed to be preserved in the original space. Also, being a linear model, it cannot readily capture nonlinearities that might be present in the data in addition to non-Gaussian features. Extending this technique to space and time results is a substantial increase in the dimensions of  $A$  and  $B$ , which can be cumbersome and computationally intensive in some cases. Stepwise approaches that use fewer parameters, but require several stages to complete the process have been proposed (Lane, 1979; Salas et al. 1980; Grygier and Stedinger, 1988) along with condensed models, which reduce the number of parameters but model only select cross correlations (Pereira et al., 1984; Lane, 1982; Olivera et al., 1988) to reduce computational cost. Koutsoyiannis (1992) and Santos and Salas (1992) continued this effort, while attempting to maintain summability of the disaggregated values.

In a significant shift that improved upon the above traditional approach, Tarboton et al. (1997) put forth a non-parametric technique that is data driven and can capture any arbitrary distributional (Gaussian, or non-Gaussian) or functional relationship (i.e., linear or nonlinear). This approach is, however, computationally intensive especially when extending it to a large spatial-temporal disaggregation such as on the Colorado River. Prairie et al. (2007) modified this kernel based approach to a K-Nearest Neighbor (KNN) resampling method. They demonstrated this on the Colorado River Basin, which showed it to be simple, efficient, computationally less involved and able to simulate at large number of spatial locations. Therefore, such an approach is adapted for this work. The methodology is described in the following section.

### **4.3 KNN Space-Time Disaggregation**

The schematic of the disaggregation for the Gunnison Basin is shown in Figure 35. The implementation methodology, largely abstracted from Prairie et al. (2007), is described below.  $X$  is a matrix of observed data that is  $D$  (dimensions, i.e., number of months or locations) by  $N$  (years of observations) in size.  $Z$  is the aggregate vector of all dimensions for each year or aggregate gauging site.

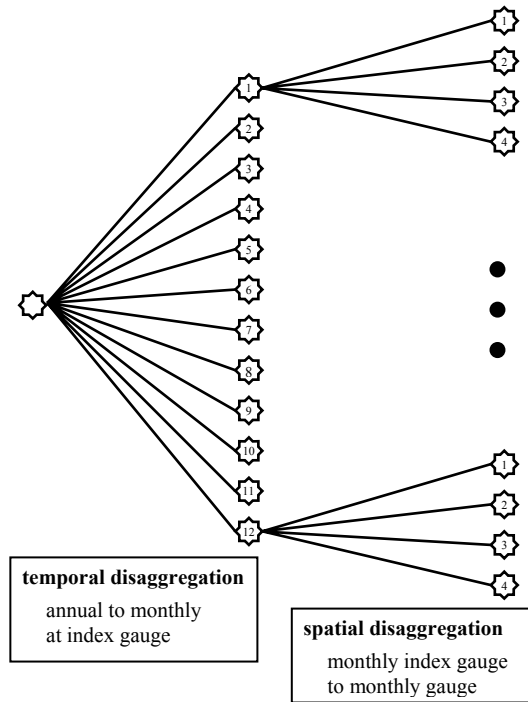


**Figure 35 Space-time disaggregation schematic.**

$$X = [ \ ]_{D \times N}$$

**Equation 15**

$$Z = [ \ ]_{N \times 1}$$

**Equation 16**

$R$  is a  $D \times D$  matrix such that  $R$  transpose is equal to  $R$  inverse. This matrix is dependant only upon the number of dimensions ( $D$ ) and is used to transform  $X$  into the orthonormal space, represented by  $Y$ .

$$R \in \{M_{D \times D} \mid M^T = M^{-1}\}$$

**Equation 17**

$$Y = RX$$

**Equation 18**

$Z_{sim}$  (simulated value to be disaggregated) and  $Z$  are transformed into the orthonormal space as described below.

$$Z' = Z / \sqrt{D}$$

**Equation 19**

$$Z'_{sim} = Z_{sim} / \sqrt{D}$$

**Equation 20**

At this point, a KNN resampling of the  $Z'$  values is conducted to identify the “nearest neighbor” to  $Z'_{sim}$ . Say that the selected neighbor (year) is index  $j$  in vector  $Z'$ . The  $(1:D-1)$  corresponding values from matrix  $Y$  are identified as  $U_j$ .

$$U_j = Y_{1:(D-1),j}$$

**Equation 21**

$U_j$  is then combined with  $Z'_{sim}$  to form vector  $Y^*$ . The last value,  $Y_{D,j}$  is not included because it can be calculated as the remaining flow required to sum to the aggregate.  $Y^*$  is then be back-transformed into the original space to give the disaggregated values ( $X_{sim}$ ) as shown below.

$$Y^* = (U_j, Z'_{sim})$$

**Equation 22**

$$X_{sim} = R^T Y^*$$

**Equation 23**

As a check, the sum  $X_{sim}$  should equal  $Z_{sim}$ , providing disaggregated values for all  $D$  dimensions. It should be noted that the above described method provides a single domain disaggregation (i.e., space or time), and thus for our purposes (disaggregation of a single, annual flow to monthly values at multiple sites), the data must be disaggregated in two steps to achieve the desired results. For the second disaggregation, it was found that the best results were produced when the same observed year was used for both domains. This obviates the need to conduct a KNN

resampling of the data in the second implementation, which further reduces computational intensity.

#### **4.4 Model Evaluation**

The aggregate variable, in this case the annual flow at the downstream gauge (Site 4), is generated using the recommended techniques from Chapters 2 and 3. These are then disaggregated using the nonparametric space-time disaggregation technique described above. From each of the two methods, 1000 simulations, 30 years in length are generated. As before, a suite of statistics are computed from the simulations at the four locations and compared to the observed data. The basic statistics computed are mean, skew, standard deviation, lag-1 correlation, max and min and cross-correlation, at the monthly and annual time scale. The results are displayed as boxplots (described in the previous chapters) with the observed values identified by a solid triangle - as before if the observed values fall within the IQR of the boxplot it can be taken that the statistic is well captured by the simulations. In addition, probability density function (PDF) is also computed.

#### **4.5 Results**

To begin the disaggregation evaluation, boxplots of annual flow PDFs are presented at the four locations (Figure 36-Figure 39) along with the historical PDF. It can be seen that the observed PDF is captured very well at all the locations. Also note that the annual PDF is based on the sum of the monthly disaggregated flows, and thus, is not explicitly designed to be reproduced. Furthermore, it can be seen that all the four PDFs are non-Gaussian, which would make it very difficult for traditional disaggregation techniques to capture.

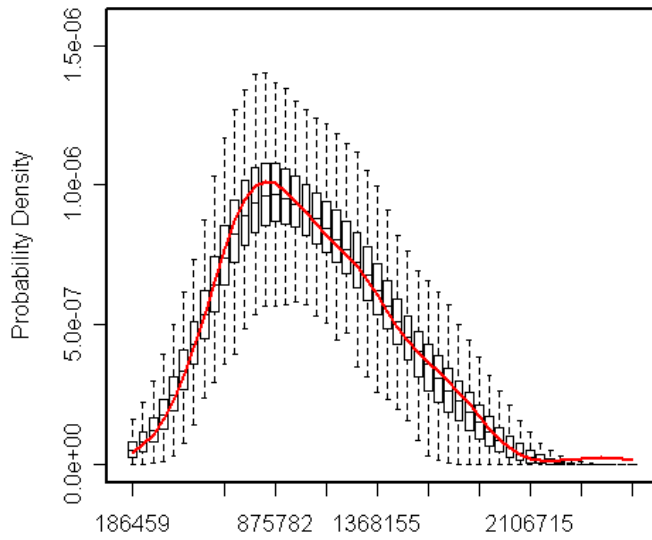


**Figure 36 Annual flow PDF (acre-ft/yr) at site 4.**

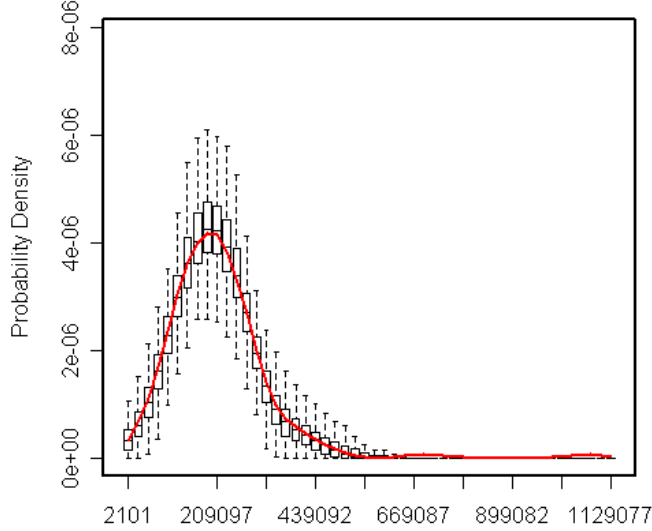


**Figure 37 Annual flow PDF (acre-ft/yr) at site 3.**

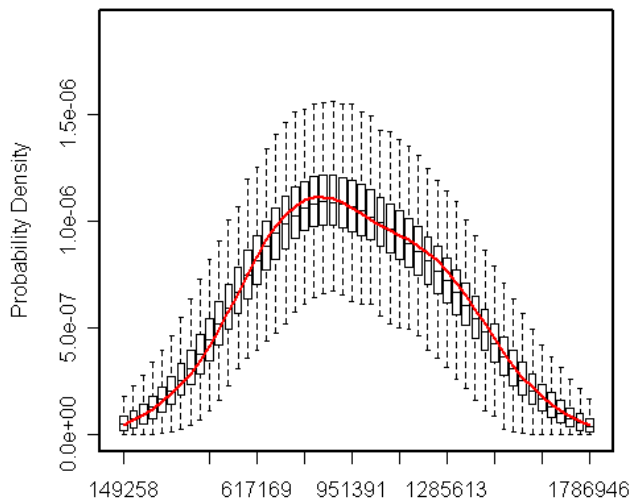


**Figure 38 Annual flow PDF (acre-ft/yr) at site 2.**

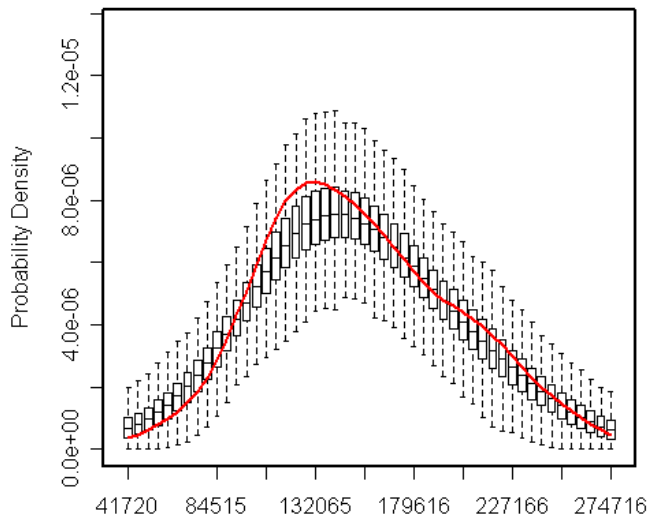


**Figure 39 Annual flow PDF (acre-ft/yr) at site 1.**

The monthly PDFs for each location are presented to evaluate the ability of the temporal disaggregation (Figure 40-Figure 43). Here too, all the monthly PDFs at all the locations are very well reproduced. Notice the variety of distributions, which are anything but Gaussian. This is the powerful aspect of this nonparametric disaggregation technique relative to traditional, parametric approaches.

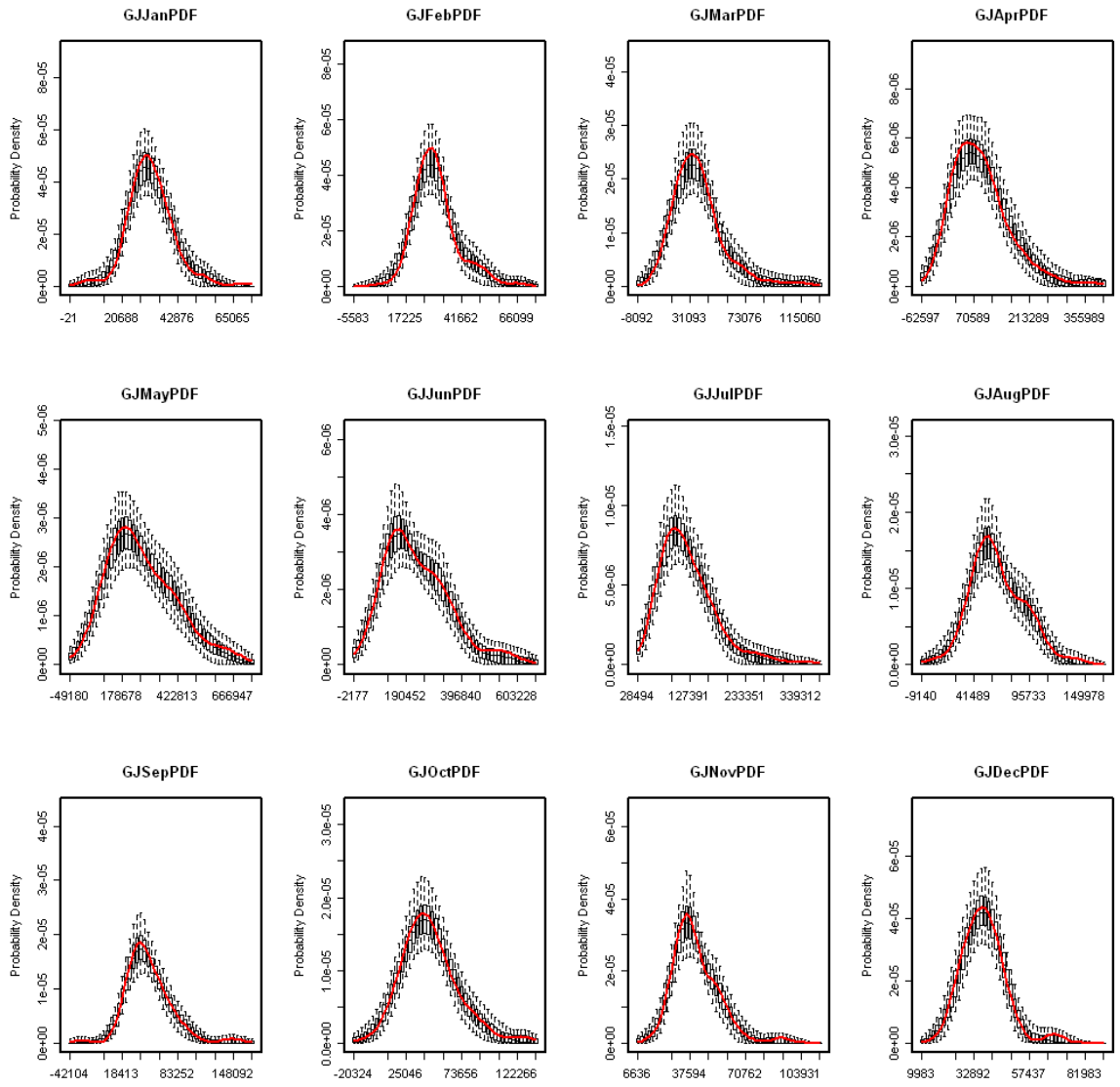


Figure 40 Monthly flow PDFs (acre-ft/yr) at site 4.

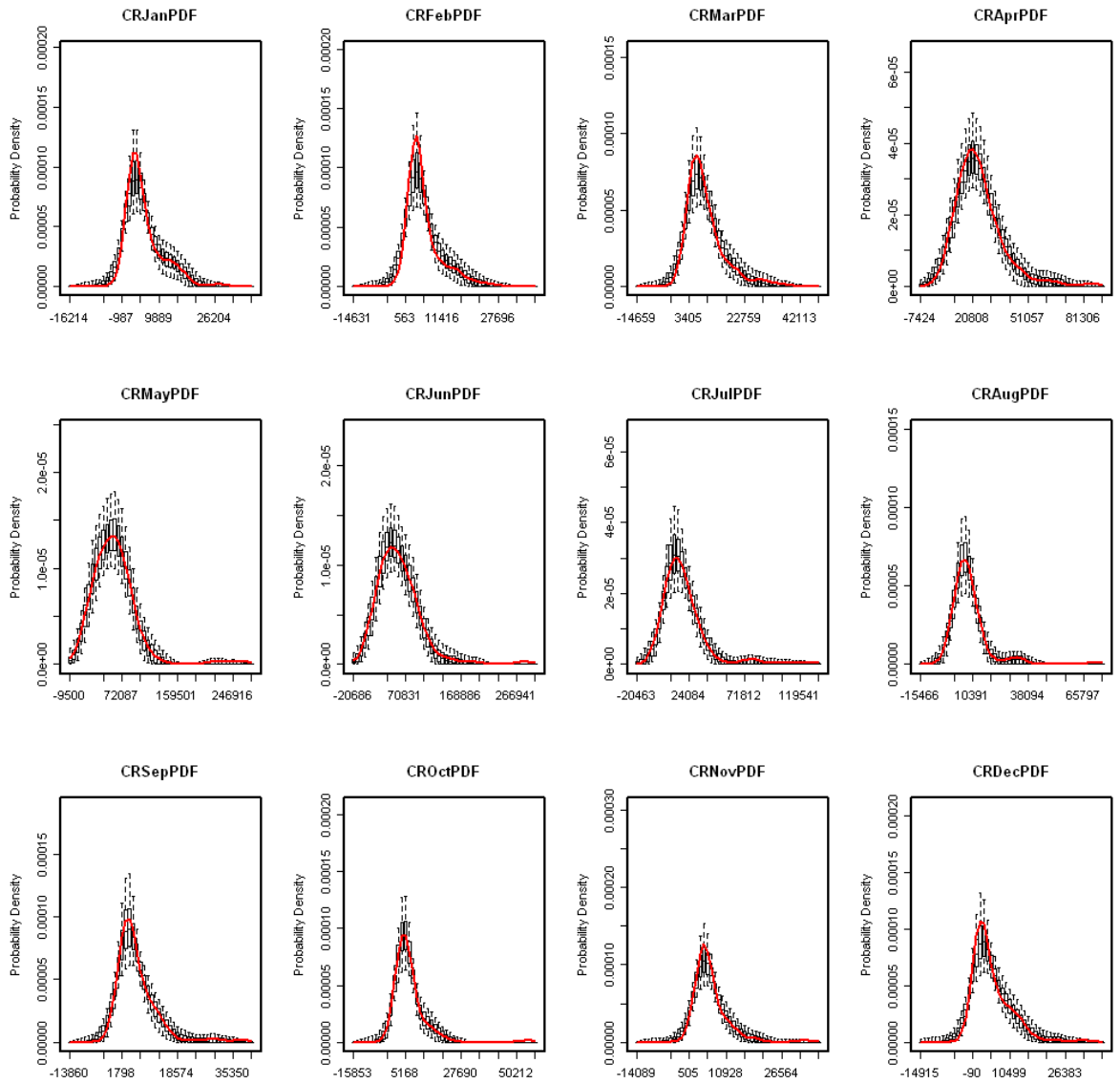


Figure 41 Monthly flow PDFs (acre-ft/yr) at site 3.

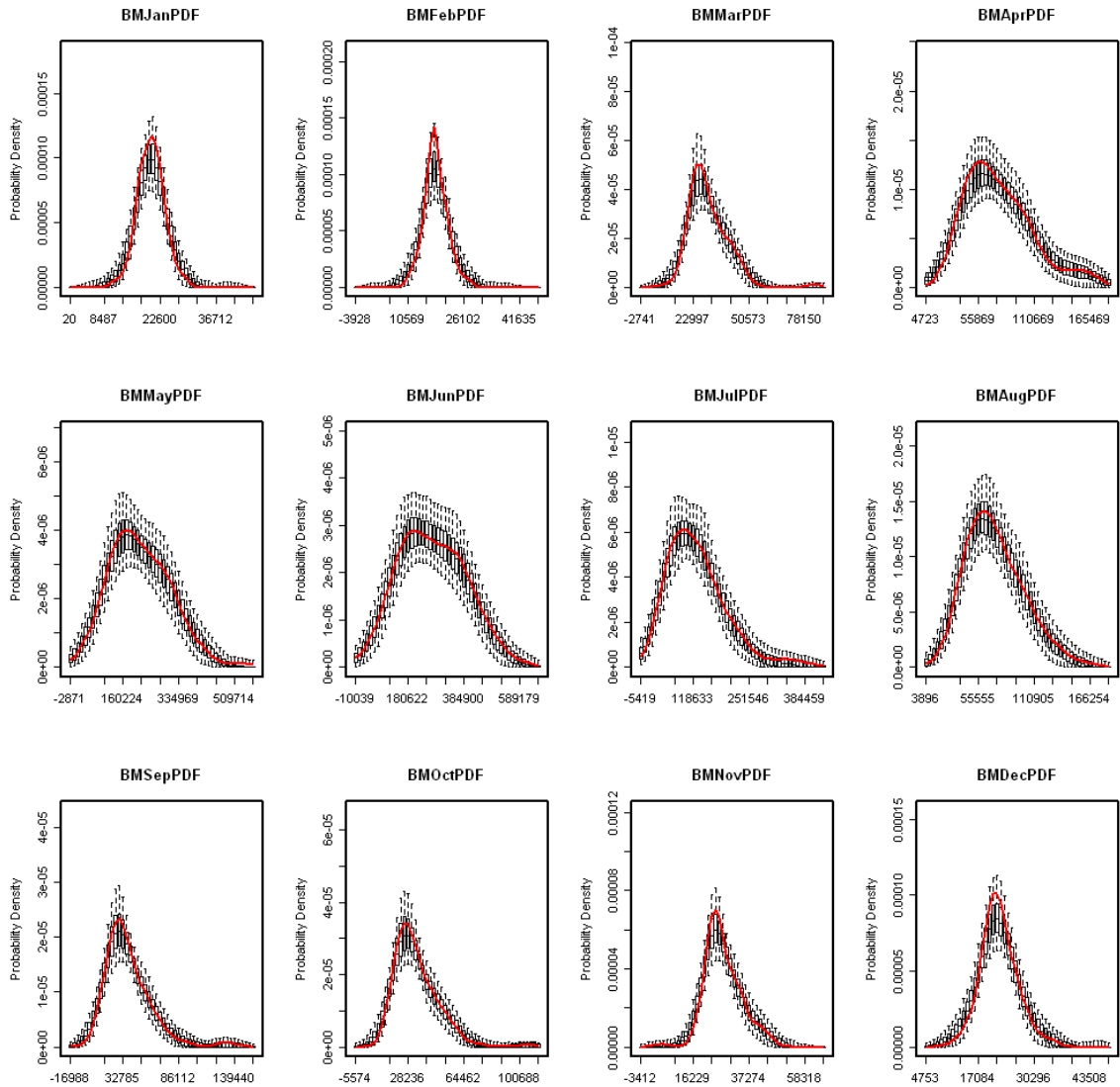
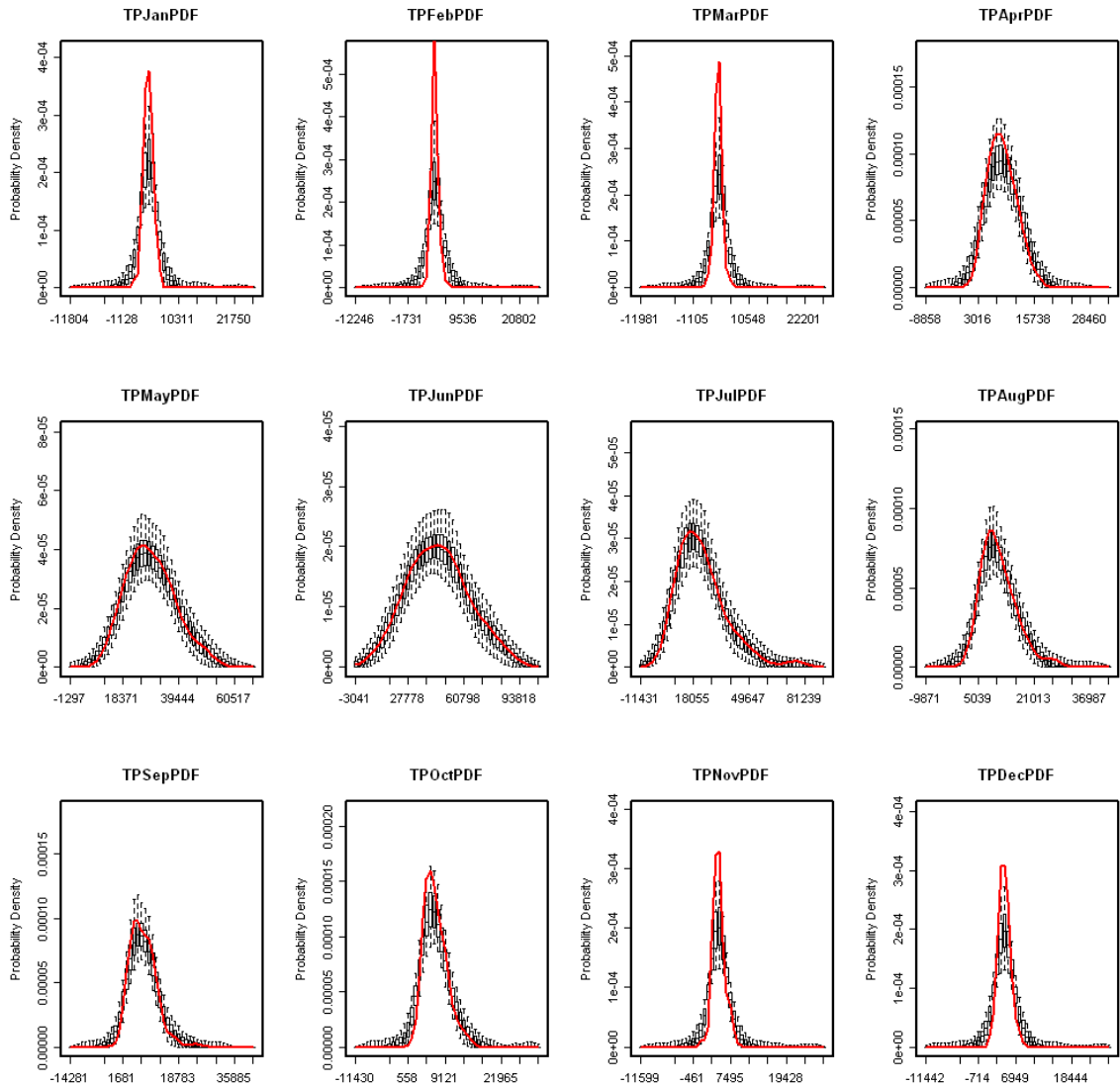


Figure 42 Monthly flow PDFs (acre-ft/yr) at site 2.



**Figure 43 Monthly flow PDFs (acre-ft/yr) at site 1.**

The boxplots of the basic statistics for the index gauge and the four sites are shown in Figure 45 through Figure 49. These plots show that for the most part, the statistics are reproduced well at both the annual and monthly timesteps throughout the basin. At all five locations, the January backward lag-1 correlation fails to be captured. This particular statistic relates the first month's flow of the current year with the last month's flow of the previous year. Since this correlation is not taken into account when selecting neighbors in the disaggregation process, it should be

expected that this poor reproduction would occur. This can be improved by including the flow from the last month of the previous year's disaggregation in the neighbor selection for the current year – but it tends to somewhat degrade the cross-correlation for the other months. Since January historically has very low flows, it was deemed the least important of the months to preserve.

The flows at the sites are ‘intervening’ flows, as was mentioned earlier – which means they can be negative, indicative of a losing reach. However, at site 1, which is the upper most gauge, flows should all be positive since the intervening flow and total flow are interchangeable for this reach. However, the disaggregation simulates negative values at site 1 (as can be seen in Figure 49) - this is most likely due to the large difference in flow magnitude between sites 1 and 2. An easy way around this issue is to use only those simulations with non-negative values at site 1. The other way is to slightly modify the disaggregation framework wherein, instead of disaggregating to sites 1-4 simultaneously, flow to site 4, site 3 and an aggregate of sites 1 and 2 is first split, thus reducing the number of locations to three. Once these values have been assigned, the observed data are used to determine monthly percentages representative of the flow breakdown between sites 1 and 2 from the “aggregate site.” This process ensures that flows above Taylor Reservoir will be positive and is based on reliable observed data. The schematic of this is shown in Figure 44.

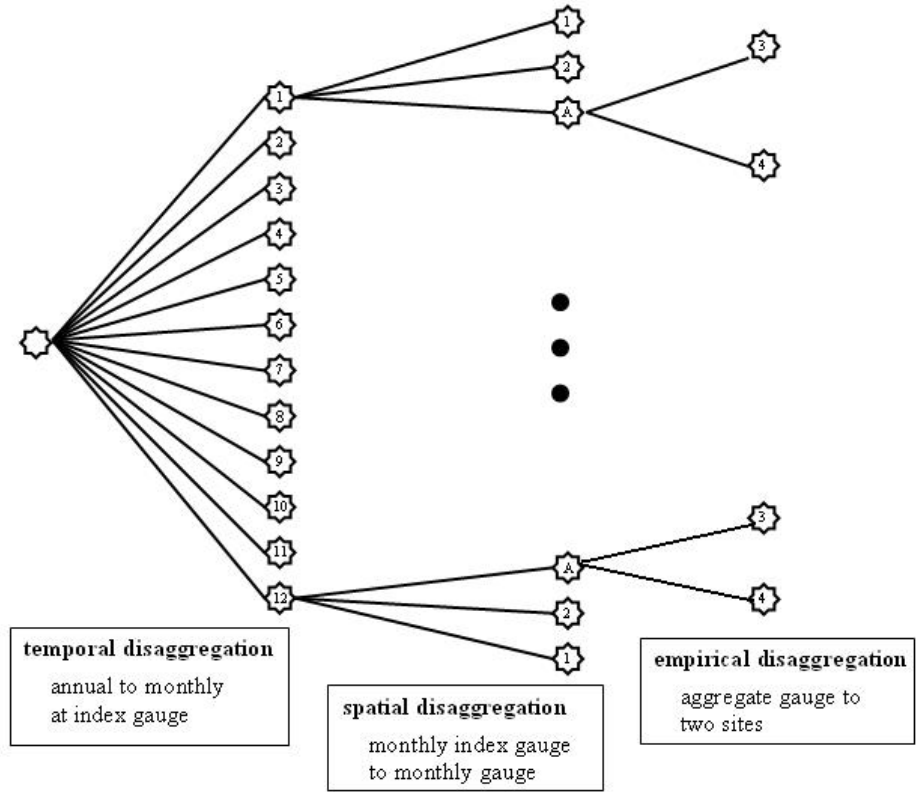


**Figure 44 Two step spatial disaggregation.**

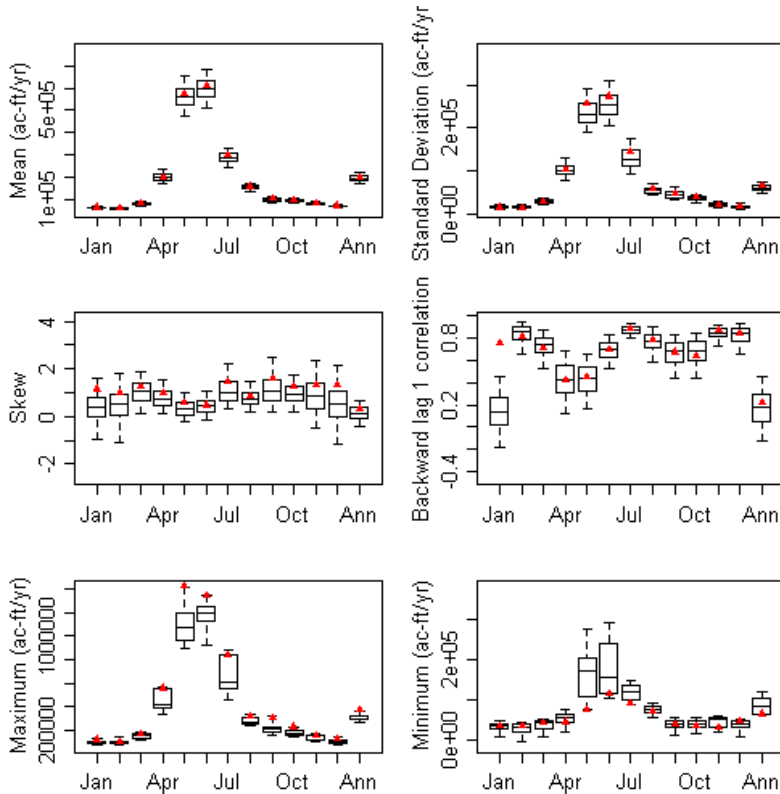


**Figure 45 Monthly statistics at the index gauge.**

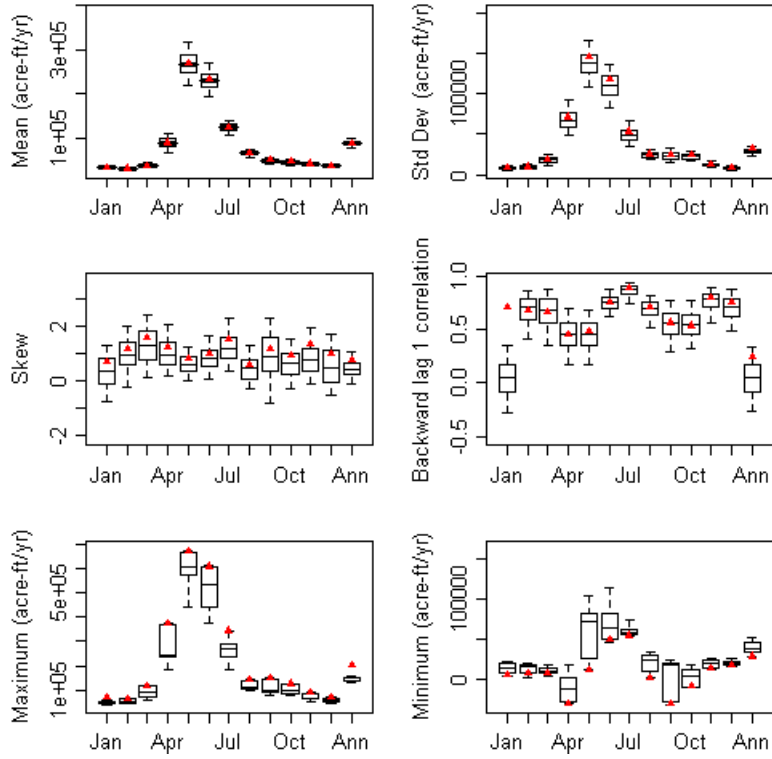


**Figure 46 Monthly statistics at site 4.**

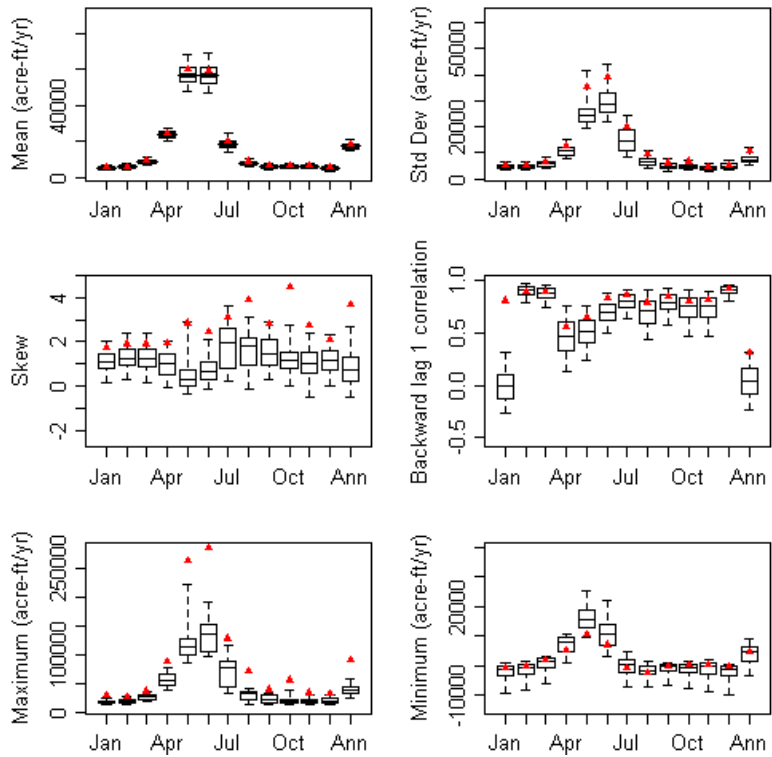


**Figure 47 Monthly statistics at site 3.**

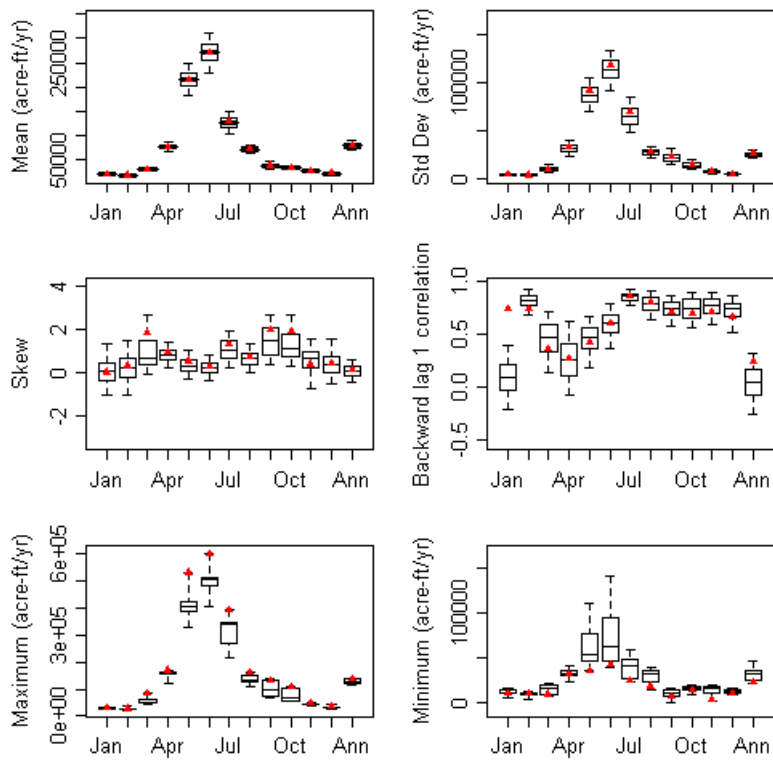


**Figure 48 Monthly statistics at site 2.**

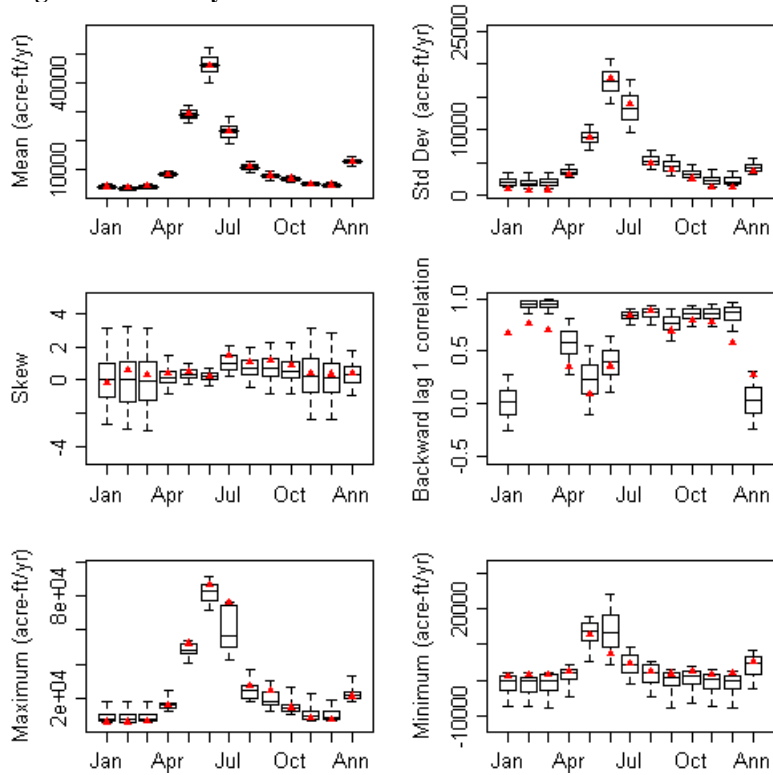


**Figure 49 Monthly statistics at site 1.**

One of the main drivers for the use of this space-time disaggregation technique is the need to capture the spatial and temporal correlations. Figure 50 shows the inter-month and month-annual correlation at the aggregate location of Site 4. The x-axis specifies the particular correlations - for example, 1-2 identifies the correlation between January and February, while 3-A depicts the March to annual correlation, and so on. This figure clearly shows that temporal cross-correlations are very well captured. Similarly, Figure 51 illustrates high effectiveness at reproducing spatial correlations at the monthly timestep. The annual spatial correlations are slightly overestimated by the disaggregation.

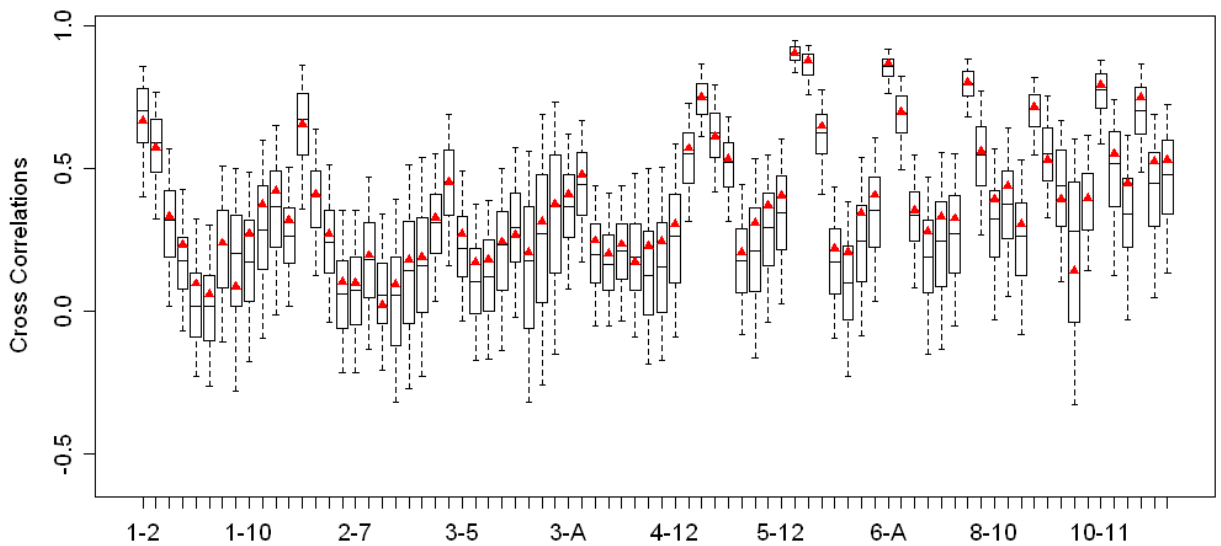


**Figure 50** Temporal correlations at site 4.

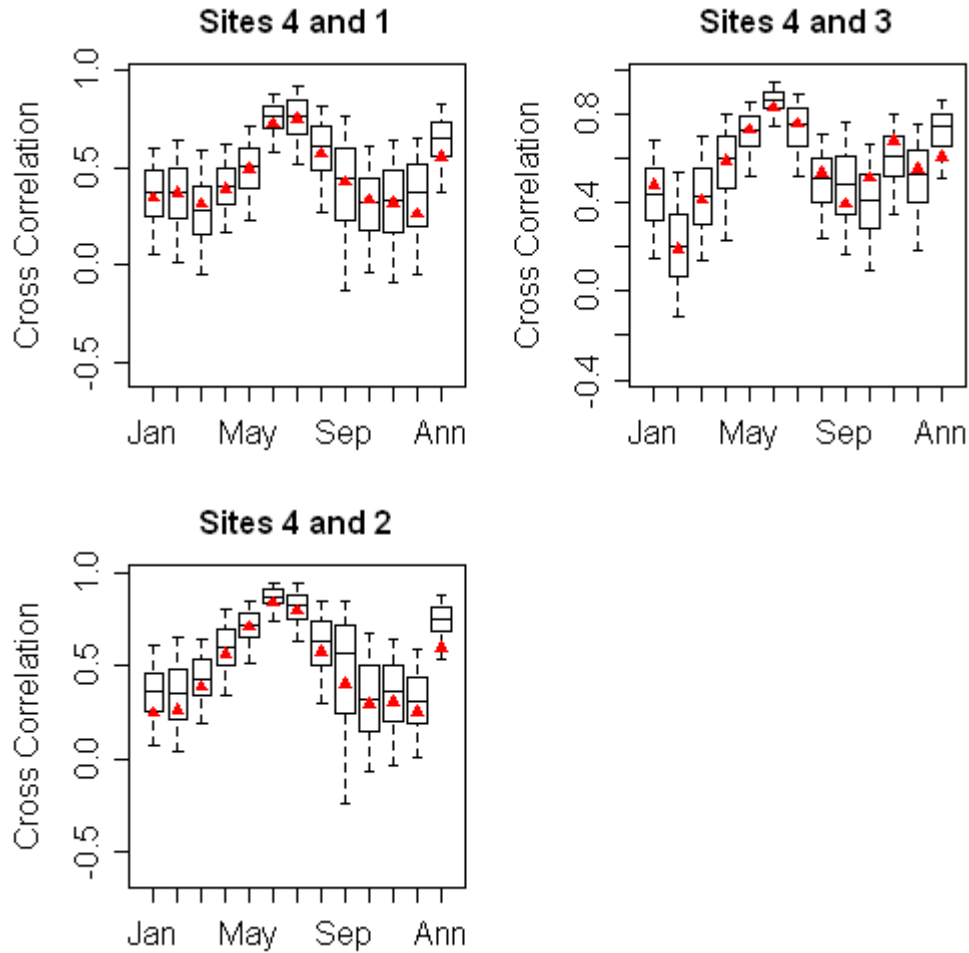


**Figure 51 Spatial correlations at monthly and annual timesteps.**

#### 4.6 Summary

The nonparametric KNN stochastic disaggregation technique of Prairie et al. (2007) was implemented for the Gunnison Basin, including the Aspinall Unit. The disaggregation method demonstrated great ability to capture all the distribution and cross correlation features present in the data. This method is simple to implement and robust relative to traditional methods. The utility of this technique is substantial in that the user must only generate annual flows at the aggregate location, in order to obtain values throughout the basin at a monthly timestep

## **CHAPTER 5: ASPINALL UNIT OPERATIONS MODELING**

### **5.1 Introduction**

The previous chapters provided a thorough investigation into the generation of stochastic flow sequences, identifying strengths and weaknesses of techniques and data. From this, we present a K-Nearest Neighbor bootstrap and Non-Homogeneous Markov model to generate single-site, annual flow traces, followed by a nonparametric space-time disaggregation. This provides robust, synthetic data that can be used for a variety of water management applications. Chapter 5 utilizes these two data sets to drive a model of the Gunnison River Basin under two operational regimes - a no action condition (current operations) and policies designed to meet the recommended fish flows (RFF). The goal is to demonstrate the utility of using synthetic hydrologies when assessing policy changes such as those anticipated as a result of the Aspinall Unit Operations EIS.

### **5.2 Water Management and Need for Modeling Tools**

Over time, water management has become an increasingly complex task due to competing demands (e.g., diversions, storage, hydropower facilities, environmental needs, recreation, etc) that must be considered when allocating water. This challenge is not specific to the southwestern United States, but rather a global issue facing water managers worldwide. As demands continue to increase and systems become more complex, it is necessary to examine and explore different management strategies under a variety of hydrologic conditions, to allow for future planning and optimization of water use. Thus, the need for a flexible water management tool is presented.

One such tool is Riverware, an extremely versatile basin modeling tool, developed by CADSWES (Center for Advanced Decision Support for Water and Environmental Systems) at the University of Colorado Boulder (Zagona et al., 2001). Riverware has proven highly effective due to its adaptability to model any basin and it is used by numerous agencies including United States Bureau of Reclamation, Tennessee Valley Authority and the Army Corps of Engineers. A graphical user interface (GUI) is employed in Riverware, allowing water managers/modelers to “click and drag” objects to represent reaches, diversions and reservoirs into the modeling canvas. Within each object, there are slots for user-defined values (e.g., reach routing parameters, reservoir storage volume tables), as well as slots for model outputs (e.g., storage, flow, power generation, etc.). Objects can then be linked together (e.g., reservoir outflow to reach inflow) by the same “point and click” approach, thus creating a model of the entire basin.

In addition to being able to model virtually any basin, another strength of Riverware is the option to solve models in different simulation modes. The simplest is pure simulation, where the user must specify all inputs required to solve an object (e.g., for a reservoir, inflow, outflow and previous storage must be specified to return the current storage). Rule-based simulation allows a modeler to represent management strategies through the Riverware Policy Language (RPL) and then rank the rules based on priority. The RPL interface is also user friendly and employs a similar GUI structure for selecting expressions and functions that comprise the rules. In turn, the rules appropriately assign slot values during simulation based on seasonal demands, storage targets or power needs to name a few. This mode is particularly

useful when assessing a given management strategy under a variety of hydrologic conditions. For the purpose of this work, rule-based simulation will be employed so as to analyze the basin policies under the simulated hydrologies of Chapters 2 and 3. A total of four simulations are run, each hydrology under the requirements of the EIS and the current no action policies. A description of the Gunnison River Basin is first presented, followed by a background of the Aspinall Unit EIS process, then a detailed account of the modeling and finally results/discussion.

### **5.3 Aspinall EIS**

The National Environmental Policy Act (NEPA) process governing the Aspinall Unit EIS began in the late 1990's as a component of the Upper Colorado River Recovery Implementation Program (Recovery Program). The Recovery Program was established in 1988 to aid in the revival of four endangered Colorado River fish species (Humpback Chub, Bonytail, Colorado Pikeminnow and Razorback Sucker). The Colorado Pikeminnow and Razorback Sucker can be found in the Gunnison River, while the Bonytail and Humpback Chub reside downstream of the confluence with the Colorado River. Therefore, the focus of the Aspinall Unit EIS is on the Pikeminnow and Razorback Sucker. However, the other species will undoubtedly benefit from the recommended flows as well. The Recovery Program has five specific components; habitat management, habitat development, non-native species management, endangered fish propagation and stocking and research/monitoring. The RFF specifically address the habitat management portion of the Recovery Program (USBR, 2004a).

As discussed in Chapter 1, the recommended flow for a particular year is dependant upon the forecasted runoff season (April-July) inflow to the basin. This forecast is identified as being in one of six hydrologic states ranging from wet to dry (Table 2). Corresponding to each state are minimum base flow values for the summer, fall and winter seasons (Table 4). The state also determines the number of “high flow” days for the spring season, in an effort to restore a more natural hydrograph that will improve fish habitat (Table 3). The “high flow” days are broken into ½ bank and full bank discharges, and for each state a range for both is specified. Furthermore, each state specifies an instantaneous annual peak flow value. These large releases aim to inundate flood plains and generate off-channel habitats rich in food for growth and development. High flows are necessary for effective sediment transport to remove silt and restore cobble substrate breeding habitats, while also serving as a spawning cue for the fish. These recommendations are to be met at USGS gauge number 09152500 near Grand Junction (USFWS, 2003).

<b>Hydrologic Category</b>	<b>Description</b>
Wet	(0—10% exceedance)—A year during which the forecasted April—June runoff volume has been equal or exceeded in 10% or less of the years since 1937.
Moderate Wet	(10—30% exceedance)—A year during which the forecasted April—July runoff volume has been equaled or exceeded in 10—30% of the years since 1937.
Average Wet	(30—50% exceedance)—A year during which the forecasted April—July runoff volume has been equaled or exceeded in 30—50% of the years since 1937.
Average Dry	(50—70% exceedance)—A year during which the forecasted April—July runoff volume has been equaled or exceeded in 50—70% of the years since 1937.
Moderate Dry	(70—90% exceedance)—A year during which the forecasted April—July runoff volume has been equaled or exceeded in 70—90% of the years since 1937.
Dry	(90—100% exceedance)—A year during which the

	forecasted April—July runoff volume has been equaled or exceeded in 90% or more of the years since 1937.
--	--

**Table 2 Hydrologic categories. (source: USFWS, 2003)**

Hydrologic Category	Flow Target and Duration		Instantaneous Peak Flow (cfs)
	½ Fullbank Discharge Days/Year ≥ 8,070 (cfs)	Fullbank Discharge Days/Year ≥ 14,350 (cfs)	
Wet	60-100	15-25	15,000-23,000
Moderate Wet	40-60	10-20	14,350-16,000
Average Wet	20-25	2-3	≥14,350
Average Dry	10-15	0	≥8,070
Moderate Dry	0-10	0	≥2,600
Dry	0	0	900-4,000

**Table 3 Gunnison River spring flow recommendations. (source: USFWS, 2003)**

Hydrologic Category	Gunnison River at USGS gauge 09152500 (cfs)
Wet	1,500-2,500
Moderate Wet	1,050-2,500
Average Wet	1,050-2,000
Average Dry	1,050-2,000
Moderate Dry	750-1,050
Dry	750-1,050

**Table 4 Summer, fall and winter recommended flow ranges for Gunnison River. (source: USFWS, 2003)**

## 5.4 Basin Description and Operations

### 5.4.1 General Overview

The Gunnison River is located on the western slope of the Rocky Mountains and is a major tributary of the Colorado River, draining roughly 8,000 mi<sup>2</sup>, approximately half of which is regulated by the Aspinall Unit and Taylor Park Reservoir (Figure 52). Completed in 1977; the Aspinall Unit is comprised of three power-generating reservoirs; Blue Mesa, Morrow Point and Crystal. These reservoirs

have a combined capacity of 291 MW, over half of which is located at Morrow Point. Furthermore, Morrow Point and Crystal have a combined storage of approximately 143,190 acre-ft, while Blue Mesa can store over 940,000 acre-ft. Thus, Blue Mesa serves primarily as a storage reservoir to meet downstream demands, while Morrow Point and Crystal focus on maintaining optimal pool levels for the generation of hydropower. Taylor Park has no power generating capacity, and thus serves mainly to meet downstream demands. In addition to these dams, another major anthropogenic impact is the Uncompahgre Project, in which trans-basin deliveries are made via the Gunnison Diversion Tunnel, located just downstream of Crystal Reservoir. The Diversion Tunnel has a capacity of 1,300 cfs and is almost six miles long. At the outlet, water enters a series of canals before eventually meeting the Uncompahgre River to supply irrigation demands.

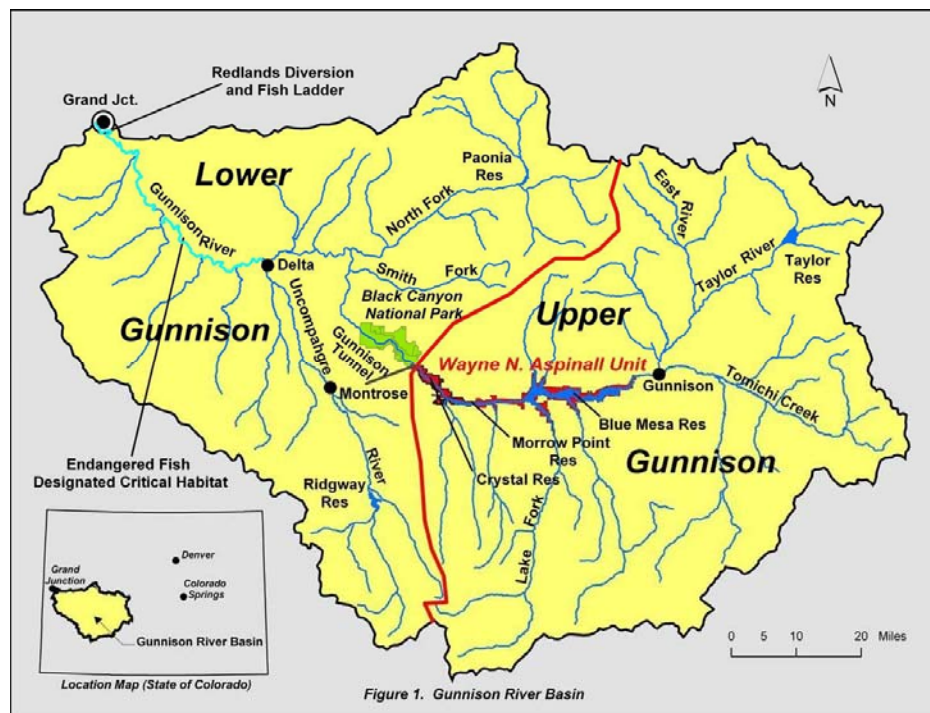
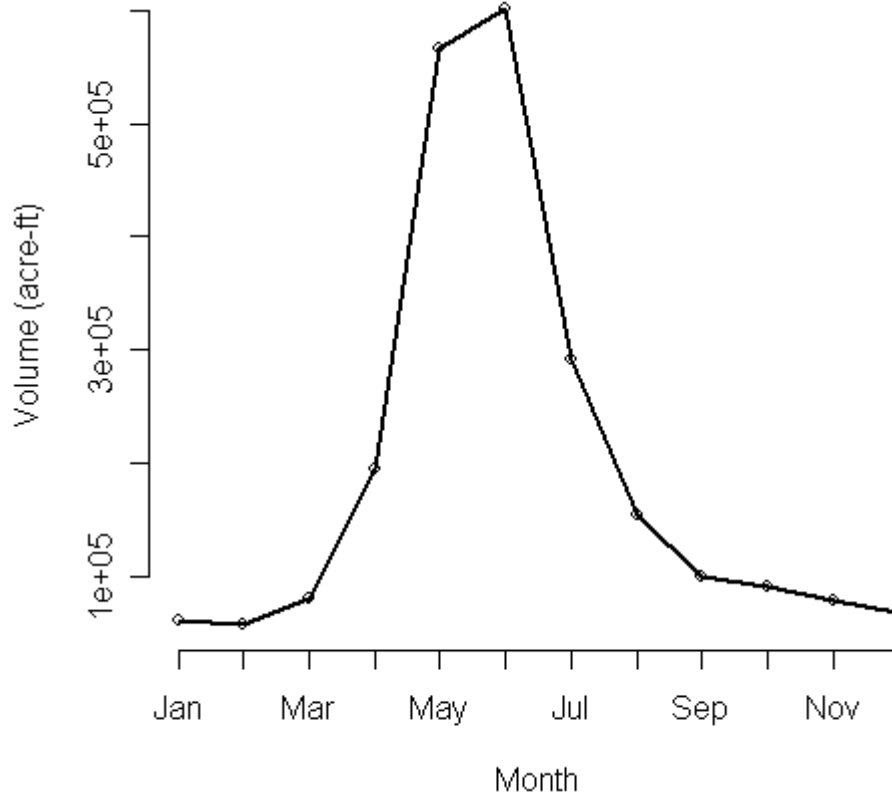


Figure 52 Gunnison River Basin. (source: USBR, 2004b)

In addition to the Aspinall Unit, other noteworthy components of the Gunnison River Basin include Curecanti National Recreation area and the Black Canyon of the Gunnison National Park. These areas attract visitors for a variety of recreational activities including hiking, camping, boating and fishing. The Black Canyon of the Gunnison has been designated a gold medal fishery by the Colorado Division of Wildlife and Taylor River provides excellent opportunities as well, drawing anglers from across the country. Blue Mesa is also a recreation destination, as it is the largest body of water in Colorado. As a result, the region receives well over a million recreational users annually, which is undoubtedly a large portion of the local economy. Thus, environmental preservation is of great importance.

Like many basins in the state of Colorado, the Gunnison has a snowmelt driven annual hydrograph, as seen in Figure 53. Such basins receive a majority of their annual flow during the spring melt period. For the Gunnison, the run-off season typically occurs from mid April to early July. Thus, there is a need for storage reservoirs to reliably supply water throughout the year, especially for summer irrigation demands, while also providing flood control. The objectives of the Aspinall Unit are precisely these: flood control, storage and the generation of hydropower. Enhancement of fish, wildlife and recreation are also considered to be primary objectives of the Unit. With so many objectives, effective management of the unit is vital to the surrounding area. The following aims to demonstrate the utility of using synthetic traces when evaluating operational implications of meeting new objectives, such as the RFF.



**Figure 53 Gunnison River natural flow hydrograph near Grand Junction.**

The following provides a brief outline of operational strategies at the four reservoirs.

#### **5.4.2 Taylor Park**

Taylor Park, like the Gunnison Diversion Tunnel, is part of the Uncompahgre Project and was constructed approximately thirty years prior to the Aspinall Unit. During the pre-Aspinall unit period, it provided the storage and releases to meet demands at the Diversion Tunnel. However, with the construction of the Aspinall unit, particularly the large storage/flexibility at Blue Mesa, the importance of Taylor Park has been reduced. Furthermore, there is no hydropower capacity at Taylor Park, and thus, it serves only as a storage reservoir. The primary objectives are to maintain

storage within a target range of approximately 25,000 acre-ft to 106,000 acre-ft (max capacity) and provide seasonal flows (fish flows and tunnel diversion).

### **5.4.3 Blue Mesa**

Blue Mesa has over six times the storage of the other three reservoirs combined, providing the ability to smooth inter-annual flow variability and meet growing demands. Thus, meeting demands downstream of the Aspinnall Unit is the largest operational goal at Blue Mesa. Fish flows and the Diversion Tunnel dominate the downstream demands; therefore, releases are made to supplement the forecasted local inflow so as to meet the required flows. Under the RFF, baseflows are specified at USGS gauge number 0912500 near Grand Junction (Table 4), but there must also be a minimum instream flow of 300 cfs throughout the entire reach from Crystal to the gauging station. Blue Mesa's operations are also aimed at maximizing hydropower output, which is primarily accomplished by minimizing spill (releases not through turbines) whenever possible. Releases also seek to minimize spilling at the downstream reservoirs, thus maximizing power for the Unit as a whole. Several seasonal targets help to meet these operational goals. The first is to draw down the storage by the end of December to approximately 585,000 acre-ft, thus providing ample available storage to capture spring run-off, control flooding and eliminate icing problems. Second, the reservoir should amass a storage of 803,000 acre-ft (roughly 95% capacity) during the filling season (April-July), ensuring the ability to meet the diversion requests and high fish flows.

#### **5.4.4 Morrow Point and Crystal**

The main purpose of Morrow Point and Crystal is to generate hydropower. These reservoirs have relatively small storage capacities that, alone, are ineffective at meeting downstream demands. Thus, pool elevations are maintained at optimal levels for power generation and releases from Blue Mesa to meet demands are effectively “passed through.” Also, spill is minimized at all times, although this is mainly controlled by Blue Mesa, because the nominal storage capacities of Morrow Point and Crystal provide little ability to absorb a large inflow.

#### **5.5 Modeling**

In order to provide a realistic but simple analysis of Gunnison River Basin operations, it was decided that modeling should occur at the monthly timestep. This is a logical choice because monthly modeling is fine enough to capture the seasonality of flows while avoiding the complexities of daily operations. Thus, the Riverware model developed and utilized by Regonda (2006) was adapted for the purposes of this work. A screenshot of the model can be seen in Figure 54. The four major reservoirs are clearly represented, as is the Diversion Tunnel. Flow data and demands are contained within the EISData and MiscData data objects (square yellow icons not linked to the basin model). The intervening flows obtained in Chapter 4 through the space-time disaggregation serve as model inputs at five locations; Taylor Park Inflow, Gunnison Above Blue Mesa Local Inflow, Gunnison Above Morrow Point Local Inflow, Gunnison Above Crystal Local Inflow and Gunnison Below Crystal Local Inflow. The unmodified rule set from Regonda (2006) serves as a no action model, while this work develops rules to govern operations under the RFF. Hence, with three hydrology data sets to drive the model (observed, KNN and NHM)

and two operational policies, a total of six modeling scenarios are conducted to assess the results from the different stochastic techniques and rulesets. The following describes the EIS and no action rulesets used in the modeling process presented on a per reservoir basis.

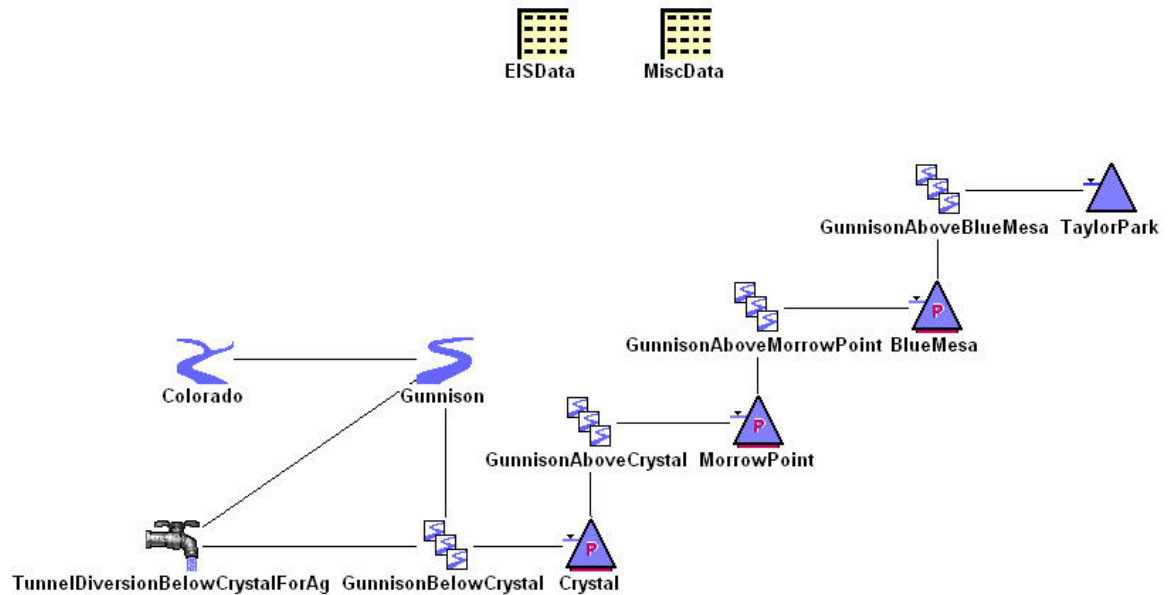


Figure 54 Riverware model.

## 5.5.1 No Action

### 5.5.1.1 Taylor Park Reservoir

1. Solve Taylor Park demand by subtracting downstream intervening flows from required flows (e.g., Diversion Tunnel, spawning releases).
2. Release from the reservoir is the larger of the minimum outflow and the computed demand, unless storage drops below the target range, in which only the minimum release is made.

3. At any time, reservoir elevation is neither allowed to go below its suggested minimum elevation (9270 feet) nor is allowed to exceed its maximum elevation (9328 feet).

#### **5.5.1.2 Blue Mesa Reservoir**

4. Solve Blue Mesa demand by subtracting downstream intervening flows from required flows (e.g., Diversion Tunnel, spawning releases, etc.).
5. During irrigation season (March – September), reservoir releases are made to meet the following goals
  - (a) fill reservoir by end of July to prepare for summer demands;
  - (b) satisfy downstream demands;
  - (c) avoid unnecessary spilling.
6. For winter season (October – February), demands are estimated and releases made to
  - (a) continue to meet downstream demands;
  - (b) bring BM elevation down to 7490 feet or lower by end of December;
  - (c) maintain consistency in river levels throughout rest of the winter.

#### **5.5.1.3 Morrow Point Reservoir**

7. Solve so as to maintain optimal power producing storage.
8. If reservoir spills unnecessarily, then attempt to modify Blue Mesa Reservoir releases, which is the only controllable source of reservoir inflows.

#### **5.5.1.4 Crystal Reservoir**

9. Solve so as to maintain optimal power producing storage.
10. If reservoir spills unnecessarily, then attempt to modify Blue Mesa Reservoir releases, which is the only controllable source of reservoir inflows.

Furthermore, all reservoirs are operated so as to maintain storage within a target range, while always meeting the minimum flow of 300 cfs. This prevents reservoir drying at the occasional cost to downstream demands (Regonda, 2006).

#### **5.5.2 RFF Policy**

Under the policy designed to meet the RFF, current objectives of the Aspinall Unit will not change. Thus, the above no action ruleset is simply added to, in order to accommodate the additional demands with a few small modifications. A brief outline of the operating rules developed to satisfy the RFF are presented, followed by specific details.

1. In January of each year, the estimated April-July inflow to Blue Mesa is used to determine which one of the six previously discussed hydrologic states the current year falls into.
2. Based on the classification determined, target flows are set for the next 12 months.
3. The no action policies are implemented as described above, with the additional demands taken into account when computing releases.

For the purpose of this work, a perfect forecast is used to assign appropriate the hydrologic category for each year. This is possible because all monthly flows are

known at the start of each model run. In reality this is not the case – it has been shown that forecasts made before snowpack has fully accumulated have significant uncertainty (Regonda, 2006). One approach to address this is to perturb the perfect forecast by a percent that is consistent with the uncertainty in the actual forecasts.

Since the RFF are specified at timesteps finer than that of this model, it was necessary to convert the values to monthly volumes. For the summer, fall and winter baseflows, this was accomplished by selecting the median of the recommended range, computing a daily volume based on that flow and then multiplying by the number of days in the particular month. For the Gunnison Basin, peak run-off months are traditionally April – July, making it the logical spring release period. Within that range, the highest flows occur in May and June. For developing monthly spring flow volumes, the recommended flows (again, when a range was listed, the median value was selected) were distributed over the April-July period using the following process. Fullbank discharges are distributed in the high flow months of May and June with additional volume for the instantaneous peak flow requirement in May. Next, the halfbank discharges are distributed evenly between the unused portions of the April-May and June-July periods with priority on May and June. The remaining days of the entire April-July period are then set to the baseflow value. With flows assigned to each day in the spring period, these values are converted to daily volumes and summed for each month. These volumes represent the amount of water that, when properly released, will satisfy the RFF.

While the current operational objectives of the Aspinall Unit will remain a priority when trying to meet the RFF, certain aspects of the no action ruleset require

modification. Specifically, in order to meet the RFF during spring peak flows, rules which attempt to minimize spill can be overridden by the need for high volume releases. It should be noted that this only applies when the average daily release for a given month is greater than turbine release capacity. Thus, for a month that requires spill for a few days to meet the RFF, the average daily discharge is most likely still within the turbine release capacity and therefore, that spill is not documented in this modeling.

## **5.6 Validation and Results**

The purpose of this work is to demonstrate the use of synthetic hydrologies when assessing the impact of meeting the RFF on the Aspinall Unit. Thus, it should be verified that the additional operating policies developed meet the RFF. The validation is first presented, followed by modeling results. In the interest of brevity, the following presents modeling results from NHM inputs only – it will be shown that the KNN inputs produce very similar results.

Figure 55 shows the probability of modeled flows at USGS gauge number 09152500 near Grand Junction, not falling within the target range as specified by the RFF for the NA and RFF policies. These values are computed by dividing the number of times the flow near Grand Junction failed to be within the RFF range for a given month by the total number of times that month was modeled. The RFF policy shows considerable reduction in risk. However, it can be seen that some fish flow violations do occur. Under the RFF policy, the majority of violations occur in the period following peak run-off, when reservoirs are fullest. Furthermore, these failures to stay within the recommended range are mostly due to flows exceeding the

upper bounds of the range, not being too low. This suggests that a wetter than usual summer may present challenges for water managers when trying to maintain stable baseflows.

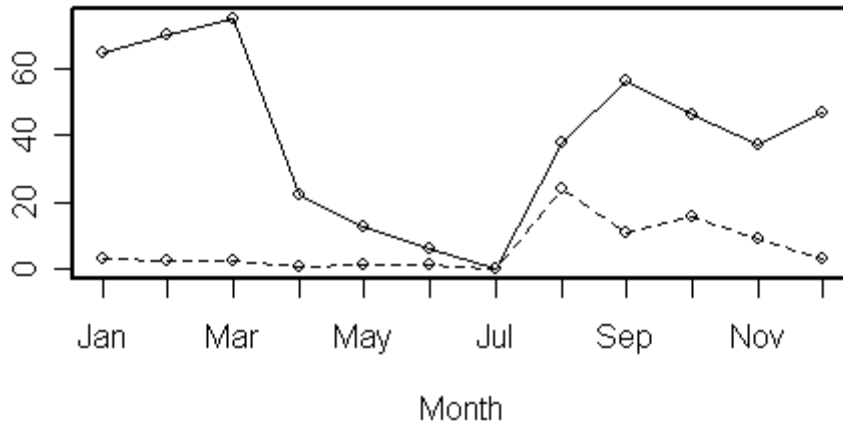


**Figure 55 Probability (%) of not meeting fish flows with NHM data inputs, RFF policy shown as dashed and NA policy as solid.**

In addition, the results of applying RFF policies based on the computed natural flow data are compared to those from modeling driven by the NHM data.

Figure 56 indicates that similar risk trends are found using both data sets.

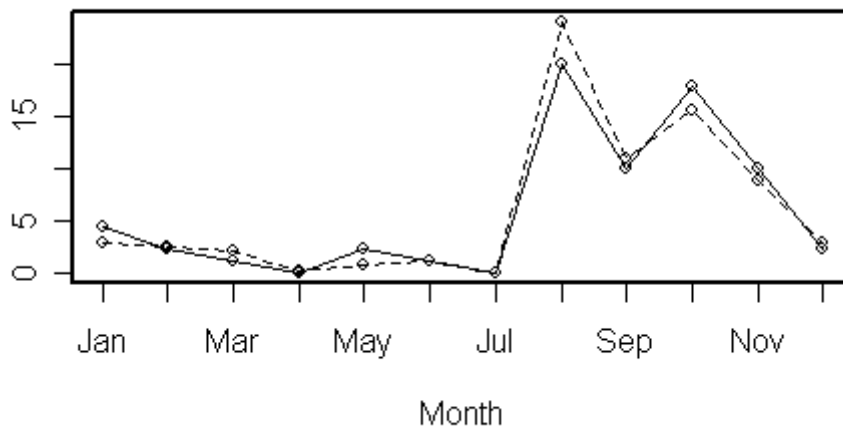


**Figure 56 Probability (%) of not meeting fish flows under RFF policy with results from NHM data inputs shown as dashed and computed natural flow inputs as solid.**

In order to assess the utility of synthetic hydrologies when investigating impacts of meeting the RFF, changes in storage, power generation and water spilled are compared based on modeling using computed natural flow versus synthetic data inputs.

As discussed earlier, Morrow Point has more than half of the power generating capacity of the Aspinall Unit, and thus it provides an effective way to gauge overall power production. It can be seen (Figure 57) that with both the RFF and NA policies, there is greater variability in hydropower generated under the synthetic hydrologies as compared to the computed natural flow data. For reference, annual generation under the various scenarios averaged in the low to mid 400 GWh range. Over the period of 1995-2004, Morrow Point annual production ranged from 200-510 GWh (USBR, 2005). Thus, the modeled results are realistic, but perhaps a little high. It should be noted that 1995-2004 includes the worst drought on record, and thus, may not be completely representative of the long-term averages. Furthermore, monthly modeling fails to capture day to day operations in which power may not be generated all of the time or perhaps turbines are taken offline for maintenance, etc., all resulting in a reduction in power generated. Also, hydropower is quite valuable in the December-March season, when winter temperatures are coldest and heating demands greatest. This will cause power authorities to request greater releases for hydropower during cold spells— a factor that is impossible to account for in most models.

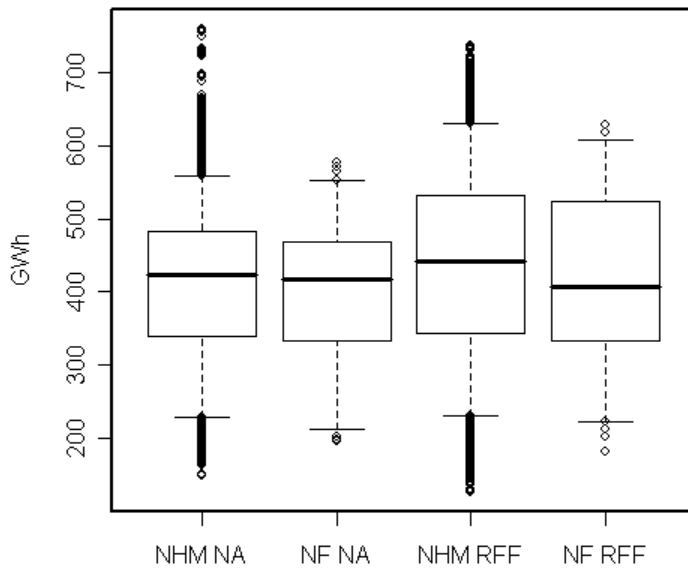
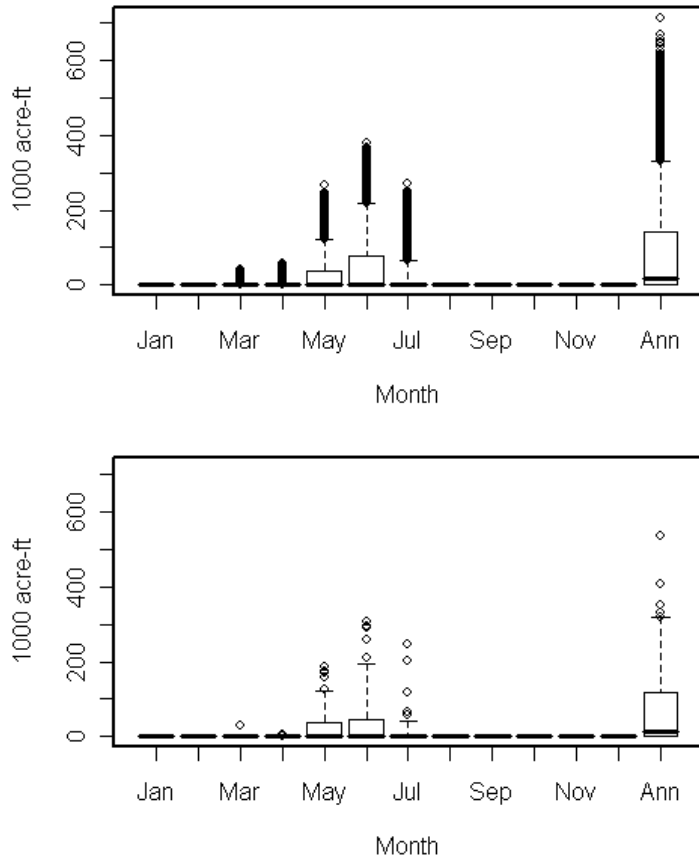


**Figure 57 Annual hydropower generation for Morrow Point under NHM and computed natural flow data inputs.**

Currently, the power generating facilities of the Aspinall Unit are operated in peaking mode, meaning that they provide supplemental power to the grid during times of high energy use (i.e., mornings and evenings – especially during summer months). This can still be accomplished at Morrow Point and Blue Mesa under the RFF policy, but Crystal will need to make more consistent releases to keep the fish flows stable near Grand Junction. These releases cannot be properly modeled at monthly timesteps – it is believed that daily modeling will uncover necessary changes in terms of day to day operations when comparing policies to meet the RFF and current policies. Thus, for this work, the best option available is to employ a power calculation method in which the computed release is divided into time at baseflow and time at “peaking release.” This provides realistic modeling of power generation given a monthly model. Again, daily modeling will undoubtedly provide the most insight regarding this topic.

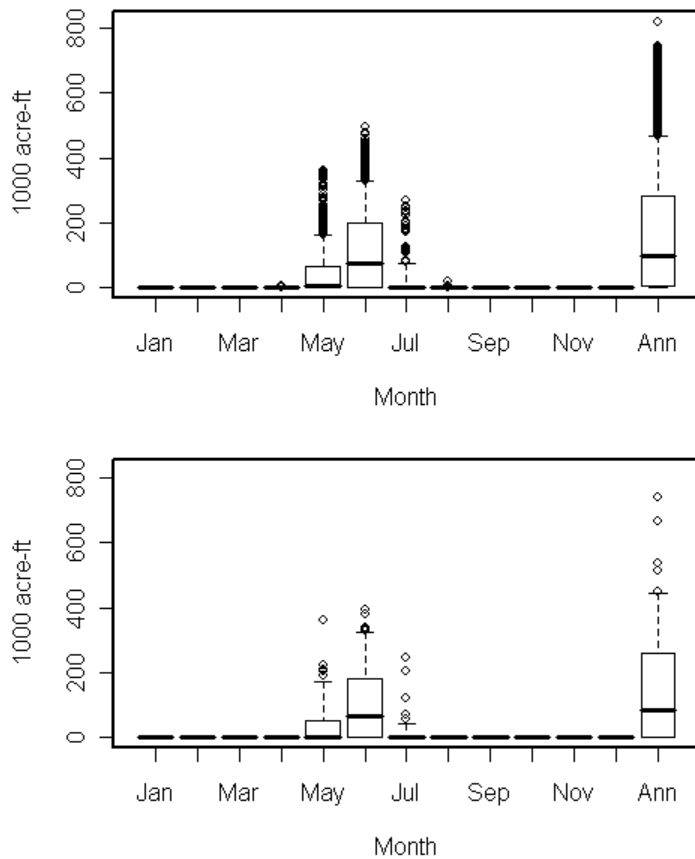
In most years, the total volume released from a given reservoir under both policies is quite similar. However, there is a difference in the distribution of that release. During the peak run-off season (April-July), both policies tend to make releases greater than the turbine capacities, and thus generate similar hydropower. For the rest of the year, the summer, fall and winter RFF releases are greater than those of the no action policy, thus producing more hydropower during this period, which accounts for slightly more power production under RFF policy (Figure 57).

Closely tied to the distribution of the releases is the volume of water spilled – that is, water released, but does not pass through a turbine to generate hydropower. Water managers attempt to minimize spill as much as possible because it wastes potential energy. Thus, when assessing new policies, changes in spill are of considerable interest. Figure 58 shows Blue Mesa monthly and annual spill for model runs driven by NHM and computed natural flow data. For the Aspinall Unit, spill at Blue Mesa is of particular interest because the reservoirs below are maintained at high pool elevations for optimal power generation. The implication of this is that spill from Blue Mesa generally causes Morrow Point and Crystal to spill as well. It can be seen that the general trend in spill is similar between the two scenarios; however, the NHM inputs provide more variability in the model results.



**Figure 58 Monthly and annual spill at Blue Mesa under RFF policy with NHM inputs (top) and computed natural flow data input (bottom).**

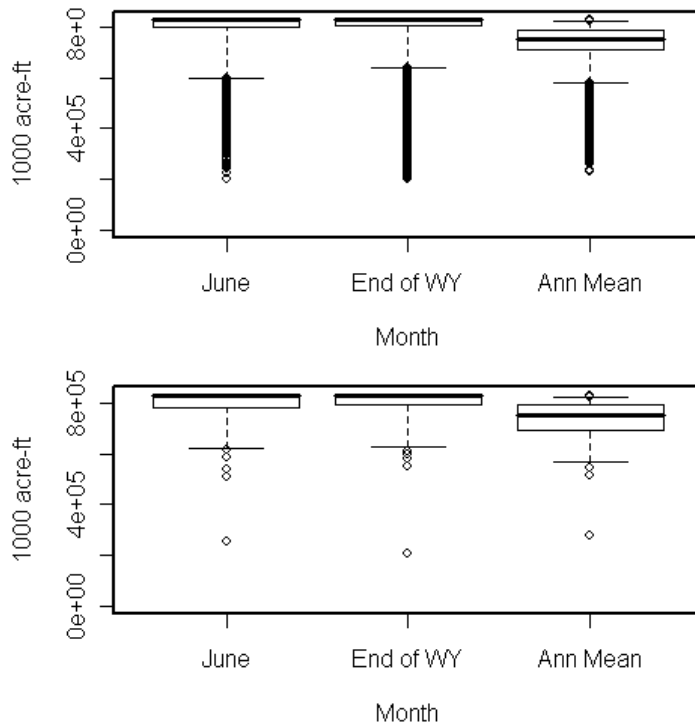
From the modeling results, the no action policy resulted in similar trends in seasonal spilling, with slightly more, in some cases, compared to the RFF policy (see Figure 58 and Figure 59). As discussed earlier, during the peak run-off season, both policies specify releases greater than the turbine capacities, thus resulting in spilled water. Therefore, the fish flows are often not the underlying factor contributing to spilled water. Furthermore, since the no action policy has fewer demands in the summer, fall and winter, pool elevations tend to remain higher throughout the year and thus, during drawdown and peak run-off, more water must be spilled to accommodate the additional water.



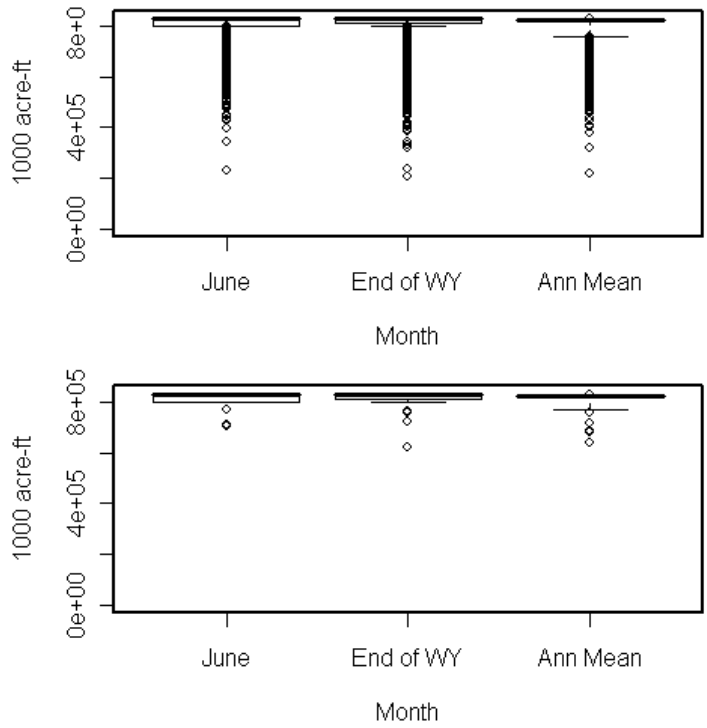
**Figure 59 Monthly and annual spill at Blue Mesa under NA policy with NHM inputs (top) and computed natural flow data input (bottom).**

Figure 60 and Figure 61 show Blue Mesa storage for key times during the year; Blue Mesa is of particular interest regarding storage, as it contains approximately 80% of the Aspinall Unit’s capacity. Increased demands throughout the year as a result of the RFF produce slightly less storage, as seen in Figure 60 compared to Figure 61 (NA policy). Under both NA and RFF policies, the NHM driven modeling results show more variability than those of the computed natural flow data. This further supports the use of synthetic hydrologies for such analyses. Crystal and Morrow Point both remained near full for all model runs, which is consistent with the operating policies discussed earlier. Taylor Park however, shows

significantly less storage under the RFF policy, compared to the no action alternative. It can be seen that storage approaches the upper and lower bounds of the acceptable range fairly frequently (Figure 62). This may seem peculiar, as Blue Mesa is considerably larger and could help to reduce the strain on the smaller reservoir. However, reverting back to goals of the Aspinall Unit, it is in the interest of generating hydropower that Blue Mesa maintains a high pool elevation. Taylor Park has no hydroelectric capacity, and thus, as long as the storage is maintained within the acceptable range, the results of the modeling are indicative of effective water management. This is allowed by the 1975 exchange agreement, in which storage can be transferred from Taylor Park to Blue Mesa to benefit the resources of the upper Gunnison Basin (USBR, 2008).



**Figure 60 Blue Mesa Reservoir Storage under RFF policy with NHM inputs (top) and RFF policy with computed natural flow data inputs (bottom).**



**Figure 61 Blue Mesa Reservoir Storage under NA policy with NHM inputs (top) and NA policy with computed natural flow data inputs (bottom).**

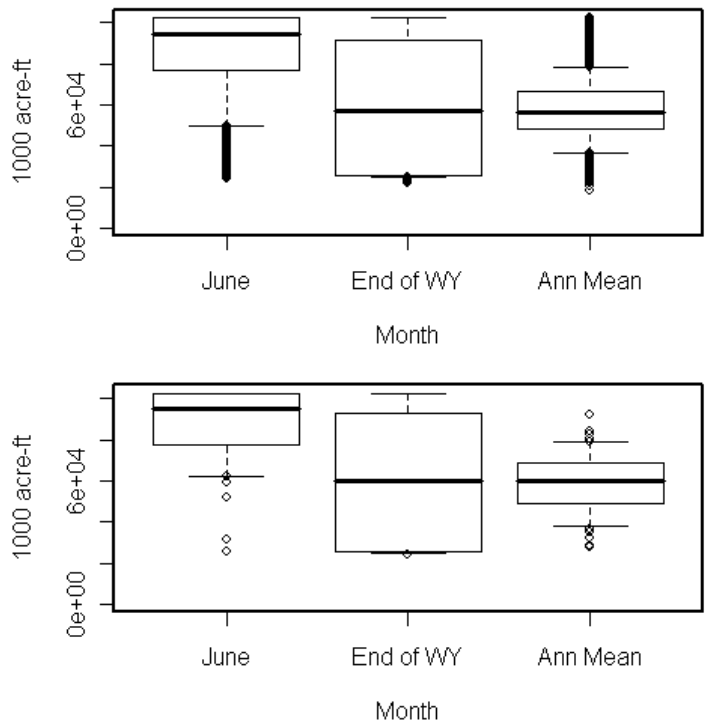


**Figure 62 Taylor Park Reservoir Storage RFF policy with NHM inputs (top) and computed natural flow data inputs (bottom).**

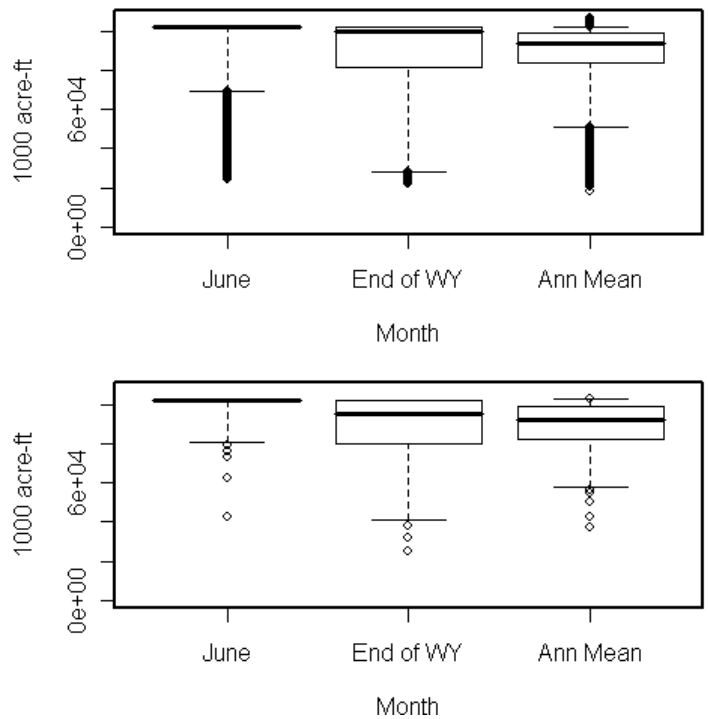


**Figure 63 Taylor Park Reservoir Storage under NA policy with NHM inputs (top) and NA policy with computed natural flow data inputs (bottom).**

Thus far, it has been shown that the RFF policy effectively meets the required fish flows while showing little impact on the operational objectives of the Unit. In some cases, specifically hydropower and water spilled, there were slight improvements over the no action policy. To investigate this, Figure 64 and Figure 65 show the modeled flow at USGS gauge 09152500 as monthly boxplots. The red triangles represent the average modeled flow using computed natural flow data from 1977-2006 to drive the model. Blue circles show the average monthly computed natural flow near Grand Junction for the same time period and green squares are monthly historic (as observed by gauging station) means, also from the 1977-2006 period. This makes for an effective comparison of the various points.

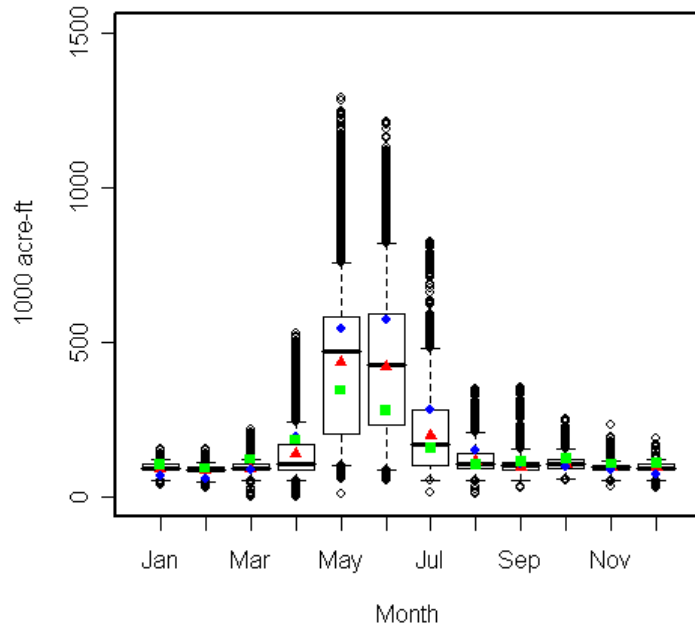


**Figure 64** Modeled flows at USGS gauge 09152500 under RFF policy and NHM input data. Blue circles represent average computed natural flow, red triangles the average modeled flow results using computed natural flow inputs and green squares the average historic data at this location, all from 1977-2006.

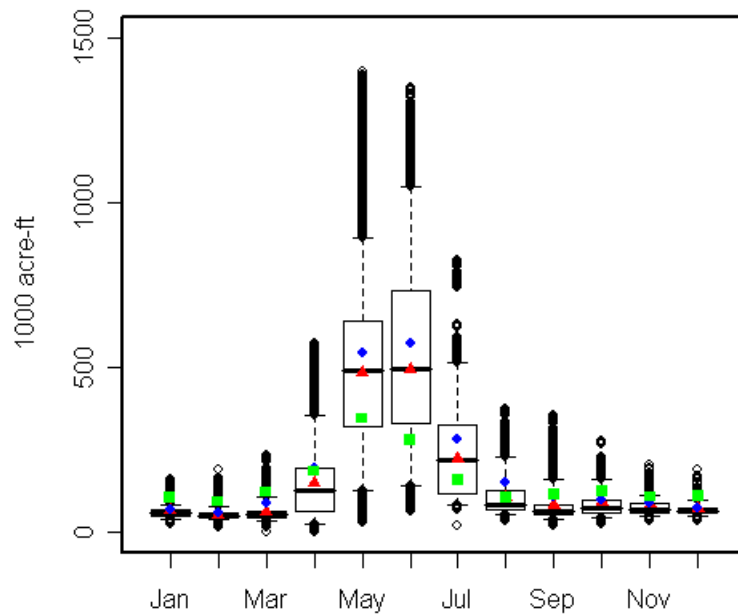


**Figure 65** Modeled flows at USGS gauge 09152500 under NA policy and NHM input data. Blue circles represent average computed natural flow, red triangles the average modeled flow results using computed natural flow inputs and green squares the average historic data at this location, all from 1977-2006.

The results from these plots are two-fold. As discussed earlier, the no action policy results in higher peak run-off releases, which corresponds with the slight increase in spill. Also, reduced releases throughout the rest of the year result in the lower hydropower production. The no action policy captures the computed natural flow data quite well, while the RFF policy mimics the historic (gauge data). In theory, the no action policy should have captured the historic, as it aims to model the current policy. Furthermore, the RFF hydrograph is more smoothed than that of the no action policy, which seems counter-intuitive because the RFF aim to restore natural “high flow” events.

The no action policy rules represent the broad operational objectives of the Aspinall Unit. However, these rules do not explicitly govern the operation of the Gunnison Basin; water managers make daily and even hourly decisions based on current and anticipated demands and conditions that simply can not be represented by the “if then” logic of modeling. Furthermore, while the Fish and Wildlife Service flow recommendations have only been officially available since 2003, water managers have attempted to make releases beneficial to fish, when possible, for some time now. Unofficial policies and nuances such as these contribute greatly to why the RFF policy seems to capture the observed flow more so than the NA rules.

## **5.7 Summary**

As mentioned earlier, the modeling results from KNN and NHM flows were similar enough to merit presenting NHM figures only. However, Crystal spill from modeling with NHM data and NA policies in Figure 66 shows slightly more variability than that of Figure 67 (modeled with KNN data). This is consistent with

the results of Chapters 2 and 3, as the NHM technique was shown to produce slightly longer periods of drought and surplus.

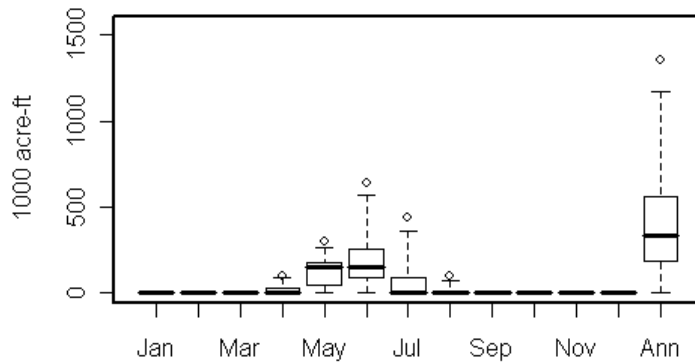


**Figure 66 Crystal spill results from modeling with NHM data and NA policy.**

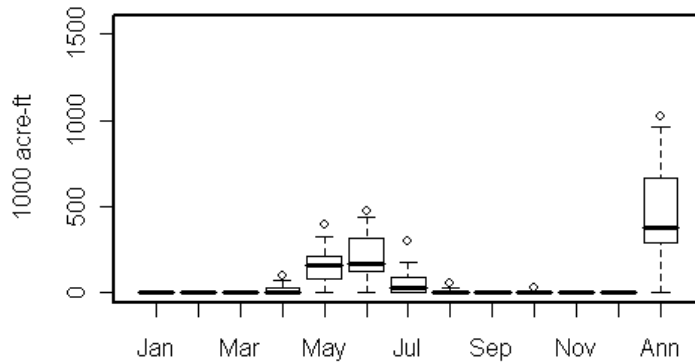


**Figure 67 Crystal spill results from modeling with KNN data and NA policy**

The results of this modeling effort have provided a broad overview of Aspinall Unit operations under two different policy sets. From the analysis, the no action results may not be completely indicative of current operations, however, there is undoubtedly a need for policy changes in order to accommodate the additional fish flows. Figure 65 suggests that the majority of these changes will occur on a daily timestep, as monthly releases to meet fish flows are consistent with the historic releases. Thus, the storage capacities of the four reservoirs should be able to effectively meet the various demands throughout the basin with high reliability. Furthermore, it should be noted that the RFF for a given year are dependant upon the

hydrologic state. For example, if due to climate change, the number of category wet years greatly reduces, water managers are not tied in any way to those flows - more years will simply fall in the dry categories. This also indicates that the system is robust enough to meet additional demands. Last, the modeled hydropower, spill and storage values all indicate that synthetic hydrologies such as those generated using the NHM and KNN techniques provide more variability than the observed data alone and thus allow for more robust modeling and risk analysis.

## **CHAPTER 6: CONCLUSION AND RECOMMENDATION FOR FUTURE WORK**

### **6.1 Conclusions**

This research develops a DSS model for the Gunnison River Basin and is driven by synthetic flow sequences in order to assess the implications of meeting the RFF and demonstrate the utility of stochastic techniques. This is accomplished through four phases, shown in Chapters 2 through 5. Techniques for generating flow sequences based purely on observed data are examined in Chapter 2. Methods for incorporating paleo reconstructed flows with the observed data are explored in Chapter 3 in order to introduce increased variability and capture long-term epochal trends. Chapter 4 employs a nonparametric space time disaggregation developed by Prairie et al. (2007) to break the single site annual hydrologies into monthly flows throughout the basin. A Riverware model of the Gunnison Basin is developed in Chapter 5, which uses the disaggregation results to model Aspinall Unit operations under a variety of hydrologic conditions, in addition to meeting new fish flows. This modeling provides a coarse overview of the operational changes necessary to comply with the RFF and the consequent impact on system components, such as hydropower and storage.

#### **6.1.1 Observed Data Techniques**

The findings from this effort can be summarized as follows. The KNN-bootstrap and modified KNN techniques generate a rich variety of flow sequences that also capture the statistical properties of the observed data. ISM and AR-1 models were also investigated; however, ISM is limited in the variety it can produce and ARMA based models fail to capture non-Gaussian distributions, as discussed in

Chapter 2. The rich variety of sequences from the nonparametric approach provide a better estimate of system risk/reliability, a useful strength in water management.

Beyond the evaluation of techniques, it is shown that the wet/dry state threshold (i.e., the median of the observed flow), used to compute the drought/surplus statistics, is somewhat subjective. Furthermore, such thresholds are sensitive to the length of the observed data. Thus, as the data set grows, a year classified as wet may become dry and vice versa. Therefore, a demand and storage based approach, such as the sequent-peak algorithm, seems to be a better way to quantify drought and surplus.

### **6.1.2 Paleo Techniques**

The techniques presented in this section allow for the generation of more varied traces, compared to the observed data only methods. In particular, the NHM approach is highly effective at introducing variability to the stochastic sequence generation process, while preserving distributional statistics. While it is slightly more intensive to implement than the other methods discussed, it has several benefits. By resampling transition probabilities to generate new binary sequences, an unlimited number of unique traces can be produced. Other techniques that can generate unseen traces compute a single transition probability matrix (TPM) for a portion of or the entire paleo record, resulting in undue smoothing or bias toward a particular transition, an obvious detractor. The epochal nature of the paleo data is undoubtedly reproduced to some extent by all methods; however, the NHM approach produces the most realistic results – longer periods of drought (or surplus) are generated with the possibility of an occasional wet (or dry) year interspersed.

This section also contributes to the stochastic modeling field guidelines for using the Least Squares Cross Validation (LSCV) method to select band widths for markov chain-type applications. Specifically, recommendations are made for how to proceed when no clear minimum is presented.

### **6.1.3 Flow Disaggregation**

The nonparametric disaggregation technique employed in Chapter 4 has substantial advantages over its traditional parametric counterparts. Results show successful preservation of distributional statistics in both space and time. Furthermore, observed spatial and temporal correlations are also reproduced quite well and at no increase in computational intensity. This is particularly significant as parametric methods are not effective at modeling non-linear correlations and quickly become intensive when attempting to capture these relationships at more than a few locations.

### **6.1.4 Application of Synthetic Flows to Gunnison Operations Model**

This section applies generated flows to a decision support modeling tool for the simulation of the Aspinall Unit operations. The stochastic flow sequences developed in Chapters 2 and 3, which are disaggregated to monthly intervening flows, drive this model. It is shown that the DSS model is effective at meeting the RFF in addition to the other downstream demands. The NHM and KNN techniques provide the flow sequence variability needed for robust planning applications. The results of the modeling effort led to the following conclusions. Monthly operations of the Aspinall Unit, specifically discharge volume, will change little to accommodate the fish flows; however, daily modeling of reservoir operations is recommended, as there

will need to be changes to the distribution of the release throughout the high flow months.

Hydropower generation, storage and spill results from modeling with the NHM flows all showed more variability, compared to the output when modeling with computed natural flow. Robust, stochastic sequences make it possible for water managers and policy makers to analyze a wide range of scenarios and appropriately characterize system risk and reliability. This information is useful in providing guidance when making necessary modifications to operating policies such as those currently being examined as part of the NEPA process governing the Aspinall Unit EIS.

## **6.2 Future Work**

### **6.2.1 Further Development of Paleo Techniques**

Chapter 3 discusses the importance of capturing the epochal nature of the paleo record in the stochastic flow traces developed in this work. This highlights the importance of properly understanding and modeling the sequencing of high and low flow events. To this end, a modification to the nonhomogeneous markov (NHM) technique is proposed. First, a smoothing of the paleo data is conducted (typically a 5 or 10 year moving average is sufficient) to identify wet and dry epochs. Next, TPMs are developed for the wet and dry epochs. The epoch signal (the smoothed data) is converted to 1 (wet epoch) and 0 (dry epoch) and resampled in blocks of the desired length. Then, based on the epoch at any given time and the hydrologic state of the previous timestep, the appropriate TPM is used to generate the current hydrologic state. Once the hydrologic states have been assigned, the KNN-based conditional resampling is used to assign observed flow magnitudes. This approach is expected to

produce similar results to the NHM, as it can generate new, previously unseen sequencing while still modeling the epochal nature of the data in a realistic manner.

### **6.2.2 Climate Change and Water Management**

The paleo data used in this work indicates that the pre-observational period was, on average, slightly more wet than the past century. This is undoubtedly useful information to water managers. However, it should be interpreted with caution, as the paleo record may not be indicative of future conditions. Factors such as global warming and anthropogenic basin impacts may shape future climate more so than the past trends. Incorporating the variability of the past with the predicted future trends will be the next step in generating flow sequences for reservoir management. Furthermore, developing operational policies that properly address such changes will be paramount for the future of the southwestern United States.

## REFERENCES

- Apipattanavis, S., G. Podesta', B. Rajagopalan, and R. W. Katz (2007), A semiparametric multivariate and multisite weather generator, *Water Resour. Res.*, 43, W11401, doi:10.1029/2006WR005714.
- Chourre, M. and S. Wright. "Population Growth of the Southwest United States, 1900-1990." *U.S. Geological Survey* (1997): <<http://geochange.er.usgs.gov/sw/changes/anthropogenic/population/>> (19 June 2008)
- Efron, B. (1982), *The Jackknife, the Bootstrap and Other Resampling Plans*, Society for Industrial and Applied Mathematics, Providence, RI.
- Fukunaga, K. (1990), *Introduction to statistical pattern recognition*, Academic, San Diego, California.
- Gosset C, Rives J, Labonne J. Effect of habitat fragmentation on spawning migration of brown trout (*Salmo trutta* L.). *Ecology of Freshwater Fish* 2006: 15: 247–254.
- Grygier, J.C. and J.R. Stedinger (1988), Condensed Disaggregation Procedures and Conservation Corrections for Stochastic Hydrology, *Water Resour. Res.*, 24(10), 1574-1584.
- Harms, A. A., and T. H. Campbell (1967), An extension to the Thomas-Fiering model for the sequential generation of streamflow, *Water Resour. Res.*, 3 (3), 653-661.
- Hidalgo, H.G., T.C. Piechota, and J.A. Dracup (2000), Alternative principal components regression procedures for dendrohydrologic reconstructions, *Water Resour. Res.*, 36(11), 3241-3249.
- Koutsoyiannis, D. (1992), A nonlinear disaggregation method with a reduced parameter set for simulation of hydrologic series, *Water Resour. Res.*, 28(12), 3175-3191.
- Lall, U. (1995), Recent advances in nonparametric function estimation: Hydraulic applications, *Rev. Geophys.*, 33, 1093-1102.
- Lall, U. and A. Sharma (1996), A nearest neighbor bootstrap for resampling hydrologic time series, *Water Resour. Res.*, 32(3), 679-693.
- Lane, W. L. (1979), *Applied stochastic techniques, users manual*, Engineering and Resource Center, Bureau of Reclamation, Denver, Colo.
- Lane, W.L. (1982), Corrected parameter estimates for disaggregation schemes, in *Statistical Analysis of Rainfall and Runoff*, edited by V. P. Singh, Water Resources Publications, Littleton, Colo.
- Loucks, D.P., J.R. Stedinger, and D.A. Haith (1981), *Water Resource System Planning and Analysis*, Prentice-Hall, Inc., New Jersey.

- Mejia, J. and J. Rousselle (1976), Disaggregation Models in Hydrology Revisited, *Water Resources Research*, 12(2), 185-186.
- Oliveira, G.C., J. Kelman, M.V.F. Pereira and J.R. Stedinger (1988), A representation of spatial correlations in large stochastic seasonal streamflow models, *Water Resour. Res.* 24(5), 781–785.
- Ouarda, T., J.W. Labadie, and D.G. Fontane (1997), Index sequential hydrologic modeling for hydropower capacity estimation, *J. of the American Water Resources Association*, 33(6), 1337-1349.
- Pereira, M.V.F., G.C. Oliveira, C.C.G. Costa and J. Kelman (1984), Stochastic streamflow models for hydroelectric systems, *Water Resour. Res.* 20(3), 379–390.
- Prairie, J. and R. Callejo (2005), *Natural flow and salt computation methods*, U.S. Dept. of Interior, Salt Lake City, Utah.
- Prairie, J.R., B. Rajagopalan, T.J. Fulp, and E.A. Zagona (2006), Modified K-NN model for stochastic streamflow simulation, *ASCE Journal of Hydrologic Engineering*, 11(4), 371-378.
- Prairie, J., B. Rajagopalan, U. Lall, and T. Fulp (2007), A stochastic nonparametric technique for space-time disaggregation of streamflows, *Water Resour. Res.*, 43, W03432, doi:10.1029/2005WR004721.
- Prairie, J., K. Nowak, B. Rajagopalan, U. Lall, and T. Fulp (2008), A stochastic nonparametric approach for streamflow generation combining observational and paleo reconstructed data, *Water Resour. Res.*, (in press).
- Rajagopalan, B. and U. Lall.(1999), A k–nearest-neighbor simulator for daily precipitation and other weather variables, *Water Resour. Res.*, 35(10), 3089-3101.
- Rajagopalan, B., U. Lall, and M.A. Cane (1997), Anomalous ENSO Occurrences: An Alternate View, *Journal of Climate*, 10(9), 2351-2357.
- Rajagopalan, B., U. Lall, and D.G. Tarboton (1996), Nonhomogeneous Markov model for daily precipitation, *Journal of Hydrologic Engineering*, 1(1), 33-39.
- Regonda, S.K. (2006), Intra-annual to Inter-decadal Variability in the Upper Colorado Hydroclimatology: Diagnosis, Forecasting and Implications for Water Resources Management, PhD thesis, University of Colorado.
- Rieman, B., Peterson, J.T., Clayton, J., Howell, P., Thurow, R., Thompson, W. and Lee, D., 2001. Evaluation of potential effects of federal land management alternatives on trends of salmonids and their habitats in the interior Columbia River basin. *Forest Ecology and Management*. 153, 43–62.
- Salas, J.D., J.W. Delleur, V. Yevjevich, and W.L. Lane (1980), *Applied Modeling of*

*Hydrologic Time Series*, 484 pp., Water Resources, Littleton, Colo.

- Santos, E.D. and J.D. Salas (1992), Stepwise Disaggregation Scheme for Synthetic Hydrology. *ASCE Journal of Hydrologic Engineering*, 118(5), 765-784.
- Sharma, A. and R. O'Neill (2002), A nonparametric approach for representing interannual dependence in monthly streamflow sequences, *Water Resour. Res.*, 38(7),1100, doi: 10.1029/2001WR000953, 2002.
- Sharma, A., D.G. Tarboton, and U. Lall (1997), Streamflow simulation: a nonparametric approach, *Water Resour. Res.*, 33(2), 291-308.
- Souza, F. A., and U. Lall, Seasonal to interannual ensemble streamflow forecasts for Ceara, Brazil: Applications of amultivariate, semiparametric algorithm, *Water Resour. Res.*, 39(11), 1307, doi:10.1029/2002WR001373, 2003.
- Tarboton, D.G., A. Sharma, and U. Lall (1998), Disaggregation procedures for stochastic hydrology based on nonparametric density estimation, *Water Resour. Res.*, 34(1), 107-119.
- Thomas, H.A., and M.B. Fiering, Mathematical synthesis of streamflow sequences for the analysis of river basins by simulation, *Design of Water –Resource Systems*, by A. Maass, M. M. Hufschmidt, R. Doffman, H. A. Thomas, Jr., S. A. Marglin, and G. M. Fair, Harvard University Press, Cambridge, MA., 1962.
- Thompson, P. D., and F. J. Rahel. 1998. Evaluation of artificial barriers in small Rocky Mountain streams for preventing the upstream movement of brook trout. *North American Journal of Fisheries Management* 18: 206– 210.
- United States Bureau of Reclamation (USBR) (2004a). “Aspinall Unit Operations Environmental Impact Statement Background Material.” Western Colorado Area Office, Upper Colorado Region, Grand Junction, CO.
- United States Bureau of Reclamation (USBR) (2004b). “Scoping Report -Aspinall Unit Operations EIS.” Western Colorado Area Office, Upper Colorado Region, Grand Junction, CO.
- United States Bureau of Reclamation (USBR) (2005). “Morrow Point Powerplan.” Western Colorado Area Office, Upper Colorado Region, Grand Junction, CO.
- United States Bureau of Reclamation (USBR) (2007). Western Colorado Area Office, Water Operations: Taylor Park Reservoir. <<http://www.usbr.gov/uc/wcao/water/rsvrs/ds/taylor.html>> (August 8, 2007)
- United States Bureau of Reclamation (USBR) (2008). “Aspinall Unit Operations Environmental Impact Statement Background Material.” Western Colorado Area Office, Upper Colorado Region, Grand Junction, CO.

- United States Fish and Wildlife Service (USFWS) (2003). "Flow Recommendations to Benefit Endangered Fishes in the Colorado and Gunnison Rivers." U.S. Fish and Wildlife Service, Denver, Colorado.
- Valencia, D. R., and J. C. Schaake (1973), Disaggregation processes in stochastic hydrology, *Water Resour. Res.*, 9, 580-585.
- Woodhouse, C.A., S.T. Gray, and D.M. Meko (2006), Updated streamflow reconstructions for the Upper Colorado River Basin, *Water Resour. Res.*, 42, W05415, doi:10.1029/2005WR004455.
- Yates, D., S. Gangopadhyay, B. Rajagopalan, and K. Strzepek, A technique for generating regional climate scenarios using a nearest-neighbor algorithm, *Water Resour. Res.*, 39(7), 1199, doi:10.1029/2002WR001769, 2003.
- Zagona, E.A., Fulp, T.J., Shane, R., Magee, T.M. and Goranflo, H.M. (2001). "RiverWare: A Generalized Tool for Complex Reservoir System Modeling." *Journal of the American Water Resources Association*, 37(4), 913-929.

# APPENDIX A RFF RIVERWARE RULES

RiverWare 5.0

RPL Set: C:\Documents and Settings\nowakkc\Desktop\RESERVOIR-STORAGES\Gunnison\_Ruleset\_KEN\_EIS\_1

RPL Set: C:\Documents and Settings\nowakkc\Desktop\RESERVOIR-STORAGES\Gunnison\_Ruleset\_KEN\_EIS\_1

Policy Group: Policy Group1

**Rule: BMOutflowGivenStorage**

```
BlueMesa.Outflow [ ] = IF ( BlueMesa.Outflow [ ] > Max ( MiscData.BM Res Data [ 0, ],
    ComputeOutflowAtStorage ( % "BlueMesa",
    82.00000000 ["1000 acre-feet"] ) ) ) THEN
    Max ( MiscData.BM Res Data [ 0, ],
    ComputeOutflowAtStorage ( % "BlueMesa",
    82.00000000 ["1000 acre-feet"] ) )
ENDIF
```

**Rule: CR sprill II**

```
MorrowPoint.Outflow [ ] = IF ( Crystal.Spill [ ] > 0.00000000 ["acre-feet/month"] AND MorrowPoint.Spill [ ] <= 0.00000000 ["acre-feet/month"] ) THEN
    Max ( MorrowPoint.Outflow [ ] - Crystal.Spill [ ],
    Max ( MiscData.MP Res Data [ 0, ],
    ComputeOutflowAtElevation ( % "MorrowPoint",
    7199.00000000 ["feet"] ) ) )
ENDIF
```

**Rule: MP spill II**

```
TaylorPark.Outflow [ ] = IF ( MorrowPoint.Spill [ ] > 0.00000000 ["acre-feet/month"] AND TaylorPark.Spill [ ] <= 0.00000000 ["acre-feet/month"] ) THEN
    Max ( TaylorPark.Outflow [ ] - MorrowPoint.Spill [ ],
    Max ( MiscData.TP Res Data [ 0, ],
    ComputeOutflowAtElevation ( % "TaylorPark",
    9335.00000000 ["feet"] ) ) )
ENDIF
```

**Rule: CR Res Values**

```
Crystal.Outflow [ ] = IF ( Crystal.Outflow [ ] < MiscData.DemandsAtCR [ ] AND @"t" <= @"Start Timestep" ) THEN
    Min ( # Computes storage at In active capacity
    ComputeOutflowAtStorage ( % "Crystal", MiscData.Crystal Res Data [ 0, 3 ] ), MiscData.DemandsAtCR [ ] )
ENDIF
```

**Rule: Crystal Rule Curve Storage**

```
Crystal.Storage [ ]
= IF ( CrystalRuleCurveRelease ( ) > MaxRelease ( % "Crystal" ) ) THEN
    CrystalStorageAtMaxRelease ( )
ELSE
    IF ( CrystalRuleCurveRelease ( ) < MiscData.Crystal Res Data [ 0, ]
    AND CrystalStorageAtMinRelease ( ) >= # In Active Capacity
    MiscData.Crystal Res Data [ 0, 3 ] ) THEN
        CrystalStorageAtMinRelease ( )
    ELSE
        # Live Capacity
        MiscData.Crystal Res Data [ 0, 2 ]
    ENDIF
ENDIF
```

ENDIF

**Rule: Demands at CR**

```
MiscData.DemandsAtCR []
= # Demands = Tunnel Diversions+ 300 cfs - Intervening Flows
( ( TunnelDiversionBelowCrystalForAg.Diversion Requested [] )
  + EISData.EIS [ EISData.EISdmd [@"t"],
                  GetMonth( @"t" )
                  - 1.00000000 ]
  - GunnisonBelowCrystal:TunnelDivBelowCrystalForAg.Local Inflow [@"t"] )
```

**Rule: MP Res Values**

```
MorrowPoint.Outflow [] = IF( MorrowPoint.Outflow [] < MiscData.DemandsAtMP [] AND @"t" == @"Start Timestep" )THEN
  Min( # Computes storage at In active capacity
        ComputeOutflowAtStorage( % "MorrowPoint", MiscData.MP Res Data [ 0 , 3 ], MiscData.DemandsAtMP [] )
      )
ENDIF
```

**Rule: MP Rule Curve Storage**

```
MorrowPoint.Storage []
= IF( MPRuleCurveRelease( ) > MaxRelease( % "MorrowPoint" ))THEN
  MPStorageAtMaxRelease( )
ELSE
  IF ( MPRuleCurveRelease( ) < MiscData.MP Res Data [ 0 ,
                                                       0 ] AND MPStorageAtMinRelease( ) >= # In Active Capacity
        MiscData.MP Res Data [ 0 ,
                               3 ] ) THEN
    MPStorageAtMinRelease( )
  ELSE
    # Live Capacity
    MiscData.MP Res Data [ 0 ,
                          2 ]
  ENDIF
ENDIF
```

**Rule: Demands at MP**

```
MiscData.DemandsAtMP []
= # Demands = Tunnel Diversions+ 300 cfs - Intervening Flows
( ( TunnelDiversionBelowCrystalForAg.Diversion Requested [] )
  + EISData.EIS [ EISData.EISdmd [@"t"],
                  GetMonth( @"t" )
                  - 1.00000000 ]
  - ( GunnisonBelowCrystal:TunnelDivBelowCrystalForAg.Local Inflow [@"t"]
      + GunnisonAboveCrystal:InterveningAboveCrystal.Local Inflow [@"t"] ) )
```

**Rule: New BM out**

```
BlueMesa.Outflow [@"t"] = IF ( MiscData.BM Res Data [ 0 ,
                                                       2 ] < SolveStorage( % "BlueMesa",
                                                                    BlueMesa.Inflow [@"t"],
                                                                    Max( MiscData.DemandsAtBM [@"t"],
                                                                    MiscData.BM Res Data [ 0 ,
                                                                    0 ] )
                                                                    )
                                                                    BlueMesa.Storage [@"t - 1"],
                                                                    @"t" ) ) THEN
```

```

SolveOutflow ( % "BlueMesa",
               BlueMesa.Inflow [@"t"],
               MiscData.BM Res Data [ 0,
                                       2 ],
               BlueMesa.Storage [@"t - 1"],
               @"t" )
ELSE
IF ( SolveStorage ( % "BlueMesa",
                  BlueMesa.Inflow [@"t"],
                  Max ( MiscData.DemandsAtBM [@"t"],
                      MiscData.BM Res Data [ 0,
                                              0 ] ),
                  BlueMesa.Storage [@"t - 1"],
                  @"t" ) < 200000.00000000 ["acre-ft"] ) THEN
MiscData.BM Res Data [ 0,
                      0 ]
ELSE
Max ( MiscData.DemandsAtBM [@"t"],
      MiscData.BM Res Data [ 0,
                            0 ] )
ENDIF
ENDIF
ENDIF

```

**Rule: BM DJF Flows**

```

BlueMesa.Outflow [ ] = IF ( Winter Season ( ) AND BlueMesa.Outflow [ ] < BMDJFFlowsFunction ( ) ) THEN
BMDJFFlowsFunction ( )
ENDIF

```

**Rule: BlueMesa Res Rule**

```

PRINT "Inflow: " CONCAT GetDisplayVa ( BlueMesa.Inflow, @"t" )
PRINT "Outflow: " CONCAT GetDisplayVa ( BlueMesa.Outflow, @"t" )
PRINT "Storage " CONCAT GetDisplayVa ( BlueMesa.Storage, @"t" )
BlueMesa.Outflow [ ] = IF ( Irri Season ( ) ) THEN
IF ( 100000.00000000 ["acre-ft"] > SolveStorage ( % "BlueMesa",
                                                BlueMesa.Inflow [@"t"],
                                                BM Irri Season DS Releases ( ),
                                                BlueMesa.Storage [@"t - 1"],
                                                @"t" ) ) THEN
MiscData.BM Res Data [ 0,
                      0 ]
ELSE
BM Irri Season DS Releases ( )
ENDIF
ELSE
BM Winter Season DS Releases ( )
ENDIF
ENDIF

```

**Rule: Winter Available Water**

```

PRINT "Winter Season: " CONCAT Winter Season ( )
PRINT "Blue Mesa Inflow: " CONCAT ( BlueMesa.Inflow [ ] )
MiscData.BM Winter Available Water [ ] = IF ( Winter Season ( ) ) THEN
SumSlot ( BlueMesa.Inflow, @"t", FinalMonthOfWinter ( @"t", @"Finish Timestep" ) )
ENDIF

```

**Rule: Winter Demands**

```
PRINT "Winter Season: " CONCAT Winter Season( )
MiscData.Winter Required Releases [ ] = IF( Winter Season( ))THEN
    SumSlot( MiscData.DemandsAtBM , @"t" , FinalMonthOfWinter( @"t" , @"Finish Timestep" ))
ENDIF
```

**Rule: Demands at BM**

```
FOREACH( DATETIME index IN @"Start Timestep" TO @"Finish Timestep" )DO
    MiscData.DemandsAtBM [ index ]
    = TunnelDiversionBelowCrystalForAg.Diversion Requested [ index ]
    + ( EISData.EIS [ EISData.EISdmd [ index ] ,
        GetMonth( index )
        - 1.00000000 ] )
    - ( GunnisonAboveMorrowPoint: InterveningAboveMorrowPoint.Local Inflow [ index ]
        + ( GunnisonAboveCrystal: InterveningAboveCrystal.Local Inflow [ index ]
            + GunnisonBelowCrystal: TunnelDivBelowCrystalForAg.Local Inflow [ index ] ) ) )
ENDFOREACH
```

**Rule: TPFutureOutflowsStorages**

```
FOREACH( NUMERIC INDEX IN GetNumbers( 0.00000000 , ( LENGTH Function2( ))- 1.00000000 , 1.00000000 ))DO
    TaylorPark.Storage [ OffsetDate( @"t" , INDEX , "1 Months" ) ] = GET NUMERIC @INDEX INDEX FROM Function2( )
ENDFOREACH
PRINT @"t"
PRINT FinalMonthOfWinter( @"t" , @"Finish Timestep" )
```

**Rule: Taylor Irri Season Res Rule**

```
TaylorPark.Outflow [ ] = IF( Irri Season( ))THEN
    TP Irri Season DS Releases( )
ENDIF
```

**Rule: Demands at TP**

```
FOREACH( DATETIME index IN @"Start Timestep" TO @"Finish Timestep" )DO
    MiscData.DemandsAtTP [ index ]
    = TunnelDiversionBelowCrystalForAg.Diversion Requested [ index ]
    + ( EISData.EIS [ EISData.EISdmd [ index ] ,
        GetMonth( index )
        - 1.00000000 ] )
    - ( GunnisonAboveBlueMesa: InterveningAboveBlueMesa.Local Inflow [ index ]
        + GunnisonAboveCrystal: InterveningAboveCrystal.Local Inflow [ index ]
        + ( GunnisonAboveMorrowPoint: InterveningAboveMorrowPoint.Local Inflow [ index ]
            + GunnisonBelowCrystal: TunnelDivBelowCrystalForAg.Local Inflow [ index ] ) ) )
ENDFOREACH
```

**Rule: Flow**

```
EISData.Flow [ @"t" ] = EISData.EIS [ EISData.EISdmd [ @"t" ] , GetMonth( @"t" )- 1.00000000 ]
```



```

+ FlowToVolume ( GunnisonAboveMorrowPoint: InterveningAboveMorrowPoint. Local Inflow [ NextDate ( index , ) ] , )
                ( NextDate ( index , ) )
                ( @ "April" )
+ FlowToVolume ( GunnisonAboveMorrowPoint: InterveningAboveMorrowPoint. Local Inflow [ NextDate ( index , ) ] , )
                ( NextDate ( index , ) )
                ( @ "May" )
+ FlowToVolume ( GunnisonAboveMorrowPoint: InterveningAboveMorrowPoint. Local Inflow [ NextDate ( index , ) ] , )
                ( NextDate ( index , ) )
                ( @ "June" )
+ FlowToVolume ( GunnisonAboveMorrowPoint: InterveningAboveMorrowPoint. Local Inflow [ NextDate ( index , ) ] , )
                ( NextDate ( index , ) )
                ( @ "July" )
+ FlowToVolume ( GunnisonAboveCrystal: InterveningAboveCrystal. Local Inflow [ NextDate ( index , ) ] , )
                ( NextDate ( index , ) )
                ( @ "April" )
+ FlowToVolume ( GunnisonAboveCrystal: InterveningAboveCrystal. Local Inflow [ NextDate ( index , ) ] , )
                ( NextDate ( index , ) )
                ( @ "May" )
+ FlowToVolume ( GunnisonAboveCrystal: InterveningAboveCrystal. Local Inflow [ NextDate ( index , ) ] , )
                ( NextDate ( index , ) )
                ( @ "June" )
+ FlowToVolume ( GunnisonAboveCrystal: InterveningAboveCrystal. Local Inflow [ NextDate ( index , ) ] , )
                ( NextDate ( index , ) )
                ( @ "July" )
+ FlowToVolume ( GunnisonBelowCrystal: TunnelDivBelowCrystalForAg. Local Inflow [ NextDate ( index , ) ] , )
                ( NextDate ( index , ) )
                ( @ "July" )
+ FlowToVolume ( GunnisonBelowCrystal: TunnelDivBelowCrystalForAg. Local Inflow [ NextDate ( index , ) ] , )
                ( NextDate ( index , ) )
                ( @ "June" )
+ FlowToVolume ( GunnisonBelowCrystal: TunnelDivBelowCrystalForAg. Local Inflow [ NextDate ( index , ) ] , )
                ( NextDate ( index , ) )
                ( @ "April" )
+ FlowToVolume ( GunnisonBelowCrystal: TunnelDivBelowCrystalForAg. Local Inflow [ NextDate ( index , ) ] , )
                ( NextDate ( index , ) )
                ( @ "May" )

```

```

+ FlowToVolume( TaylorPark.Inflow [ NextDate( index , @"July" ) ] ,
               NextDate( index , @"July" ) )
+ FlowToVolume( TaylorPark.Inflow [ NextDate( index , @"April" ) ] ,
               NextDate( index , @"April" ) )
+ FlowToVolume( TaylorPark.Inflow [ NextDate( index , @"June" ) ] ,
               NextDate( index , @"June" ) )
ENDIF
ENDFOREACH

```

**Utility Group:** Utility Group1

**Function:** Irri Season  
**Return Type:** BOOLEAN  
**Arguments:** ( )

```
@"t" >= @"24:00:00 March 1, Current Year" AND @"t" <= @"24:00:00 September 30, Current Year"
```

**Function:** Winter Season  
**Return Type:** BOOLEAN  
**Arguments:** ( )

```
@"t" >= @"October" AND @"t" <= @"December" OR ( @"t" >= @"January" AND @"t" <= @"February" )
```

**Function:** TP Irri Season DS Releases  
**Return Type:** NUMERIC  
**Arguments:** ( )

```

IF( # If reservoir is not full
    TaylorPark.Storage [@"t - 1"] < ElevationToStorage( % "TaylorPark", 9328.00000000 ["ft"] ) ) THEN
    # In April elevation should not go beyond 9305 ft
    IF( @"t" == @"April" AND ComputeOutflowAtElevation( % "TaylorPark", 9305.00000000 ["ft"] ) < MiscData.DemandsATP [ ] ) THEN
        ComputeOutflowAtElevation( % "TaylorPark", 9305.00000000 ["ft"] )
    ELSE
        Max( MiscData.DemandsATP [ ] , ComputeOutflowAtElevation( % "TaylorPark", 9328.00000000 ["ft"] ) )
    ENDIF
ENDIF
ELSE
    # If reservoir is full
    IF( @"t" == @"April" AND ComputeOutflowAtElevation( % "TaylorPark", 9305.00000000 ["ft"] ) < MiscData.DemandsATP [ ] ) THEN
        ComputeOutflowAtElevation( % "TaylorPark", 9305.00000000 ["ft"] )
    ELSE
        IF( @"t" <= @"July" ) THEN
            # If it is filling season
            Max( MiscData.DemandsATP [ ] , ComputeOutflowAtElevation( % "TaylorPark", 9328.00000000 ["ft"] ) )
        ELSE
            Max( MiscData.DemandsATP [ ] , TaylorPark.Inflow [ ] )
        ENDIF
    ENDIF
ENDIF
ENDIF

```

**Function:** TP Winter Season DS Releases

**Return Type:** NUMERIC

**Arguments:** ( )

```
IF ( # If reservoir is not full
    TaylorPark.Storage [ @'t' - 1 ] < ElevationToStorage( % "TaylorPark", 9328.0000000 ["ft"] ) ) THEN
    MiscData.DemandsAtTP [ ]
ELSE
    # If reservoir is full
    Max( MiscData.Taylor Park Fish Releases [ @'t', 1 ], TaylorPark.Inflow [ ] )
ENDIF
```

**Function:** TP Winter Season DS Releases Arg

**Return Type:** NUMERIC

**Arguments:** ( DATETIME date, LIST TpStorages )

```
IF ( # If reservoir is not full "GET NUMERIC @..." is Re. Storage [prev.timestep]
    ( GET NUMERIC @INDEX( LENGTH TpStorages ) - 1.0000000 FROM TpStorages ) < ElevationToStorage( % "TaylorPark",
    9328.0000000 ["ft"] ) ) THEN
    MiscData.DemandsAtTP [ date ]
ELSE
    # If reservoir is full
    Max( MiscData.DemandsAtTP [ date ],
    TaylorPark.Inflow [ date ] )
ENDIF
```

**Function:** Spawning Period

**Return Type:** BOOLEAN

**Arguments:** ( )

```
@'t' == @"October" OR '@'t' == @"November"
```

**Function:** BM Irri Season DS Releases

**Return Type:** NUMERIC

**Arguments:** ( )

```
IF ( # If reservoir is not full then release demands
    ( BlueMesa.Storage [ @'t' - 1 ] < ElevationToStorage( % "BlueMesa", 7516.4000000 ["feet"] ) ) ) THEN
    Max( MiscData.DemandsAtBM [ ], ComputeOutflowAtElevation( % "BlueMesa", 7516.4000000 ["feet"] ) )
ELSE
    IF ( # It is not a filling season, so releases - inflows ) THEN
        ( @'t' > @"24:00:00 July 31, Current Year" )
        Max( MiscData.DemandsAtBM [ ], BlueMesa.Inflow [ ] )
    ELSE
        Max( MiscData.DemandsAtBM [ ], ComputeOutflowAtElevation( % "BlueMesa", 7516.4000000 ["feet"] ) )
    ENDIF
ENDIF
```

**Function:** BM Winter Season DS Releases

**Return Type:** NUMERIC

**Arguments:** ( )

```
IF( BlueMesa.Storage [@"t - 1"] >= ElevationToStorage( % "BlueMesa", 7516.40000000 ["feet"] ))THEN
  # If the reservoir is full
  Max( BMWinterSeasonDSReleasesDetailsSub( ), BlueMesa.Inflow [ ] )
ELSE
  # If reservoir is not full
  BMWinterSeasonDSReleasesDetailsSub( )
ENDIF
```

**Function:** BMWinterSeasonDSReleasesDetailsSub

**Return Type:** NUMERIC

**Arguments:** ( )

```
IF( MiscData.BM Winter Available Water [ ] >= MiscData.Winter Required Releases [ ] )THEN
  ( ( MiscData.BM Winter Available Water [ ] - MiscData.Winter Required Releases [ ] ) /
    ( LENGTH GetDates( @"t", FinalMonthOfWinter( @"t", @"Finish Timestep" ), "1 months" ) ) ) + MiscData.DemandsAtBM [ ]
ELSE
  MiscData.BM Res Data [ 0, 0 ]
ENDIF
```

**Function:** TPFutureStorages

**Return Type:** LIST

**Arguments:** ( LIST dates )

```
FOR( DATETIME date IN dates )WITH LIST TpStorages = { TaylorPark.Storage [@"t - 1"] } DO
  TpStorages
  = IF( 25000.00000000 ["acre-ft"] > ( GET NUMERIC @INDEX( LENGTH TpStorages )
    - 1.00000000 FROM TpStorages
    + FlowToVolume( TaylorPark.Inflow [date]
    - TP Winter Season DS Releases Arg( date, TpStorages ),
    date ) ) THEN
    APPEND SolveStorage( % "TaylorPark",
      TaylorPark.Inflow [date],
      MiscData.TP Res Data [ 0, 0 ],
      GET NUMERIC @INDEX( LENGTH TpStorages )
      - 1.00000000 FROM TpStorages,
      date ) ONTO TpStorages
  ELSE
    APPEND SolveStorage( % "TaylorPark",
      TaylorPark.Inflow [date],
      TP Winter Season DS Releases Arg( date, TpStorages ),
      GET NUMERIC @INDEX( LENGTH TpStorages )
      - 1.00000000 FROM TpStorages,
      date ) ONTO TpStorages
  ENDIF
ENDFOR
```

**Function:** Function2

**Return Type:** LIST

**Arguments:** ( )

REMOVE ITEM @INDEX 0 FROM TPFutureStorages( @"t" TO FinalMonthOfWinter( @"t" , @"Finish Timestep" ))

**Function:** FinalMonthOfWinter

**Return Type:** DATETIME

**Arguments:** ( DATETIME datecurrent, DATETIME datefinal )

```
IF( datecurrent >= @"October" AND datecurrent <= @"December" )THEN
  IF( GetYear( datecurrent )== GetYear( datefinal ))THEN
    datefinal
  ELSE
    IF( datefinal == @"24:00:00 January Max DayOfMonth, Next Year" )THEN
      @"24:00:00 January Max DayOfMonth, Next Year"
    ELSE
      @"24:00:00 February Max DayOfMonth, Next Year"
    ENDIF
  ENDIF
ENDIF
ELSE
  IF( ( datecurrent >= @"January" AND datecurrent <= @"February" ) )THEN
    IF( datefinal == @"24:00:00 January Max DayOfMonth, Current Year" )THEN
      @"24:00:00 January Max DayOfMonth, Current Year"
    ELSE
      @"24:00:00 February Max DayOfMonth, Current Year"
    ENDIF
  ELSE
    datecurrent
  ENDIF
ENDIF
```

**Function:** BMDJFFlowsFunction

**Return Type:** NUMERIC

**Arguments:** ( )

```
IF( BlueMesa.Storage [@"t - 1"] >= ElevationToStorage( % "BlueMesa" ,
  7516.40000000 ["feet"] ))THEN
  # If the reservoir is full
  IF( @"t" == @"October" OR @"t" == @"November" )THEN
    Max( BlueMesa.Inflow [ ] ,
      Min(
        ComputeOutflowAtElevation( % "BlueMesa" ,
          7490.00000000 ["feet"] )
        + ( MiscData.BM Winter Available Water [ ]
          - MiscData.Winter Required Releases [ ] )
        / (
          LENGTH GetDates( @"t" ,
            @"24:00:00 December Max DayOfMonth, Current Year" ,
            "1 months"
          )
        )
      ,
      80.00000000 ["1000 acre-feet/month"]
    )
  ELSE
    Max( BlueMesa.Inflow [ ] ,
      Min(
        ComputeOutflowAtElevation( % "BlueMesa" ,
          7490.00000000 ["feet"] )
        ,
        120.00000000 ["1000 acre-feet/month"]
      )
    )
  ENDIF
```

```

ELSE
# If reservoir is not full and storage is > Storage (7490 feet)
IF ( BlueMesa.Storage [ @t - 1 ] > ElevationToStorage ( % "BlueMesa",
7490.00000000 ["feet"] ) ) THEN
IF ( @t == @ "October" OR @t == @ "November" ) THEN
Min (
ComputeOutflowAtElevation ( % "BlueMesa",
7490.00000000 ["feet"] )
,
LENGTH GetDates ( @t ,
@ "24:00:00 December Max DayOfMonth, Current Year" ,
"1 months"
)
80.00000000 ["1000 acre-feet/month"]
)
ELSE
Min ( ComputeOutflowAtElevation ( % "BlueMesa",
7490.00000000 ["feet"] )
,
120.00000000 ["1000 acre-feet/month"]
)
ENDIF
ELSE
IF ( # Irrigation season outflow values carried into the Winter starting season. To avoid this if it is winter season this wonot work. ) THEN
( @t != @ "October" )
BlueMesa.Outflow [ @t - 1 ]
- 10.00000000 ["1000 acre-feet/month"]
ENDIF
ENDIF
ENDIF
ENDIF

```

---

**Utility Group:** RuleCurve Functions

**Function:** MaxRelease  
**Return Type:** NUMERIC  
**Arguments:** ( OBJECT res )

res . "Maximum Controlled Release" [ 0 , 0 ]

**Function:** CrystalRuleCurveRelease  
**Return Type:** NUMERIC  
**Arguments:** ( )

SolveOutflow ( % "Crystal" , Crystal.Inflow [ ] , MiscData.Crystal Res Data [ 0 , 2 ] , Crystal.Storage [ @t - 1 ] , @t )

**Function:** CrystalStorageAtMaxRelease  
**Return Type:** NUMERIC  
**Arguments:** ( )

SolveStorage ( % "Crystal" , Crystal.Inflow [ ] , MaxRelease ( % "Crystal" ) , Crystal.Storage [ @t - 1 ] , @t )

**Function:** CrystalStorageAtCRDemands  
**Return Type:** NUMERIC  
**Arguments:** ( )

SolveStorage ( % "Crystal" , Crystal.Inflow [ ] , # Demands at CR  
MiscData.DemandsAtCR [ ] , Crystal.Storage [ @t - 1 ] , @t )

**Function:** ComputeTPElevationGivenDemands

**Return Type:** NUMERIC

**Arguments:** ( )

---

```
StorageToElevation( % "TaylorPark",  
SolveStorage( % "TaylorPark",  
TaylorPark.Inflow [],  
# Demands at TP  
MiscData.DemandsAtTP [],  
TaylorPark.Storage [@"t - 1"],  
@"t" ) )
```

**Function:** CrystalStorageAtMinRelease

**Return Type:** NUMERIC

**Arguments:** ( )

---

```
SolveStorage( % "Crystal", Crystal.Inflow [], # Min. Release  
MiscData.Crystal Res Data [0, 0], Crystal.Storage [@"t - 1"], @"t" )
```

**Function:** MPRuleCurveRelease

**Return Type:** NUMERIC

**Arguments:** ( )

---

```
SolveOutflow( % "MorrowPoint", MorrowPoint.Inflow [], MiscData.MP Res Data [0, 2], MorrowPoint.Storage [@"t - 1"], @"t" )
```

**Function:** MPStorageAtMaxRelease

**Return Type:** NUMERIC

**Arguments:** ( )

---

```
SolveStorage( % "MorrowPoint", MorrowPoint.Inflow [], MaxRelease( % "MorrowPoint" ), MorrowPoint.Storage [@"t - 1"], @"t" )
```

**Function:** MPStorageAtMinRelease

**Return Type:** NUMERIC

**Arguments:** ( )

---

```
SolveStorage( % "MorrowPoint", MorrowPoint.Inflow [], # Min. Release  
MiscData.MP Res Data [0, 0], MorrowPoint.Storage [@"t - 1"], @"t" )
```

**Function:** MPStorageAtMPDemands

**Return Type:** NUMERIC

**Arguments:** ( )

---

```
SolveStorage( % "MorrowPoint", MorrowPoint.Inflow [], # Demands at MP  
MiscData.DemandsAtMP [], MorrowPoint.Storage [@"t - 1"], @"t" )
```

**Function:** ComputeStorageAtReleases

**Return Type:** NUMERIC

**Arguments:** ( OBJECT res, NUMERIC outfl )

---

```
SolveStorage( res, res . "Inflow" [], # Releases/Outflows  
res . "Outflow" [], res . "Storage" [@"t - 1"], @"t" )
```

**Function:** ComputeOutflowAtElevation

**Return Type:** NUMERIC

**Arguments:** ( OBJECT res, NUMERIC elev )

---

```
SolveOutflow( res, res . "Inflow" [], ElevationToStorage( res, elev ), res . "Storage" [@"t - 1"], @"t" )
```

**Function:** ComputeOutflowAtStorage

**Return Type:** NUMERIC

**Arguments:** ( OBJECT res, NUMERIC stora )

---

```
SolveOutflow( res , res . "Inflow" [ ] , stora , res . "Storage" [@"t - 1" ] , @"t" )
```

**Function:** MP Outflows

**Return Type:** NUMERIC

**Arguments:** ( )

---

```
IF( MorrowPoint.Outflow [ ] < MiscData.DemandsAtMP [ ] )THEN  
  Min( # Computes storage at In active capacity  
    ( ComputeOutflowAtStorage( % "MorrowPoint" , MiscData.MP Res Data [ 0 , 3 ] ) , MiscData.DemandsAtMP [ ] )  
  )  
ELSE  
  MorrowPoint.Outflow [ ]  
ENDIF
```

**Function:** CR Outflows

**Return Type:** NUMERIC

**Arguments:** ( )

---

```
IF( Crystal.Outflow [ ] < MiscData.DemandsAtCR [ ] )THEN  
  Min( # Computes storage at In active capacity  
    ( ComputeOutflowAtStorage( % "Crystal" , MiscData.Crystal Res Data [ 0 , 3 ] ) , MiscData.DemandsAtCR [ ] )  
  )  
ELSE  
  Crystal.Outflow [ ]  
ENDIF
```